

APPLICATION BRIEFS 2002



The views and conclusions contained in this document are those of the authors and should not be interpreted as necessarily representing the official policies or endorsements, either expressed or implied, of the Air Force Research Laboratory, the U.S. Government, the University of Hawaii, or the Maui High Performance Computing Center.

**MAUI HIGH PERFORMANCE
COMPUTING CENTER**

550 Lipoa Parkway, Kihei-Maui, HI 96753
(808) 879-5077 • Fax: (808) 879-5018
E-mail: info@mhpsc.edu
URL: www.mhpsc.edu

A Center of the Air Force Research Laboratory Managed by the University of Hawaii.

WELCOME

This is the eighth annual edition of Maui High Performance Computing Center's (MHPCC) *Application Briefs*—which highlights some of the successes our customers have achieved this year.

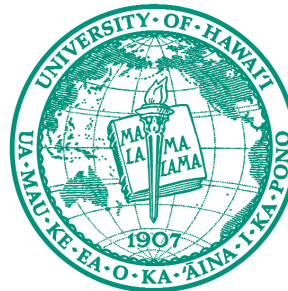
MHPCC, established in September 1993, is an Air Force Research Laboratory (AFRL) Center managed by the University of Hawaii. A leader in scalable parallel computing technologies, MHPCC is primarily chartered to support the Department of Defense (DoD) and other government organizations.

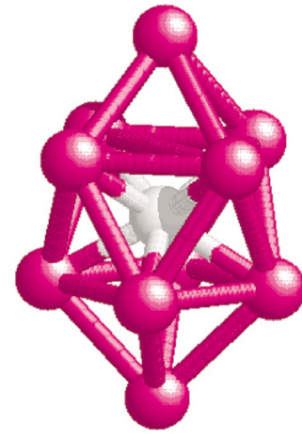
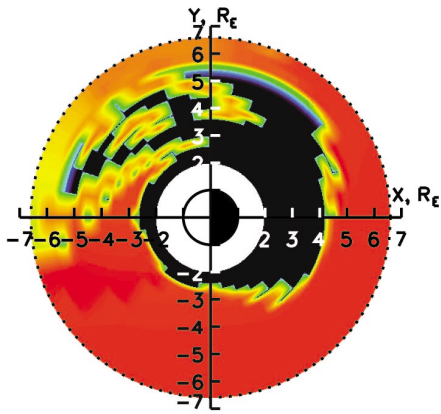
MHPCC offers an innovative environment for high performance computing applications. This includes:

- **Computational Resources:** Stable and secure parallel computing platforms for prototyping, benchmarking, and testing applications. MHPCC is ranked as one of the top computing centers in the world in terms of computational capabilities.
- **High Performance Storage:** MHPCC users have access to more than 12 terabytes (TB) of disk storage and nearly 24 TB of on-line tape storage.
- **High-Speed Communications Infrastructure:** OC3 connections, offering 155 megabit per second (Mbps) capacity, provide direct access to MHPCC resources—over the Defense Research and Engineering Network (DREN) and the Hawaii Intranet Consortium (HIC).
- **Support Services:** An expert staff provides MHPCC users with systems, network, and applications support in addition to assistance with code porting, optimization, and application development.

MHPCC is a well-established member of the High Performance Computing (HPC) community, participating in collaborations and partnerships that extend its basic capabilities. MHPCC represents the AFRL as a:

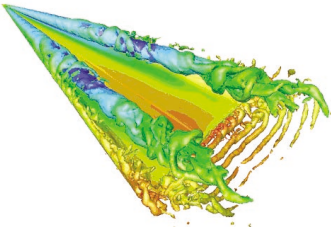
- Center within the Air Force Research Laboratory. MHPCC works closely with DoD and other government researchers to support Research, Development, Testing, and Evaluation (RDT&E) efforts.
- Distributed Center within the DoD High Performance Computing Modernization Program (HPCMP). MHPCC provides resources to the DoD research community, as well as Pacific Region DoD organizations, including the Air Force's Maui Space Surveillance Complex.
- Air Force Research Laboratory resource for the Maui Space Surveillance System (MSSS).
- Member of Hawaii's growing science and technology community.



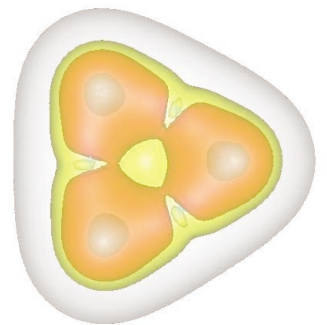


APPLICATION BRIEFS

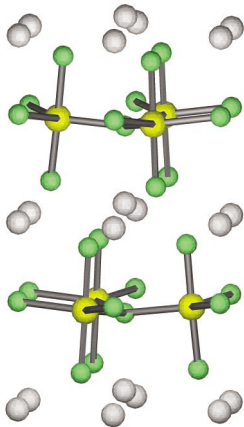
The user application briefs in this publication represent selected research efforts that have taken place at MHPCC during 2002. Each application brief was written by an individual researcher or research team, and reflects their first-hand experiences using MHPCC resources. These articles reflect the diverse nature of our users and projects.



The Application Briefs in this document are the result of the efforts of more than 80 authors representing nearly 40 organizations. We acknowledge the contributions of each of these individuals and are grateful for their work. We especially welcome back those authors who have become regular and frequent contributors. Joel T. Johnson is especially recognized for his eighth consecutive year of contributions to this publication. We also welcome those making their MHPCC Application Briefs debut this year.



The shaded box at the top of each brief's first page is a short summary of the article. Author and/or organizational contact information can be found in the shaded box at the end of each brief. The notation at the bottom of each page indicates each project's primary functional area (DoD, Government, or Academic).



And finally, feedback regarding this publication is solicited. Please direct any communications to: editor@mhpcc.edu.

Thank you for your support.

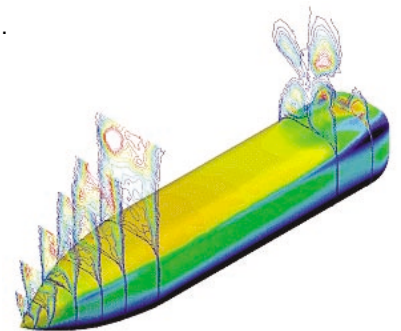
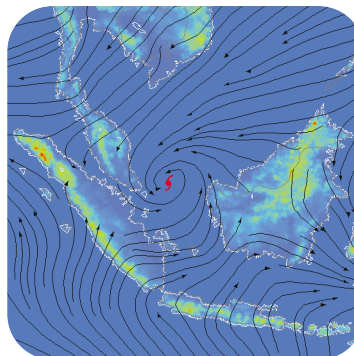


TABLE OF CONTENTS

Numerical Studies of Polarimetric Thermal Emission From Rough Sea Surfaces1 Joel T. Johnson	1
Simulations of Ring Current Ions Under AMIE Electric Field During Magnetic Storms2 Margaret W. Chen	2
Use of Covalently-Bonded Ceramics in Jet Engine Thermal Barrier Coatings4 Emily A. Jarvis and Emily A. Carter	4
Advanced Image Processing and Data Management Environment Implementation for MSSS6 Bruce Duncan, Kathy Schulze, Bob Brem, Flo Cid, Paul Billings, Chip DeMeo, Steve Gima	6
Joint Medical Asset Repository (JMAR) Implementation at MHPCC8 Bruce Duncan, Chelsea Nesbitt, Dean George, Jason Wachi, Mark Radleigh, Steve Gima, Joshua Testerman, Nathan Reish, Shirley Verbisk	8
Detached-Eddy Simulation of Massively Separated Flows Over Aircraft10 James R. Forsythe, Kyle D. Squires, Scott A. Morton, Kenneth E. Wurtzler, William Z. Strang, Robert F. Tomaro, Philippe R. Spalart	10
High Performance Computing and Web Support for Project Albert: Analysis of Entity-Based Simulations of Land Combat12 Brent Swartz, Alfred Brandstein, Gary Horne, John Kresho, Ted Meyer, Steve Upton, Mary McDonald, Bob Swanson, Maria Murphy, Ron Vilorio, D. J. Fabozzi, Bruce Duncan	12
Parallelization Development and Testing of the Operational Multiscale Environment Model With Grid Adaptivity (OMEGA)14 Thomas J. Dunn, David P. Bacon, Pius C. S. Lee, Mary S. Hall, A. Sarma	14
Visualization Support for Project Albert16 Brent Swartz, Alfred Brandstein, Gary Horne, John Kresho, Ted Meyer, Steve Upton, Mary McDonald, Bob Swanson, Maria Murphy, Ron Vilorio, D. J. Fabozzi, Bruce Duncan	16
Simulations of Multi-Color, Inverse-Tapered Free-Electron Lasers18 Eric Szarmes and Frank Price	18
The Modeling of Bubbly Flows Around Ship Hulls19 F. J. Moraga, D. A. Drew, R. T. Lahey, Jr.	19
MatlabMPI Improves Matlab Performance By 300x20 Jeremy Kepner	20
A Study of Airfoil Spin Characteristics Using Computational Fluid Dynamics22 Cadet First Class Jon Wentzel and Jim Forsythe	22
Ultra-High Bandwidth Control of Active Optics Using Chemo-Optical Computation23 Joe Ritter	23
Non-Linear Imaging Algorithm Study24 Kathy Schulze, Paul Billings, Chuck Matson, Bobby Hunt, Bob Dant	24

TABLE OF CONTENTS CONTINUED

Novel Laser Actuated Optically Addressable Adaptive Optics	26
Joe Ritter, Jim Brozik, James Newhouse, David Keller	
The Impact of Initial Conditions on the Time-Space Distribution of Long-Term Atmospheric Predictability	28
Thomas Reichler and John Roads	
Experimental High-Resolution Forecasts/Analyses for the Hawaiian Islands	30
John Roads, Jongil Han, Francis Fujioka, Kevin Roe	
High-Resolution Weather Modeling for Improved Fire Management	32
Kevin Roe and Duane Stevens	
Ab Initio Calculations Characterizing an Effective Hamiltonian for Polymeric Photonic “Muscles”	34
James Newhouse, Debi Evans, Joe Ritter	
Investigation of Small Boron Nitride Clusters	36
Sigrid Greene and Pui Lam	
Measuring the Carrier-Envelope Phase of Few-Cycle Laser Pulses Using Attosecond Cross Correlation Technique in Atoms and Molecules	38
André D. Bandrauk, Szczepan Chelkowski, Nguyen Hong Shon	
3D Visualization Concept for Complex Battlefield Simulations	40
Marie Greene, Mark Elies, Jonathan Baliquat, Peter Lentz, Ted Meyer, Michael Shrive, Brent Swartz, J. D. Vargas-Garcia, Betsy Ward	
Minima of Kr_n-H for n = 1 to 13	42
Emanuele Curotto and Jonathan H. Skone	
2D MHD Simulations Using Lattice Boltzman Methods	43
Linda Vahala, George Vahala, Angus Macnab, Min Soe	
First-Principle Methodologies for Ferroelectromagnetic Materials	44
Alessio Filippetti and Nicola A. Hill	
Cluster Computing: Communication Performance and Scalability	46
Daniele Tessera	
Electron-Impact Ionization of Hydrogen	48
Igor Bray	
INDEX OF AUTHORS	Index-1
INDEX OF ORGANIZATIONS	Index-2

Numerical Studies of Polarimetric Thermal Emission From Rough Sea Surfaces

Joel T. Johnson

Microwave radiometers are passive sensors included on Earth orbiting satellites for monitoring the global climate. One application of radiometer data involves determination of sea surface wind speed and direction due to the fact that radiometer "brightness temperatures" are influenced by roughness on the sea surface. Improving measurements of sea wind vector requires understanding the physics of microwave thermal emission from rough surfaces. Competing models for emission from rough surfaces are explored in this project to investigate their accuracy.

Methodology: The studies of this project involve predicting microwave power emitted from a rough surface. The competing models considered are a "small slope approximation" (SSA) theory, a "geometrical optics" (GO) approach, and a numerical solution of the electromagnetic boundary value problem. The SSA method provides a perturbation series for surface roughness effects. A numerical SSA algorithm is used that allows computation of these terms up to the twentieth order. The GO algorithm

includes a ray-tracing step so that multiple scattering and shadowing effects can be included approximately. The numerical solution is based on the "extended boundary condition" (EBC) formulation, and involves inversion of a large matrix equation. The simplicity of the GO method allows its results to be computed on a standard PC level platform. However, the numerical higher-order SSA method is somewhat expensive. Parallel computing resources are applied so that solutions for multiple observation angles are performed on individual nodes. The high-order SSA code also requires high precision calculations, and was implemented using the quadruple precision libraries available on the SP system. The EBC code is very computationally expensive. Solutions for a single observation angle were implemented using multiple SP nodes under the "Scalapack" parallel matrix equation library.

Results: A detailed comparison of the SSA and GO approximate theories has been completed for a simple class of surface profiles. Results showed the SSA theory to provide high accuracy compared to the EBC algorithm when convergence of the SSA series was obtained. The number of SSA series terms required was found to be a function of the length scale of the surface considered, with larger scale surface features obtaining slower convergence. Convergence of the SSA series also degraded when multiple scattering or shadowing effects were possible. The GO algorithm matched SSA results well for large scale surfaces when multiple scattering and shadowing effects were absent, but produced poor agreement for shorter scale surface features. Higher order ray-tracing contributions in the GO theory provided only minimal increases in overall accuracy.

Significance: The results of this project have further clarified the limitations of the standard theories applied for prediction of rough surface brightness temperatures. The impending launch of the Naval Research Laboratory's "WindSAT" microwave radiometer (scheduled for 2003) makes these results important for designing effective wind vector retrieval methods from WindSAT brightness measurements.

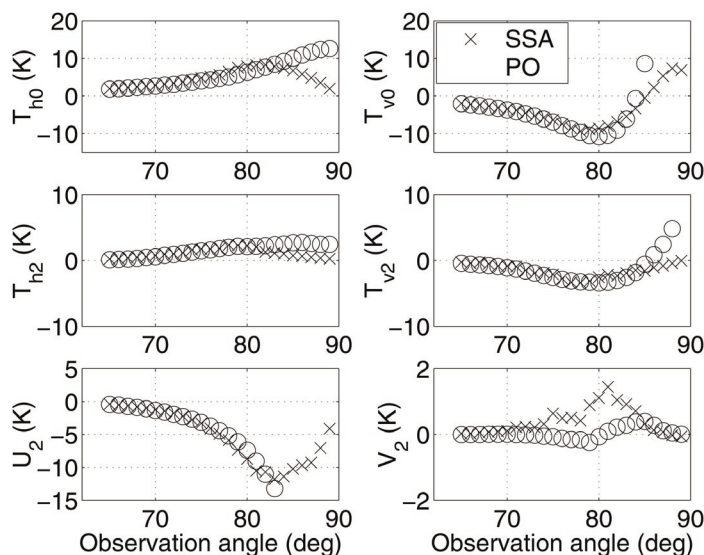


Figure 1. A sample comparison of SSA and GO results versus polar observation angle for a bi-sinusoidal sea water surface with periods 50 by 100 electromagnetic wavelengths and with amplitude 1.5 wavelengths. Zeroth and second azimuthal harmonics of the horizontal, vertical, U, and V brightness temperatures are compared. Results show significant errors in the optical method (labeled here as PO) at larger observation angles where multiple scattering and shadowing effects are more appreciable.

Author and Contact: Joel T. Johnson

Organization: The Ohio State University, 205 Dreese Laboratories, 2015 Neil Avenue, Columbus, OH, 43210

URL: <http://eewww.eng.ohio-state.edu>

Resources: 64 IBM SP nodes at MHPCC

Sponsorship: DoD

Simulations of Ring Current Ions Under AMIE Electric Field During Magnetic Storms

Margaret W. Chen

This is a simulation study of ring current ions (energies $\sim 10 - 200$ keV at 2 to 7 earth radii) under the Assimilative Model of Ionospheric Electrodynamics (AMIE)¹ mapped into a model magnetospheric magnetic field. We compute the guiding-center drifts of ions for magnetic storm events. Using the simulation results, we map the storm time phase-space distributions of protons for a given value of the first adiabatic invariant. Our simulations show the formation of an asymmetric ring current that progressively becomes more symmetric during the storm main phase. Knowledge of realistic flux distributions of ring current particles in the inner magnetosphere is relevant to Air Force and other satellite systems because long-term exposure to such an environment can cause damage to optical coatings and other surface materials.

Research Objectives: We simulate the drift of ions under the realistic AMIE electric field in a model magnetic field so as to understand better the formation of the storm time ring current. Our eventual goal is to develop a self-consistent simulation that calculates particle distributions in a magnetic field that includes the ring current itself.

Methodology: The AMIE potentials are an analytic expansion of basis functions that depend on magnetic latitude and magnetic local time in the ionosphere. These potentials are fit to electric field data that is inferred from ground-based magnetometers and available satellite and radar data. We model the magnetospheric magnetic field as a superposition

of a dipolar magnetic field and a uniform southward field parallel to the dipole axis. In this field model, the field line equation relates the magnetic latitude to the field line label L at the altitude where AMIE potentials are specified. Thus, we can describe AMIE potentials analytically everywhere in the model magnetic field, given the AMIE coefficients for a particular time period. We construct a Hamiltonian function (kinetic energy plus potential energy) of the particle motion, assuming that particles conserve their first two adiabatic invariants. This formalism facilitates the derivation of the guiding-center drift equations for which we solve numerically.

Results: We simulated the drifts of ions for different values of the first adiabatic invariant M under the AMIE electric field for selected times during the large 19 October 1998 magnetic storm. During the early main phase of the 19 October 1998 storm, the electric field in the evening sector of the AMIE model is stronger than in any other longitudinal sector. This results in rapid (about 20 to 30 minutes) inward transport of ring current ions and electrons near dusk where the partial ring current is formed. We accounted for the observed rapid formation of a partial ring current, which subsequently becomes more symmetric. We calculated ion drifts during the early main phase of the extremely large 15 July 2000 "Bastille Day" magnetic storm. We found that open drift paths of ions with M values representative of the ring current reach as low as 2 earth radii. This deep penetration of ring current ions is consistent with a very strong ring current that was observed during this storm. We found a nearly symmetric ring current at 2 to 3 earth radii near the peak of the storm main phase.

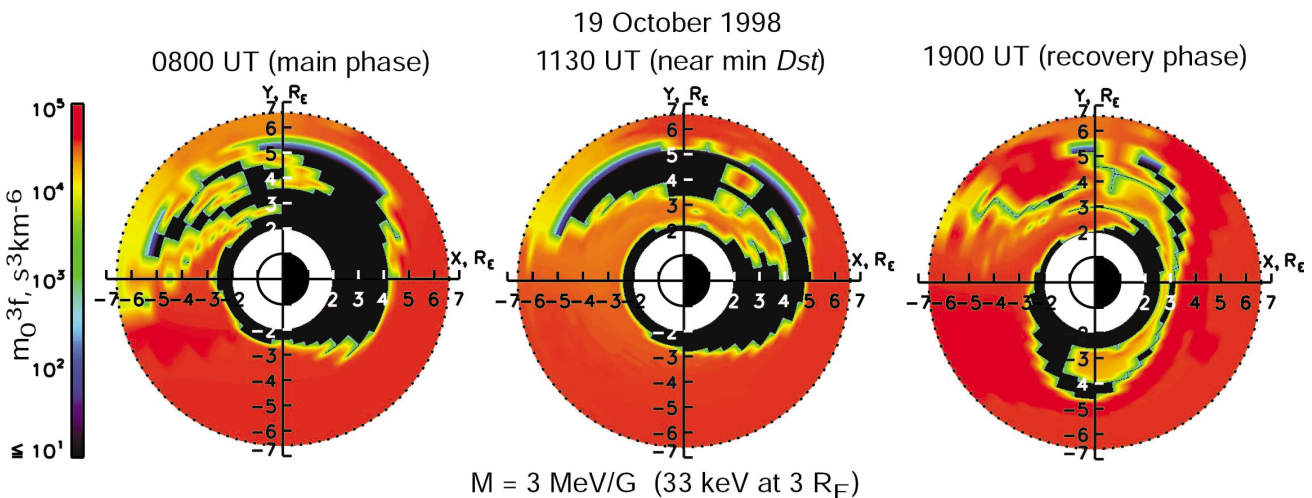


Figure 1. The panels show the phase space density f for protons with $M = 3 \text{ MeV/G}$ (energies of 33 keV at 3 earth radii) in the equatorial plane at different times during the 19 October 1998 storm. The constant m_0 is the ion rest mass. The sun is to the left. During the storm main phase a partial ring current is forming. The ring current becomes more symmetric in the storm recovery phase.

Significance: The incorporation of realistic electric field models in numerical models of inner magnetospheric dynamics is very important, as recent electric field observations² show that the storm time near-earth electric field may be much stronger than what is predicted in simplified electric field models that are commonly used. This study shows that the ion drift times and simulated phase space distributions for a couple of real magnetic storms are consistent with ring current observations. Knowledge of realistic flux distributions of ring current particles in the inner magnetosphere is relevant to Air Force and other satellite systems, because long-term exposure to such an environment can cause damage to optical coatings and other surface materials.

References:

- 1) A. D. Richmond and Y. Kamide, Mapping Electrodynamic Features of the High-Latitude Ionosphere from Localized Observations: Technique, *J. Geophys. Res.*, 92, 5471-5759, 1988.
- 2) D. E. Rowland and J. R. Wygant, Dependence of the Large-Scale, Inner Magnetospheric Electric Field on Geomagnetic Activity, *J. Geophys. Res.*, 103, 14,959-14,964, 1998.

Author and Contact: Margaret W. Chen
Organization: The Aerospace Corporation, P.O. Box 92957, M2-260, Los Angeles, CA, 90009-2957
URL: www.aero.org
Resources: IBM SP at MHPCC and Sun Enterprise 3000 at the Aerospace Corporation
Sponsorship: DoD and National Science Foundation

Use of Covalently-Bonded Ceramics in Jet Engine Thermal Barrier Coatings

Emily A. Jarvis and Emily A. Carter

Thin ceramic coatings are used to protect turbine blades from heat and corrosion. The protection afforded by these "Thermal Barrier Coating" (TBC) films permits greater power and fuel efficiency. Current coatings fail after repeated use. It is hoped that materials modifications to TBCs that enhance open-shell bonding at the interfaces will limit the materials failure mechanisms that currently plague TBCs.

Methodology: We have characterized atomic-level interactions at ideal TBC interfaces using a first principles density functional method. We found that interfaces with alumina, which is the typical oxidation product in current TBCs, exhibit weak adhesion.^{1,2,3} We postulated that one cause of the observed void formation at such interfaces is the highly ionic bonding in alumina

leading to closed-shell repulsions with the nickel metal alloy. We demonstrated how doping the ceramic-metal interface with early transition metals increases local bonding and decreases closed-shell repulsions.^{4,5} More recently, we have investigated the effect of limiting closed-shell electronic structure at the interface by replacing alumina with a more covalently bonded ceramic, silica. We found the ideal ceramic/metal and ceramic/ceramic TBC interfaces formed using silica in place of alumina permit much stronger interface adhesion. It is hoped that materials modifications to TBCs that enhance open-shell bonding at the interfaces will limit the materials failure mechanisms that currently plague TBCs.

References:

- 1) A. Christensen and E. A. Carter, *Phys. Rev.*, B 62, 16968 (2000).
- 2) A. Christensen and E. A. Carter, *J.Chem. Phys.*, 114, 5816 (2001).
- 3) E. A. Jarvis, A. Christensen, and E. A. Carter, *Surf. Sci.*, 487, 55 (2001).
- 4) E. A. Jarvis and E. A. Carter, *Comp. Sci. Eng.*, 4, 33 (2002).
- 5) E. A. Jarvis and E. A. Carter, *J. Phys. Chem.*, in press (2002).

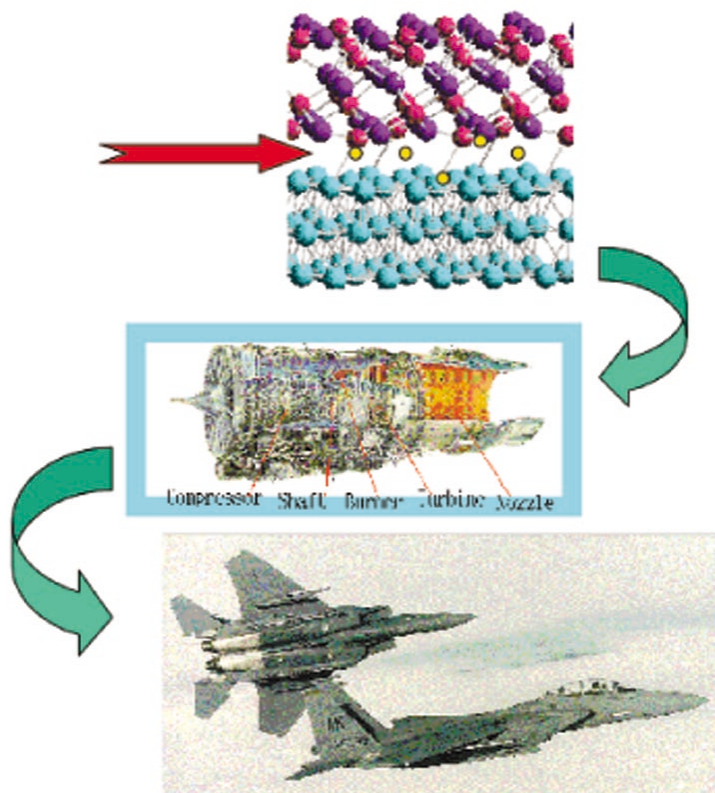


Figure 1. A schematic view tracing how the atomic-level interfacial interactions of the TBC influence the jet engine and ultimately aircraft performance and efficiency.

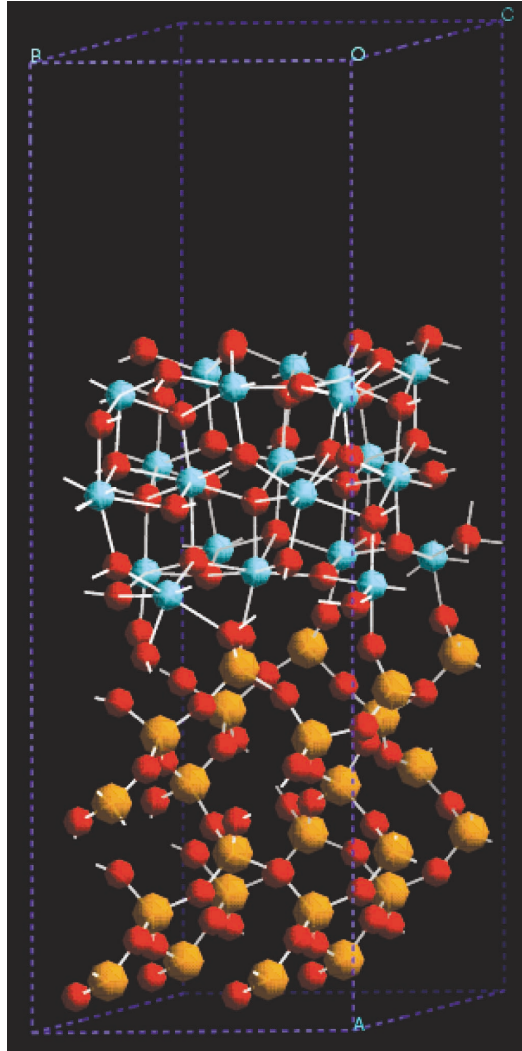


Figure 2. Periodic supercell displaying relaxed atomic coordinates of a zirconia, ZrO_2 , coating on silica, SiO_2 . ZrO_2 serves as the outermost thermal protective layer in a TBC, and SiO_2 may be a preferred oxidation product of the metal alloy for TBC applications. The red, orange, and blue spheres represent oxygen, silicon, and zirconium, respectively. The ZrO_2 film experiences a partial phase transition upon relaxation, which agrees with previous observations and predictions for ZrO_2 thin films.

Author and Contact: Emily A. Carter

Author: Emily A. Jarvis

Organization: Department of Chemistry and Biochemistry, University of California, Los Angeles, CA, 90095-1569

Resources: IBM SP P3 at MHPCC and DEC Alpha ES40 and local workstations at UCLA

Sponsorship: Air Force Office of Scientific Research and the DoD's High Performance Computing Modernization Program (HPCMP) Challenge Projects

Advanced Image Processing and Data Management Environment Implementation for MSSS

Bruce Duncan, Kathy Schulze, Bob Brem, Flo Cid, Paul Billings, Chip DeMeo, Steve Gima

Developers at Boeing LTS, Textron Systems, and KJS Consulting spent much of calendar year 2002 working under a Task Order awarded by the Air Force Research Laboratory (AFRL) to complete engineering development and to operationalize a new bispectrum algorithm in the Maui Image Manager and Online Systems Archive (MIMOSA) environment for AFRL's Maui Space Surveillance System (MSSS) GEMINI sensor. The project completion is to include passing an Operational Test & Evaluation (OT&E) to make the software useable for preparing end-use customer data products. The goal of this effort is to have the new bispectrum software operating under MIMOSA. This software will be accessible from the computers at the Maui Space Surveillance Complex (MSSC) atop Mt. Haleakala and at the Maui High Performance Computing Center (MHPCC). It is to be ready for use with GEMINI data and available for all image processing needs. Under the program plan, the MHPCC version of the code will be the primary data reduction software, with the MSSC version available as a backup.

Research Background: The AFRL operating location on Maui, Hawaii has a two-fold mission. First, it conducts research and development (R&D) and operations on the MSSS at the MSSC site. Second, it oversees operation of the MHPCC. AFRL is integrating these world-class assets to enhance space surveillance with the primary objective of detecting, tracking, and identifying space objects within its area of coverage. MSSS is a national resource that provides support to various government agencies, the scientific community, and the United States space surveillance mission. MSSS acquires gigabytes of information per day from its various sensors and instruments. AFRL and an AFRL contractor have developed a new algorithm to solve the bispectrum phase estimation equation, building on the parallel bispectrum algorithm that is currently operational on GEMINI sensor data. This new algorithm provides many enhancements over the

previous version. The new algorithm runs very efficiently in terms of CPU time and especially memory usage, and delivers photometrically accurate results in timeframes usable for the MSSS mission. In the GEMINI Near Real Time (NRT) monitoring mode, the new bispectrum version uses MHPCC computing nodes that are connected to the MSSS computer network to receive frames of raw data, perform a bispectrum recovery, and send the results back to the MSSS system in less than one second. Developers at MHPCC and AFRL contractors have also developed a data reduction environment known as the Maui Image Manager and Online Systems Archive (MIMOSA). MIMOSA is a key step in a multi-faceted plan to more closely integrate MSSS telescopes and the High Performance Computing (HPC) environment and tools of the MHPCC. MIMOSA provides a Web-browser environment that encompasses all aspects of telescope imagery data reduction including, file transfer, processing for calibration data and object imagery, file format conversion, data viewing, and storage.

Development Methodology: The MIMOSA Environment contains all of the requirements for successful post mission processing of GEMINI sensor data (Figure 1). Additional capabilities were developed this year under AFRL direction to enhance the already robust MIMOSA environment. The additional capabilities included the addition of new linear filters, an alert mechanism for disk space limits, color look-up table selection for the movie/data viewer, an "EXECUTE NOW" capability for small jobs, and adding file manipulation utilities. The new filters received from AFRL were packaged into the bispectrum code and changes were made to the MIMOSA Web page, output files, and executables. The design and development of file manipulation utilities included: view

(using MIMOSA viewing utilities), remove, and rename files and directories. The file manipulations functionality was implemented in Perl/CGI, because of Javascript file access limitations. A new Web page tab was also created with the title "FILE MANIPULATIONS." The disk status utility was created because as large amounts of data are moved between the observatory and the MHPCC *Crux* server RAID, users need to be aware of the amount of disk space available. The disk status utility displays statistics for the amount of disk space available and used on this file system. This new feature reports the amount of space unused and available on the /data filesystem. On the applicable MIMOSA Web page, in the bottom left hand corner, the ability to show the amount of available storage on the /data filesystem and the percentage utilized was added. Previously, the MIMOSA movie-viewer had no ability to display movies using any look-up table other than grayscale. Using the color look-up table options from the single frame viewer, a color look-up table selection function was added to the movie player. A function allowing users to globally scale the movie during viewing was also added.

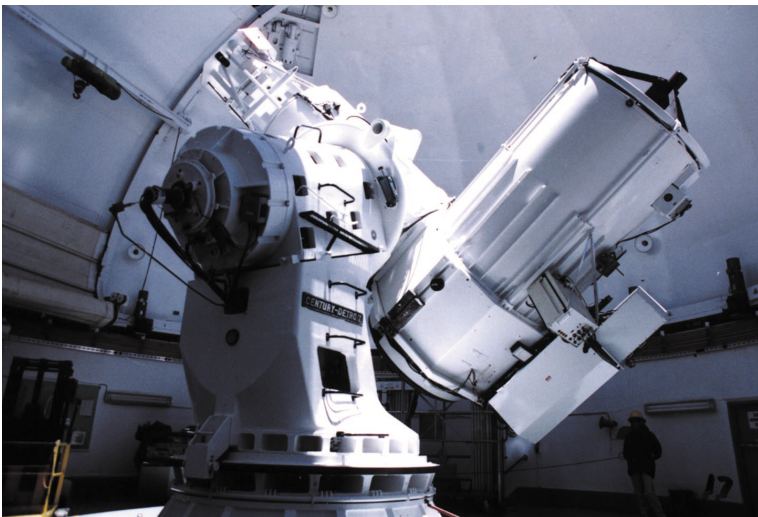


Figure 1. The GEMINI sensor is mounted on the 1.6 m telescope at the Air Force's Maui Space Surveillance Complex (MSSC) located at the 10,000 foot summit of Mt. Haleakala, Maui, Hawaii.

The project team is also implementing a Near Real Time image reconstruction monitoring option in the MIMOSA environment software that enables users who are logged into the appropriate systems using MIMOSA to view NRT image reconstruction of a pass in progress. The NRT monitoring will only be available during GEMINI operation when the NRT mode is being utilized. NRT feedback is obtained by sending raw data packets via a high speed link from the MSSS to the MHPCC parallel computing system where a bispectrum recovery is completed. The bispectrum recovery is returned to the MSSS where it is displayed on the GEMINI operator's console. This NRT feedback allows the operators to make optical parameter adjustments, such as exposure time and filter settings, using recovered imagery rather than raw imagery, thus increasing the fidelity of the collected raw data products. The required code modifications for the MIMOSA viewing capabilities to include the NRT monitoring of GEMINI have been made. NRT operator feedback was determined and an NRT design guidance document was developed. The appropriate changes were then made to the GEMINI servers to supply the raw and recovered data to the MIMOSA environment.

As of this writing, the latest version of the bispectrum software is planned to be installed on the *Koa* processor at the MSSS observatory to upgrade the processing system. This latest version of the software is identical to the version running at the MHPCC under MIMOSA. The differences in the old and new software packages have been documented, outlining the required changes to the GEMINI Graphical User Interface (GUI) for proper code execution. This included the differences between the input parameters for the old version of bispectrum currently running on *Koa* and the new version that is currently running under MIMOSA at MHPCC. This document served as the guide for all software changes that were required to integrate the new version. The document also included changes required for the post-processing pipeline. The GEMINI GUI was also updated to reflect all the changes in the bispectrum software and correctly execute the new bispectrum code. It was also necessary to modify the bispectrum code to allow it to run on the *Koa* processing system.

The project team has also begun preparing for end-to-end testing, and Operational Test & Evaluation (OT&E) passage of the Bispectrum/MIMOSA software in order to have the software validated for use for customer data products. The OT&E process is to include the software at the MHPCC and on the *Koa* SGI system at MSSS, with the same test data for MHPCC MIMOSA and *Koa* to obtain the same results. Training materials will be developed and the team will provide R&D training for the individuals who will be able to train the operators in the use of the software. The final task of the team will be to provide complete updates to all documents as required by AFRL.

Significance: MSSS GEMINI sensor operation using the new bispectrum software will result in enhanced space surveillance functions, overcome post processing challenges presented by MSSC sensors, and will provide the foundation for future imaging algorithmic designs and implementations. Use of MHPCC computing platforms and MIMOSA for data processing will also free up MSSS computational resources to be used for other purposes, such as tracking and data acquisition. This will allow much greater flexibility in MSSS operations and R&D. As an example, MSSS processing of GEMINI data is currently controlled only from the GEMINI control workstation. However, a consequence of this is that use of the workstation for data reduction means that objects of interest could possibly go unobserved. Additionally, using the workstation to control GEMINI's cameras and optics for an observation means that time-critical data cannot be processed. The MIMOSA environment tool set allows for integrated data reduction, data storage, and visualization for the purpose of producing high quality data products for our customers. MIMOSA allows users to do their jobs more efficiently and has no limit to the number of algorithms and system performance enhancements that can be integrated in the future. MIMOSA provides an overall "umbrella" environment in which many other applications can work and provides the basis for anticipated continued and expanding key research and operations activities in support of the Air Force's MSSS mission. The future successful completion of OT&E and the beginning of the operational use of MIMOSA will mark a major joint effort between the MSSS and MHPCC, providing the Air Force MSSS mission full, near real time use of the MHPCC supercomputing assets.

Author and Contact: Bruce Duncan

Authors: Bob Brem and Flo Cid

Organization: Boeing LTS, 535 Lipoa Parkway, Kihei, HI, 96753

Author: Kathy J. Schulze

Organization: KJS Consulting, PO Box 591, Georgetown, DE, 19947

Authors: Paul Billings and William "Chip" DeMeo

Organization: Textron Systems, 535 Lipoa Parkway, Kihei, HI, 96753

Author: Steve Gima

Organization: Maui High Performance Computing Center, 550 Lipoa Parkway, Kihei, HI, 96753

Resources: IBM P3 *Corona* and *Tempest* and SGI Origin 200 *Crux* and *Mango* Servers at MHPCC and SGI Onyx R4400 *Koa* Computer at MSSS

Sponsorship: Air Force Research Laboratory

Joint Medical Asset Repository (JMAR) Implementation at MHPCC

Bruce Duncan, Chelsea Nesbitt, Dean George, Jason Wachi, Mark Radleigh, Steve Gima, Joshua Testerman, Nathan Reish, Shirley Verbisk

JMAR contractor developers installed, integrated, and placed into operation advanced JMAR medical logistics automation system servers, support servers, and other related operating systems and applications software at the Maui High Performance Computing Center (MHPCC) during 2002. This project team was led by JMAR contractors working directly in support of the DoD's Defense Medical Logistics Standard Support (DMLSS) Joint Medical Asset Repository (JMAR) program office with MHPCC staff. The major elements of the JMAR concept of operations include World Wide Web access, multiple data sources, and U.S. Joint military medical mission capabilities.

Background: The Medical Logistics Total Asset Visibility (MEDLOGTAV) Project was established to ensure integration of Quad-Service medical logistics data into Joint Total Asset Visibility (JTAV) via the Joint Medical Asset Repository (JMAR). The Medical Logistics Proponent Subcommittee appointed the U.S. Army Medical Materiel Agency (USAMMA), located at Fort Detrick, Maryland as Executive Agent for the development of the JMAR in January 1997. JMAR is the DoD recognized authoritative source for joint medical logistics

information and is the medical logistics component of JTAV. Users from all levels and all Services are involved in this systems integration effort, working with the project office to identify legacy system key data elements, data mapping, query development, and user-interface testing. Effective October 1, 2001 cognizance for the JMAR project was transferred to the DoD's Defense Medical Logistics Standard Support (DMLSS) Program Office and the Joint Medical Logistics Functional Development Center located at Fort Detrick. JMAR plans call for continued development to be conducted spanning three phases through Fiscal Year (FY) 2003. During JMAR operations, DoD medical systems data is captured, pre-processed, verified, and the data is loaded into the database. The data is then mediated and useful medical information is provided to customers, as and when requested, around the world via the World Wide Web. The JMAR system provides total asset visibility of medical logistics data at the Tactical (unit and retail level), Operational (intermediate), and Strategic (wholesale) levels. This visibility encompasses all points in the medical logistics "pipeline" including assets that are: In-Storage (such as blood, vaccines, unit, retail, war reserve, and wholesale assets); In-Transit (such as medical material, pharmaceuticals, blood shipments, and Global Transportation Network information); In-Process (such as equipment under repair, maintenance trends, and material under contract); and In-Theater (such as pre-positioned stocks, patient movement items, theater medical information, and blood supplies). The third phase in the development of the JMAR is the integration of Reserve Component medical unit data and DMLSS Wholesale Readiness Management Application (RMA). It will also incorporate additional DMLSS products, as they are fielded, such as Equipment and Technology Management and Stockroom/Readiness Inventory Management. The Reserve Component target systems are the same ones identified for the Active Component. The RMA includes Commercial Asset Visibility (CAV), Industrial Preparedness Program (IPP), and Customer Demand Management Information Application (CDMIA).

JMAR Implementation Methodology at MHPCC: The JMAR project team's main objective was to migrate the operation of the JMAR system from Fort Detrick, Maryland and install an updated system at MHPCC. A detailed technical program plan and schedule were developed and implemented by the DMLSS JMAR contractor team. Early in the program process, there was efficient planning between the JMAR contractor team and MHPCC. The goals for the setup at MHPCC were to install, develop, host, and support the new JMAR development and production servers and infrastructure, including the server hardware, operating systems, and associated networks.

The first step in this process was the installation of two Hewlett-Packard (HP) N-Class N4000 computers, each with 8 processors running at 550 MHz, in an HP cabinet in the MHPCC Main Computer Room. DVD and DDS drives and a 16-port brocade switch were also installed in the first cabinet. These computers run the HP/UX operating system and the operating systems in both computers were installed identically. A second HP cabinet was populated with a VA7400 disk array, physical hard drives, an HP Sure Store Tape Library, and an 8-port brocade switch. A third general purpose cabinet was populated with a Windows NT 4.0 server to provide File Transfer Protocol (FTP) functionality and a Windows 2000 server to provide Virtual Private Network (VPN) capability. Each JMAR server is linked with the cluster's VA7400 disk array via a Fiber Channel switch, with two switches provided for redundancy. The root disks were mirrored on the two internal Ultra Wide SCSI interfaces. Alternate fiber paths were provided between all of the equipment. Three disk enclosures that hold 15 disks each were also integrated.



Figure 1. JMAR Computer Installation at MHPCC.

Each enclosure presently has 10 disks, leaving 15 total free slots for hard disks. Domain Name System (DNS) configuration for distributed, replicated, data query service and the MHPCC initial network connectivity and network filters were next established. Users services activities then occurred, including the set up of group and user accounts. Compilers were installed. Secure Shell (SSH) was installed to provide for remote access of the JMAR systems and to enable secure encrypted communications. All four platforms of the system were then hardened. Oracle installation was completed and the JMAR database was installed. The majority of systems testing was completed by early April. Final system testing occurred in mid-April. The JMAR system at MHPCC was fully activated on 15 April and the JMAR computing installation is shown in Figure 1.

JMAR Operations and Principal Applications: MHPCC is now hosting and supporting JMAR project development and production servers and other items, including the server hardware, operating systems, and associated networks. This represents a wide range of infrastructure, environmental, and operational requirements as required to meet the needs of the project. The MHPCC integrated solution is also providing operational support, computer security, system monitoring, and backup and recovery. The JMAR machines located at MHPCC are also using many hardware platforms and software applications to provide the JMAR project with a highly available FTP site, Web servers, and Oracle databases. JMAR system users upload data to the Dell PowerEdge Windows NT FTP server. Data Junction software processes the data into JMAR-readable format and sends it to the primary database server. The DMLSS JMAR project contractor staff at Ft. Detrick, MD and at Kihei, Maui, Hawaii use a Dell Dimension Windows 2000 PC as a VPN server. Another VPN server is located at Ft. Detrick, MD in order to interface with the MHPCC installation using various systems software, industry-standard languages, and Internet standard protocols. Both JMAR servers are running HP/UX. An upgrade of the HP/UX operating system is also anticipated. Oracle is presently running on the two JMAR servers. One JMAR server is used to provide Oracle database and Web server functionality. The other JMAR server is used as a development and testing server. Omniback software performs incremental backups nightly for the JMAR servers and the VPN server. Full backups are performed weekly. MC/Service Guard software provides health monitoring packages and affords automated fail-overs among the JMAR production, Web production, and Omnipkg servers. The software responds according to scripts based on the outcome of the tests. Each package has a primary node and a secondary node. MHPCC provides continuous, automated monitoring of the JMAR server platforms and, to some extent, the JMAR applications. MHPCC also maintains security for the JMAR project and infrastructure from the physical level to network and computer system levels, making extensive use of current automation tools and other methodologies. The JMAR project offices, East and West, are primarily responsible for application level security, but are also supported by MHPCC staff. MHPCC also supplies all needed network-related security patches for network devices and server operating systems to maintain a high level of security for the JMAR network infrastructure at MHPCC. As of this writing, the JMAR Project was planning to modify the server installation at MHPCC by installing two new Windows 2000 data processing servers (FTP) and possibly adding another WWW server.

Significance: Implementation of the JMAR system at MHPCC has resulted in a new, comprehensive, integrated, and robust automated system to support the DoD's Joint Total Asset Visibility program. The MHPCC implementation and operation has further increased JMAR support, operational availability, flexibility, and training capabilities. The system provides important medical logistics information to DoD users located throughout the globe, while reducing costs. Additionally, the JMAR system has the capability of being extended beyond DoD to provide utility for all Federal medical use, Homeland Defense, or other emergencies that might arise. This could provide added Federal visibility in the future for agencies such as the U.S. Public Health Service, Federal Emergency Management Agency, Center for Disease Control, and Veterans Administration.

Author and Contact: Bruce Duncan

Authors: Chelsea Nesbitt, Dean George, Jason Wachi, Mark Radleigh, Steve Gima

Organization: Maui High Performance Computing Center, 550 Lipoa Parkway, Kihei, HI, 96753

Author: Joshua Testerman

Organization: Akimeka LLC, 535 Lipoa Parkway, Kihei, HI, 96753

Author: Nathan Reish

Organization: Veridian-MRJ, 623 Porter Street, Fort Detrick, MD, 21702

Author: Shirley Verbisk

Organization: PEC Solutions, 623 Porter Street, Fort Detrick, MD, 21702

Resources: HP N-Class 4000 JMAR Servers and Windows 2000 and NT Servers provided by DMLSS, hosted at MHPCC.

Sponsorship: DoD Defense Medical Logistics Standard Support (DMLSS) Program Office

Detached-Eddy Simulation of Massively Separated Flows Over Aircraft

James R. Forsythe, Kyle D. Squires, Scott A. Morton, Kenneth E. Wurtzler,
William Z. Strang, Robert F. Tomaro, Philippe R. Spalart

Most of the flow fields encountered in DoD applications occur within and around complex devices and at speeds for which the underlying state of the fluid motion is turbulent. While Computational Fluid Dynamics (CFD) is gaining increased prominence as a useful approach to analyze and ultimately design configurations, efficient and accurate solutions require substantial effort and expertise in several areas. Geometry description and grid generation, numerical solution of the Navier-Stokes equations, and efficient post-processing are all key elements. While advances have taken place in areas such as grid generation and fast algorithms for solution of systems of equations, CFD has remained limited as a reliable tool for prediction of inherently unsteady flows at flight Reynolds numbers. To overcome the deficiencies of current turbulence models for predicting massively separated flows, Dr. Philippe Spalart and co-workers proposed Detached-Eddy Simulation (DES) with the objective of developing a numerically feasible and accurate approach combining the most favorable elements of Reynolds-Averaged Navier Stokes (RANS) models and Large Eddy Simulation (LES). The primary advantage of DES is that it can be applied at high Reynolds numbers, as can Reynolds-averaged techniques, but also resolves geometry-dependent, unsteady, three-dimensional turbulent motions as in LES.

Research Objectives: The current computations support an AFOSR project to predict aircraft spin. To predict aircraft spin, accurate calculation of forces and moments at high angles-of-attack is required. The forebody is chosen as a test case, since it is a large contributor to aircraft moments, due to its long moment arm, and accurate predictions of the flow around the forebody are crucial. The computations are performed using the unstructured-grid solver Cobalt. Cobalt is the commercial version of the CHSSI code, Cobalt₆₀. Grids used in the calculations of all the geometries summarized below are unstructured, comprised of a combination of prisms, pyramids, and tetrahedra.

Methodology: The forebody modeled is the flow at 90° angle-of-attack around a rectangular ogive, with the main cross-section a round-corner-square. Visualization of the pressure distribution on the surface and the instantaneous vorticity at eight stations along the body are shown in Figure 1.

Evident in the surface pressure prediction from the RANS computation is that along the forebody the separated structure is more coherent than that obtained in the DES, with a low pressure footprint evident along most of the forebody. The DES result is characterized by a more chaotic and three-dimensional structure over most of the body, resulting in a reasonably constant pressure region along the top (aft) surface (c.f., Figure 2). Time-averaged pressure distributions were measured in experiments at eight axial stations, corresponding to the eight locations at which vorticity contours are shown in Figure 1. Compared in Figure 2 is the pressure coefficient at 11% of the forebody length. The angle $\theta = 0^\circ$ is in the symmetry plane on the windward side, with $\theta = 180^\circ$ in the leeward side symmetry plane. As shown in the figure, the strong coherent vortices predicted in the RANS solution give rise to a large variation in pressure on the leeward side that differs markedly from the experimental measurements. The largest differences in the RANS predictions occur closest to the tip of the forebody, resulting in large errors in moment predictions.

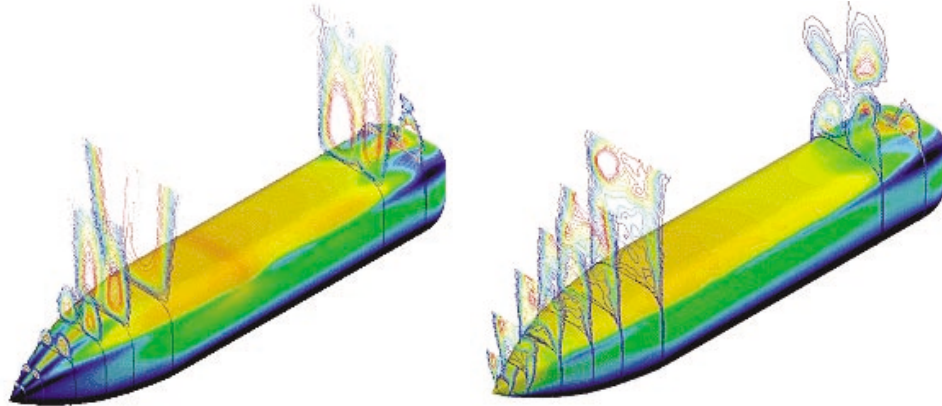


Figure 1. RANS (left) and DES (right) predictions of the flow around the rectangular-ogive forebody. The freestream flow is at 90° angle-of-attack (from top to bottom in the visualizations). Surface colored by pressure and vorticity contours at eight stations. The location of the eight stations is the same at which experimental measurements of the pressure distribution are available.

The DES prediction of the pressure coefficient, on the other hand, is in excellent agreement with the measurements, a result of the more accurate resolution of the unsteady shedding that yields a flat pressure profile on the leeward side.

To support the development of a method to predict spin, computations were performed of the flow over an F-15E aircraft at angle of attack of 65° and zero sideslip. Boeing provided the authors with a stability and control database for the F-15E that was developed from a comprehensive spin flight-test program.

Two stable spin conditions were detailed, including data for symmetric and asymmetric fuel loads. The aircraft with symmetric loading maintains a stable spin at a 65° angle of attack. Prior to computing the actual spin using rigidly moving grids (which is currently underway), the performance of the computational model was investigated at the same fixed angle of attack as for the stable spins. All computations were matched with the flight test conditions of a Mach number of 0.3 and standard day 30,000 feet. This resulted in a chord-based Reynolds number of 13.6×10^6 .

As part of this effort, a comprehensive grid refinement study was performed. Half-aircraft simulations (i.e., assuming symmetry along the reflection plane) were performed using grids consisting of 2.85×10^6 , 5.9×10^6 , and 10.0×10^6 cells. A sample solution comparing the coarse to fine grid is shown in Figure 3. A chaotic and strongly three-dimensional solution is obtained with shear layer rollup observed in the shear layers detaching from the wings. The solutions exhibit substantial unsteadiness in forces and moments, e.g., 10 % variation in the time histories of C_L . The range of mesh resolutions was such that a grid converged solution for both RANS and DES was obtained. DES predictions were within 5% of the stability and control database for lift, drag, and pitching moment. This study showed that the finest mesh (10.0×10^6 cells) was necessary to obtain a grid converged solution for DES. A doubling of this mesh is required for calculating the full aircraft in a prescribed spin, which is currently underway.

Results: The calculations documented here required between one to four wall-clock days on 256 processors of MHPCC's IBM SP3, *Tempest*. Combining the time for grid generation and solution, a DES prediction could be acquired within two weeks, given the performance of the HPC machines. The ability of DES to predict unsteady flow phenomena at high Reynolds numbers opens the possibility to handle more complex multidisciplinary problems that require an unsteady solution such as aerolasticity and aeroacoustics.

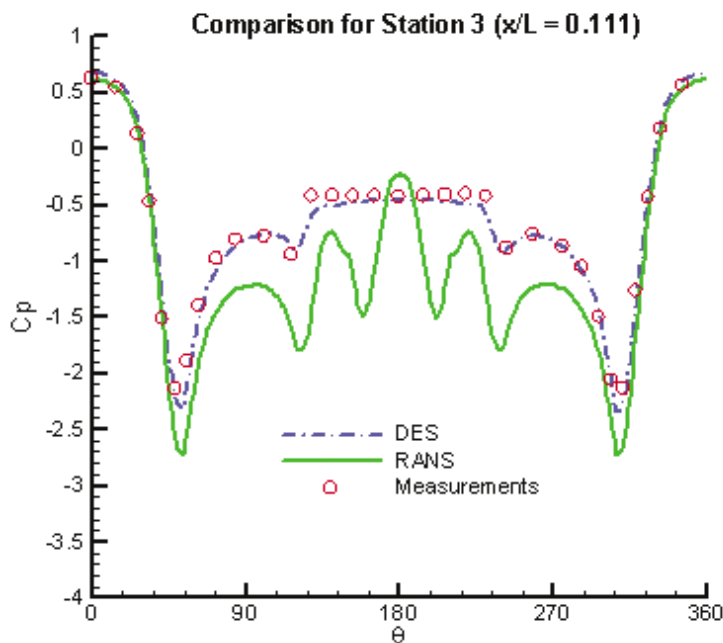


Figure 2. Pressure distribution around the rectangular ogive forebody. Comparison of DES and RANS to experimental measurements at station 3 (c.f., Figure 1).

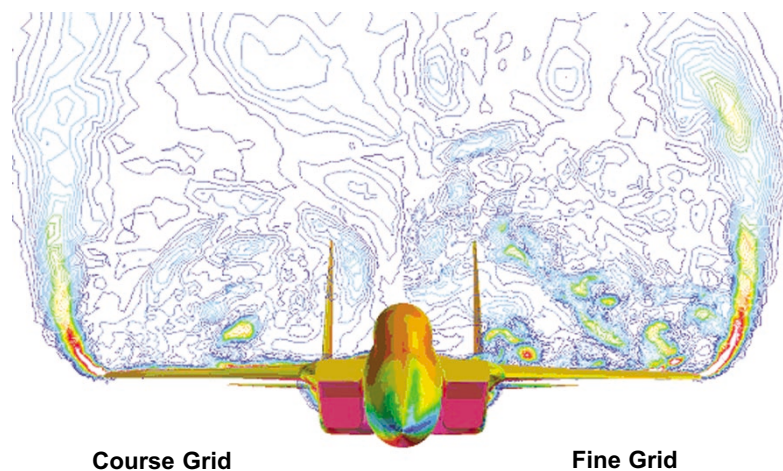


Figure 3. Flow over the F-15E at a 65° angle-of-attack – half aircraft simulation. Surface colored by pressure, and contours of vorticity over the wing – coarse vs. fine grid.

Author and Contact: James R. Forsythe

Author: Scott A. Morton

Organization: United States Air Force Academy, Colorado Springs, CO, 80840

Author: Kyle D. Squires

Organization: Arizona State University, Tempe, AZ, 85287

Authors: Kenneth E. Wurtzler, William Z. Strang, Robert F. Tomaro

Organization: Cobalt Solution, LLC, Dayton, OH, 45459

Author: Philippe R. Spalart

Organization: Boeing Commercial Airlines

Resources: IBM SP3, *Tempest*, at MHPCC

Acknowledgments: This work is partially supported by AFOSR Grant F49620-00-1-0050 (Program Manager: Dr. Tom Beutner) and F49620-02-1-0117 (Program Managers: Dr. Tom Beutner and Dr. John Schmisser). The authors are also grateful for the assistance of Dr. Glen Peters, Dr. Ken Walck, and Dr. Walt Labozzetta of Boeing Military, who provided the stability and control database and the F-15E geometry. Cadet Kory Klismith, Cadet David Hajek, and Mr. Aroon Viswanathan have assisted with grid generation and post-processing.

High Performance Computing and Web Support for Project Albert: Analysis of Entity-Based Simulations of Land Combat

Brent Swartz, Alfred Brandstein, Gary Horne, John Kresho, Ted Meyer, Steve Upton, Mary McDonald, Bob Swanson, Maria Murphy, Ron Vioria, D. J. Fabozzi, Bruce Duncan

The Marine Corps Combat Development Command's (MCCDC) Project Albert involves research to assess the general applicability of the "New Sciences" to combat and operations other than war. While simulations based on these New Sciences (or complexity theory, which models behavior and interaction at the entity level) are considered part of an infant science, they do provide insight into evolving patterns of macroscopic behavior that result from collective interactions of individual agents. Simulations based on entity-level interactions represent a significantly different approach from the traditional attrition estimation techniques based on Lanchester equations, which assert that the loss rate of forces on one side of a battle is proportional to the number of forces on the other side. The MCCDC's Project Albert is an effort to investigate how complexity theory may be applied to combat in a manner to augment and, perhaps in some cases, replace Lanchester modeling in the future.

Research Objectives: Continuing the development of a complex systems analyst's toolbox for exploiting emergent, collective patterns of behavior on the battlefield, MCCDC is using several multiagent-based simulations of notional combat, including Irreducible Semi-Autonomous Adaptive Combat (ISAAC), Socrates and Pythagoras. These models simulate the interaction between two or more variable size forces of agents. The action of each agent is determined by parameters, such as the agent's ability to sense its surroundings and to communicate with other agents. In addition to the common physical parameters measured by the model (such as range of fire and probability of kill), more abstract concepts are also modeled. Such concepts can include an agent's attraction to friendly and

opposing forces and the influence of behaviors based on determinable thresholds, such as the tendency of an agent to follow orders. The magnitude and granularity of these independent variables provide the analyst with great flexibility in simulating various hypotheses. This same flexibility, coupled with the stochastic nature of the simulations, requires a significant computational capability to determine likely outcomes with any statistical significance for each single hypothesis. This requirement becomes even greater for the analyst who wants to study hypotheses over multiple varying independent parameters, a requirement that easily overtaxes the capability of a single personal computer.

Methodology: The Maui High Performance Computing Center (MHPCC) has worked in concert with military analysts from MCCDC, and other supporting contractors, to develop methodologies and tools needed for the large-scale analysis of agent-based distillation models. This development includes the processing and data reduction required for statistical analysis of such simulations, and also the tools for analysts to visualize and comprehend the phenomenology of the simulations. Specifically, in support of MCCDC's data farming methodology, MHPCC has ported the core engine of the ISAAC, Socrates and Pythagoras models to its IBM SP parallel supercomputer, a cluster of Windows workstations, and its new Linux Supercluster. The resultant codes can execute and statistically reduce multiple combat hypotheses. The output of the multiple simulation runs is a set of statistically calculated fitness values that are used as measures of battlefield effectiveness. The Visualization Toolkit provides analysts the ability to assess the combined results of the model outputs, as well as the ability to simultaneously conduct a comparative analysis of multiple playbacks (time/space representations of battlefield agents). Advances in the Visualization Toolkit are described on page 16. The information generated from this exhaustive execution of model simulations, along with the associated mechanisms for visualization, will provide analysts with the tools required to investigate multiple hypotheses with statistical significance.



Figure 1. MCCDC's Project Albert "Chessboard" represents a distillation model. The two men depicted are computer avatars which gather information and identify relationships from the data produced by the other models, as an aid to decision makers. "Chesty" is the Marine in the picture and the other avatar is an amalgamation of potential enemy countries.

Results: This year's activities have continued to refine the current system and have provided more tools to aid the analytical process. MHPCC has developed a Web-based submission system (www.projectalbert.org) that allows analysts to submit large scenario runs over the Web, thereby allowing analysts to easily explore a given scenario in many ways. MHPCC recently added an enumeration capability, which allows the user to data farm over user supplied sub-trees of the input XML file, so that virtually any subsection of the input file can be data farmed. Also, MHPCC has modified the Web system to dynamically display parameters in the input XML file, so that any design modifications to the input file are automatically recognized by the Web system. MHPCC has also added a document retrieval and software download capability to the Web site. The Web site has been modified to allow MOE output data to be converted to various output formats, including database (.mdb), comma-separated value (CSV), and XML format. This allows the MOE output data to be passed into many existing tools.

MHPCC also continued to refine the Parallel Execution System (PES), a set of portable Java programs which allow multiple models (currently ISAAC, Socrates, and the recently added Pythagoras) to be executed in parallel on the many platforms available at MHPCC. These platforms include the IBM SP, the Condor PC cluster, and the Linux Supercluster. The PES is designed to improve the overall portability, performance, and scalability required to produce model output files. It is also designed to more easily integrate future models into the PES. This will allow these models to be run in parallel on the various MHPCC platforms, while simultaneously allowing the Visualization Toolkit to be used on the resulting output. SMP parallelism is achieved by simultaneously executing as many model runs as will fit the number of CPUs available on a computational node. MHPCC has recently modified the PES to allow the number of excursions that can be practically executed to increase by a factor of ten, allowing a hundred million model executions to be performed with a single scenario submission. An XML file is used to completely describe each user-defined scenario. This file is created by user interaction with the Web-based submission system, then passed to the PES for model execution, and finally used in the Visualization Toolkit for the display of the results. The original system allowed only exhaustive combinatorial searches of the parameter space, which could consume very large amounts of computational resources. MHPCC recently modified the Web site and PES to allow different algorithms, including genetic algorithms, to be used in the parameter space search. These alternative algorithms may allow optimal solutions to be found with a significantly reduced computational resource requirement. MHPCC also recently added a metadata database capability to the Web site, so that a user can search previously executed scenarios for scenarios that match their search criteria. The MHPCC Project Albert team is also procuring a new 3U Blade computing cluster that will be dedicated to support the program. Additional Web site and PES enhancements are also planned to provide more functionality and user empowerment.

MCCDC has successfully applied these tools to reinforce intuitive conclusions. Comparison of these results with several historical battles has further validated the various models' applicability. MCCDC has also used Project Albert and the associated products as a springboard for other collaborative research and analysis activities. Such activities include the participation of analysts from a variety of nations at international conferences, where the participants research analytical methods and a new generation of modeling tools.

Significance: This initiative has led to a continuing evolution and refinement of the new generation of analytical models and tools. MHPCC will continue to collaborate with MCCDC to further develop simulation, visualization, and statistical methodologies that may eventually improve MCCDC's ability to evaluate the applicability of these simulations to actual combat doctrine. Current efforts will expand the existing infrastructure to incorporate new technologies.

Author and Contact: Brent Swartz

Authors: Bob Swanson, Maria Murphy, Ron Vilorio, D. J. Fabozzi, Bruce Duncan

Organization: Maui High Performance Computing Center, 550 Lipoa Parkway, Kihei, HI, 96753

Author: Alfred Brandstein

Organization: Marine Corps Combat Development Command (MCCDC)

Authors: Gary Horne, John Kresho, Ted Meyer, Steve Upton

Organization: MITRE Corporation

Author: Mary McDonald

Organization: Scientific Applications International Corporation (SAIC)

URL: www.projectalbert.org

Resources: IBM P3, IBM Linux Supercluster, and Windows clusters at MHPCC

Sponsorship: MCCDC/Marine Corps Warfighting Laboratory (MCWL)

Parallelization Development and Testing of the Operational Multiscale Environment Model With Grid Adaptivity (OMEGA)

Thomas J. Dunn, David P. Bacon, Pius C. S. Lee, Mary S. Hall, A. Sarma

The Operational Multiscale Environment model with Grid Adaptivity (OMEGA) is a new atmospheric modeling system developed at Science Applications International Corporation (SAIC) with support from the Defense Threat Reduction Agency (DTRA). The OMEGA system links the latest methods in computational fluid dynamics and high resolution gridding technologies with numerical weather prediction. A unique feature of the OMEGA model is its unstructured grid. The unstructured grid permits the addition of grid elements at any point in space or time. As a result, OMEGA can increase local resolution to better capture the underlying topography and the important physical features of atmospheric flows. OMEGA has been used to simulate many types of weather-related hazards, including tropical cyclones, heavy precipitation, severe storms, and the atmospheric transport of hazardous aerosols. A parallel version of OMEGA has been developed and is undergoing testing on a number of machines including the *Huinalu* 520-processor IBM Netfinity Linux Supercluster at the Maui High Performance Computing Center (MHPCC).

Research Objective: OMEGA is a fully nonhydrostatic atmospheric simulation system that is discussed at length in Bacon et al. (2000) and Boybeyi et al. (2001). OMEGA is based on an adaptive, unstructured triangular prism grid that is referenced to a rotating Cartesian coordinate system. OMEGA's grid is unstructured in the horizontal dimension and structured in the vertical dimension. The use of an unstructured grid permits a continuously varying horizontal resolution ranging from roughly 100 km down to less than 1 km without the need for nested grids. The vertical resolution ranges from a few tens of meters in the boundary layer to 1 km in the free atmosphere. The benefit of having a structured vertical dimension is a significant reduction in the computational requirements of the model. The grid is naturally scale spanning because it permits the addition of grid elements at any point in space and time. This capability allows the full range of scales to be modeled over the domain without the wave reflecting internal boundaries of traditional nested grid models.

OMEGA uses a finite volume flux-based numerical advection algorithm. It has a detailed physical model for the planetary boundary layer and includes the Mellor-Yamada Level 2.5 turbulence closure model. Both the modified Kuo and Kain-Fritsch cumulus parameterizations are incorporated to account for the effects of subgrid-scale deep cumulus convection. OMEGA uses an extensive bulk water microphysics package to represent the precipitation fields. OMEGA uses an optimum interpolation analysis scheme to create initial and boundary conditions and supports piecewise four dimensional data assimilation using a previous forecast as the first guess for a new analysis.

OMEGA has eight major worldwide databases, including terrain elevation, land/water distribution, soil type, land use/land cover, vegetation index, sea surface temperature, subsurface temperature, and soil moisture. In addition, the OMEGA modeling system includes a highly automated grid generator, an automated meteorological and surface data assimilation system, and a user-friendly X-windows and Motif-based Graphical User Interface and graphics postprocessors.

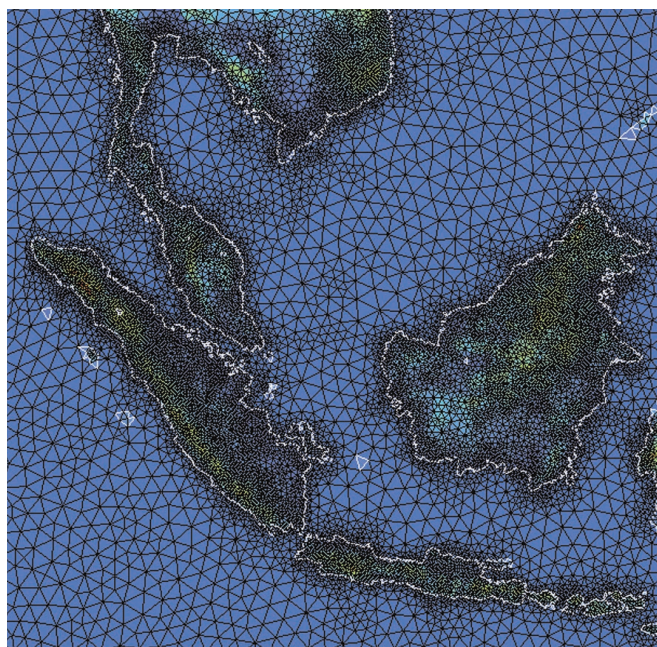


Figure 1. The OMEGA domain, grid structure, and terrain elevation for Southeast Asia.

OMEGA has achieved high (99%) vectorization efficiency. Therefore, further speedups can only be achieved from parallelization or from accelerated solution algorithms. A parallel version of OMEGA which uses the Message Passing Interface (MPI) library has been developed under the goals of portability to both shared and distributed memory machines and efficient scalability to massively parallel machines. An objective of this research is the development and testing of OMEGA's parallelization capabilities in both operational and research applications.

Methodology: OMEGA was applied successfully to the forecasting of tropical cyclones (Gopalakrishnan et al. 2002). An example of this application is presented here in which OMEGA was used to simulate the evolution of a mini tropical cyclone. Typhoon Vamei developed over the South China Sea east-northeast of Singapore by December 27, 2001 and obtained a maximum intensity of 75 knots before making initial landfall in southern Johore, West Malaysia. This storm was unusual in that it formed just 1.5 degrees north of the equator and is the first reported occurrence of a typhoon in this region. The relatively small size of this storm makes it a very difficult weather forecasting and numerical weather prediction problem.

An OMEGA grid was generated for Southeast Asia (Figure 1) using 30 arc second resolution terrain data. The grid was composed of 28,539 computational cells in each of 34 vertical layers. The grid was statically adapted only to terrain gradients and land/water boundaries. The largest and smallest cell areas were 4716 km² and 34 km², respectively. The longest cell edge length was about 140 km and the shortest edge length about 5 km. The initial fields and boundary conditions were derived from Medium Range Forecast (MRF) model 1.0 degree resolution analyses. The simulation was performed on 64 processors (32 nodes) of the MHPCC *Huinalu* cluster. Figure 2 shows the parallel domain decomposition obtained for the 64 processors on *Huinalu*.

Results: Figure 3 shows a zoomed view of the grid. The graphic is composed of the total precipitation on the surface after six hours of simulation overlaid with the surface wind field at six hours. Although the model produced high winds and locally heavy rainfall along the east coast of West Malaysia, the relatively coarse grid resolution over the initial vortex aided in the early dissipation of the storm.

The evolution of a tropical cyclone is an important forecast problem. Yet, to date, there is no operational model that can forecast both the track and intensity of a tropical cyclone reasonably well. Given accurate initial conditions, dynamical predictions of tropical cyclones can only be improved by correctly simulating the interactions between the fine-scale structure of the storm and the large-scale environment. However, to adequately resolve the fine-scale structure, model resolution on the order of 10 to 20 km or less is required.

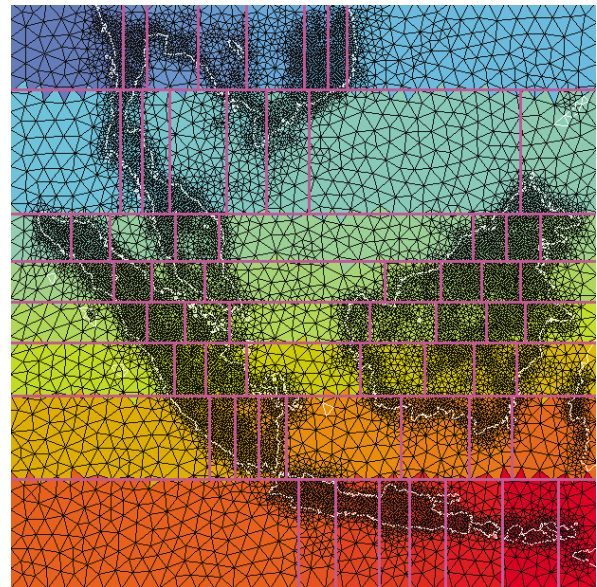


Figure 2. The OMEGA grid plus parallel domain decomposition of 64 subdomains of roughly equal numbers of computational cells.

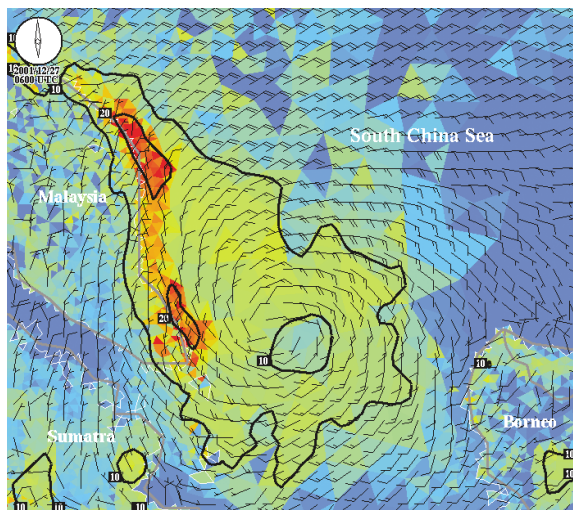


Figure 3. Total precipitation (mm) on the surface at six hours after the start of the simulation overlaid with the surface wind field at six hours. The precipitation contour interval is 10 mm. The surface wind field has been interpolated onto a regular grid overlay. The storm center is located over the South China Sea between Malaysia, Sumatra, and Borneo.

Significance: Two types of grid adaptation options for specifying the required model resolution are available in OMEGA. The static adaptation option used here creates a numerical grid by resolving static features with a resolution that varies smoothly from the maximum to the minimum specified. Dynamic adaptation adds the periodic readaptation of the grid to regions that require high resolution during the course of a simulation. Both adaptation options benefit from parallelization. Thus, future work will include further development and testing of increased parallelization in order to increase the number of processors that can be utilized, thereby increasing the resolution possible in both operational and research situations.

References:

- 1) D. P. Bacon, N. N. Ahmad, Z. Boybeyi, T. J. Dunn, M. S. Hall, P. C. S. Lee, R. A. Sarma, M. D. Turner, K. T. Waight III, S. H. Young, J. Zack, 2000: The Operational Multiscale Environment Model with Grid Adaptivity (OMEGA), *Mon. Wea. Rev.*, 128, 2044-2076.
- 2) Z. Boybeyi, N. N. Ahmad, D. P. Bacon, T. J. Dunn, M. S. Hall, P. C. S. Lee, R. A. Sarma, T. R. Wait, 2001: Evaluation of the Operational Multiscale Environment Model with Grid Adaptivity Against the European Tracer Experiment, *J. Appl. Meteor.*, 40, 1541-1558.
- 3) S. G. Gopalakrishnan, D. P. Bacon, N. N. Ahmad, Z. Boybeyi, T. J. Dunn, M. S. Hall, Y. Jin, P. C. S. Lee, D. E. Mays, R. V. Madala, A. Sarma, M. D. Turner, T. R. Wait, 2002: An Operational Multiscale Hurricane Forecasting System, *Mon. Wea. Rev.*, 130, 1830-1847.

Author and Contact: Thomas J. Dunn

Organization: SAIC, Center for Atmospheric Physics, 1565 9th Ave., San Francisco, CA, 94122

Authors: David P. Bacon, Pius C. S. Lee, Mary S. Hall, A. Sarma

Organization: SAIC, Center for Atmospheric Physics, 1710 Goodridge Dr., MS 2-3-1, McLean, VA, 22102

URL: <http://vortex.atgteam.com>

Resources: Linux Supercluster, *Huinalu*, at MHPCC

Acknowledgements: This project was sponsored by DTRA under contract DTRA01-99-C0007. Computational support was provided by MHPCC.

Visualization Support for Project Albert

Brent Swartz, Alfred Brandstein, Gary Horne, John Kresho, Ted Meyer, Steve Upton, Mary McDonald, Bob Swanson, Maria Murphy, Ron Vloria, D. J. Fabozzi, Bruce Duncan

This paper describes the Maui High Performance Computing Center's (MHPCC) visualization tool development support provided to Project Albert, which is described on page 12. The Marine Corps Combat Development Command's (MCCDC) Project Albert produces large amounts of multi-dimensional output, which must be visualized to comprehend the results of the model executions.

Research Objectives: Continuing the development of a complex systems analyst's toolbox for exploiting emergent, collective patterns of behavior in combat and operations other than war, MCCDC is using visualization tools developed by MHPCC to analyze the results of multiple model executions. A single scenario submission can contain potentially hundreds of millions of model runs. The output from these model runs can have a large number of dimensions, and analysts require visualization tools to statistically reduce, explore, and understand the output results of a given scenario.

Methodology: MHPCC has worked in concert with military analysts from MCCDC, and other supporting contractors, to develop methodologies and tools needed for the large-scale analysis of agent-based distillation models. This development includes the processing and data reduction required for statistical analysis of such simulations, as well as tools for analysts to visualize and comprehend the phenomenology of the simulations. Specifically, MHPCC has developed a Visualization Toolkit containing a landscape tool and playback tools to allow analysts to understand the output results of multiple model executions. The resultant codes can statistically reduce multiple combat hypotheses. One output of the multiple simulation runs is a set of statistically calculated fitness values that are used as measures of combat effectiveness. Another user selectable output is a playback file generated for each model execution. A playback is a spatial temporal representation of battlefield agents, depicting agent movement on the battlefield. The generalized Visualization Toolkit provides analysts the ability to assess the combined results of the model outputs, as well as the ability to simultaneously conduct a comparative analysis of multiple playbacks. The information generated from this exhaustive execution of model simulations, along with the associated mechanisms for visualization, will provide analysts with the tools required to investigate multiple hypotheses with statistical significance.

MHPCC has also been working on a subtask known as "Pocket Albert." This is a small hand-held unit (such as a PDA) in the field that can access the Internet via a wireless network connected to a satellite uplink. This could allow scenario submissions to occur from the field via the Project Albert Web site. The scenarios could then be executed on MHPCC high performance computing resources, and the results of that scenario execution could be made available via the Web site. MHPCC has demonstrated most of this functionality by installing a wireless network at MHPCC, and submitting scenarios from PDAs connected via this network. Next-generation visualization tools that MHPCC is currently designing will be accessible from the Internet, allowing the results to be viewed remotely.

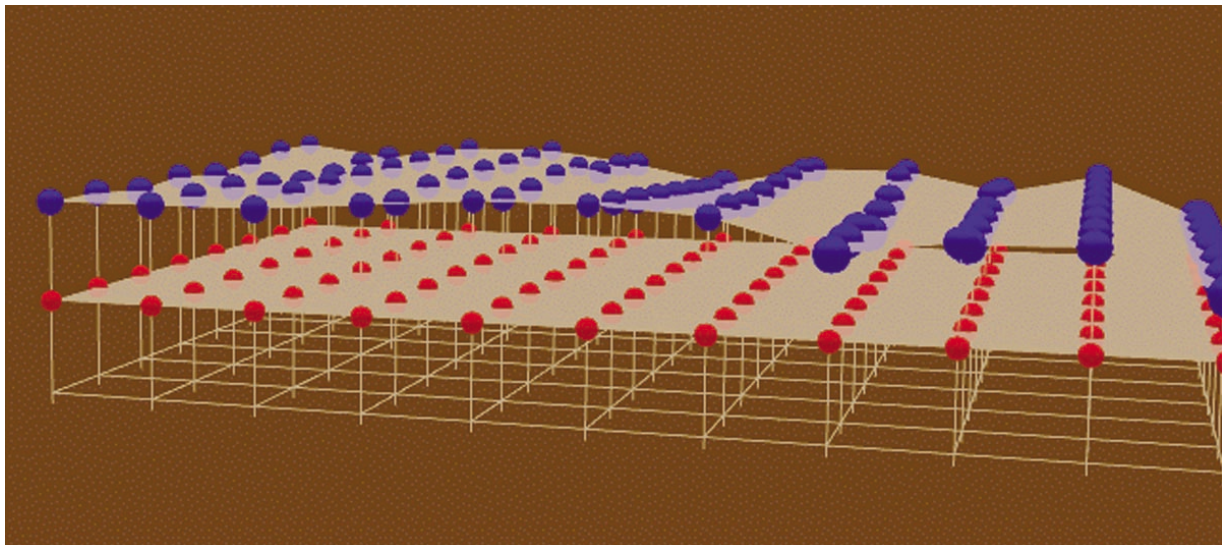


Figure 1. Mockup of Project Albert's next-generation Landscape Tool.

Results: This year's activities have continued to refine the current system and have provided more tools to aid in the analytical process. MCCDC has successfully applied the current visualization tools to reinforce intuitive conclusions. MCCDC has also used the Albert project and associated products as a springboard for other collaborative activities. Such activities include the participation of analysts from a variety of nations at international conferences, where the participants research analytical methods and a new generation of modeling tools. Feedback received from analysts at these conferences on the current Visualization Toolkit will be used during the design and development of the next-generation Visualization Toolkit.

Significance: This initiative has led to a continuing evolution and refinement of the new generation of analytical models and tools. MHPCC will continue to collaborate with MCCDC to further develop simulation, visualization, and statistical methodologies that may eventually improve MCCDC's ability to evaluate the applicability of these simulations to actual combat doctrine. Current efforts will expand the existing infrastructure to incorporate new technologies, including an end to end solution combining vendor independent next-generation versions of several visualization tools that have been developed at MHPCC as part of Project Albert. These tools provide MCCDC analysts with a variety of ways to explore the output of multiple simulations. MHPCC has been exploring the use of the VisAD, which is a framework for visualization tools based on Java3D, as the core software used in the next-generation tools. This would allow the tools to be used on a local workstation or accessed via the Internet.

Figure 1 shows a mockup of the next-generation generalized landscape tool, displaying two MOEs, represented by the red and blue spheres. The X- and Y- axes are two of the input variables chosen by the user. This tool is being designed to efficiently utilize simulation MOE output data files stored in Hierarchical Data Format (HDF), which MHPCC has been designing with other Project Albert team members. By stacking the two outputs, conclusions or questions regarding relationships between the MOEs relative to input parameters and their values can be developed. The tool will allow users to alter the viewpoint to see the data from any direction. Another new capability will be the ability to select an excursion/MOE combination by clicking on a given sphere. This will then bring up a distribution plot of the raw MOE values for the replicates (model runs with differing random seeds) associated with that excursion. The user will then have the ability to select replicates from this distribution and then have the selected replicates placed into a playback tool for analysis. The analyst could then detect patterns of interest in the agent's behavior that appear to reinforce (or reduce) the outcome of the scenario (the MOE).

Author and Contact: Brent Swartz

Authors: Bob Swanson, Maria Murphy, Ron Vilorio, D. J. Fabozzi, Bruce Duncan

Organization: Maui High Performance Computing Center, 550 Lipoa Parkway, Kihei, HI, 96753

Author: Alfred Brandstein

Organization: Marine Corps Combat Development Command (MCCDC)

Authors: Gary Horne, John Kresho, Ted Meyer, Steve Upton

Organization: MITRE Corporation

Author: Mary McDonald

Organization: SAIC

URL: www.projectalbert.org

Resources: IBM P3, IBM Linux Supercluster, and Windows clusters at MHPCC

Sponsorship: MCCDC/Marine Corps Warfighting Laboratory (MCWL)

Simulations of Multi-Color, Inverse-Tapered Free-Electron Lasers

Eric Szarmes and Frank Price

Our research using MHPCC's high performance computing resources has focused on the Free-Electron Laser (FEL). FEL technology is largely untapped, especially in the area of remote sensing. We are hoping that our research with the supercomputer simulations will lead to extreme reductions in the operational requirements of FEL systems, with enhanced operational capabilities.

Research Objectives: The Free-Electron Laser is capable of laser light production at high power with continuous tuning ranges unparalleled by any other device. The potential for FEL technology development is largely untapped, especially in remote sensing. There are some extremely sensitive spectroscopic techniques which are very difficult without a bright, tunable, and coherent multi-color

laser. Conventional FEL technology for multi-color generation is very costly. It is our purpose to explore more economical alternatives to the traditional FEL system through systematic simulation of FEL devices in various configurations. The computing power provided by MHPCC has greatly enhanced our simulation capabilities.

Results: Our most important result to date is the successful simulation of two FELs lasing from the same electron beam, but at different optical wavelengths. This is very exciting as it can lead to extreme reductions in the operational requirements of multi-color FEL systems. Further investigations seek to enhance both the efficiency and capability of this extremely powerful device.

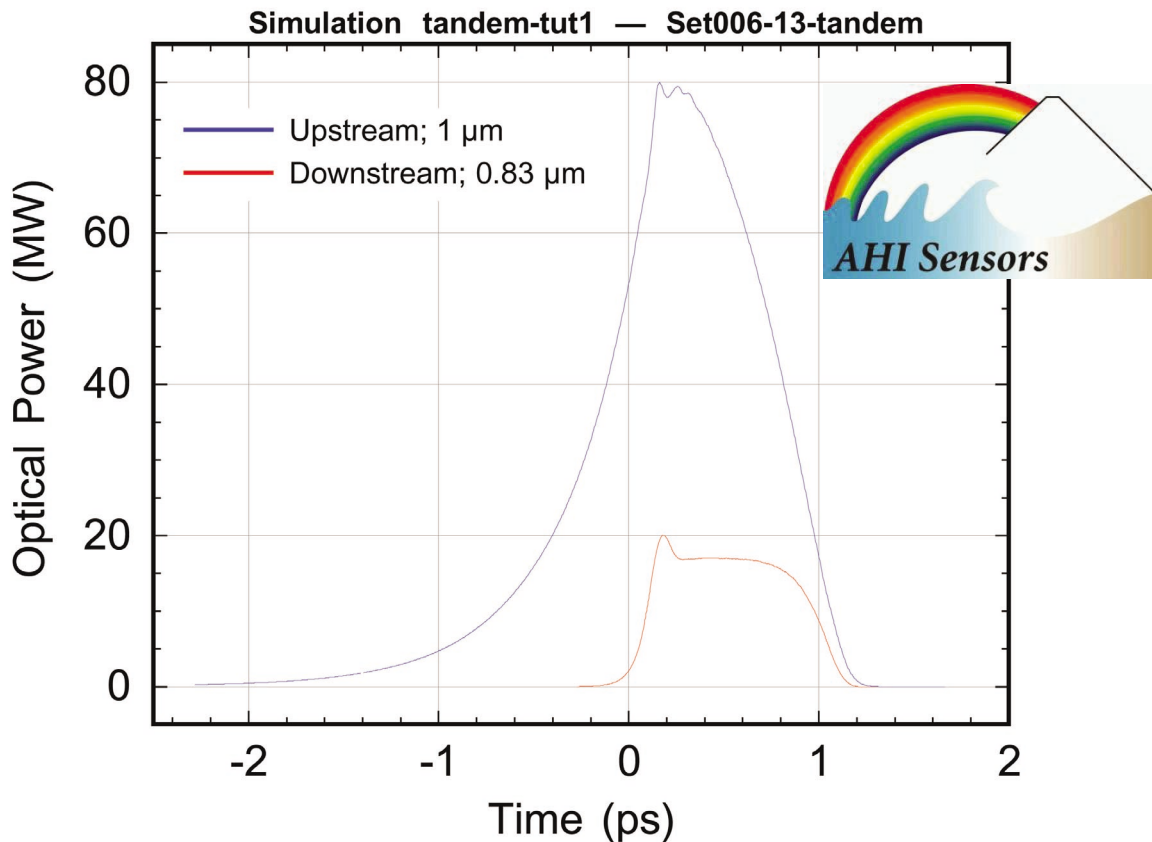


Figure 1. Optical pulses produced at 1 micron and 830 nm by same electron beam.

Author and Contact: Eric Szarmes

Author: Frank Price

Organization: University of Hawaii, Department of Physics and Astronomy, 2505 Correa Rd., Honolulu, HI, 96822

Resources: IBM SP3 at MHPCC and High Energy Physics Alpha Workstations at the University of Hawaii, Department of Physics

Sponsorship: Nuclear Treaty Programs Office; U.S. Army Space and Missile Defense Command

The Modeling Of Bubbly Flows Around Ship Hulls

F. J. Moraga, D. A. Drew, R. T. Lahey, Jr.

As a naval surface ship moves in the ocean, it entrains air bubbles into the water flow. Many of these small bubbles form a bubbly wake that extends for several ship lengths. Because of its strong acoustic signature, this bubbly wake makes all naval surface ships easily detectable by enemy sonar. Today, naval engineers neglect the bubbly wake during the ship design process. This is due to the enormous complexity of the phenomena involved in bubble formation and transport along the ship.

Methodology: To change this state of matters, Francisco J. Moraga, Donald A. Drew, and Richard T. Lahey, Jr. are developing, under the sponsorship of the Office of Naval Research, a state-of-the-art multiphase computer code, CFDSHIPM, that calculates bubbly flow around the hull of a naval surface ship. The code is intended to become a design tool for naval surface ships. Figure 1 shows the bubble distribution close to the hull for a fixed monodisperse bubble source located in front of the ship. This result was obtained using *Huinalu* at the Maui High Performance Computing Center (MHPCC).

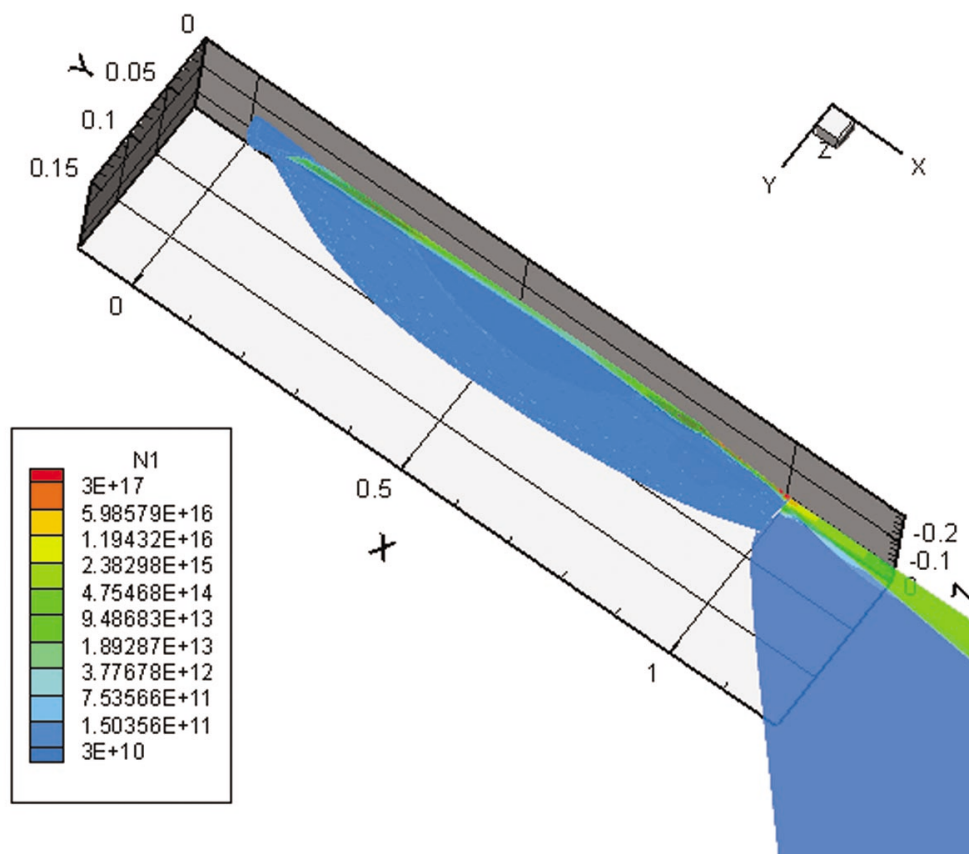


Figure 1. Fish view of the bubble number density approximately a bubble radius from the hull and at the free surface of the wake for naval combatant DTMB5415 at Reynolds number, $Re=10^8$ and zero Froude number. The bubble diameter is 80 microns.

Author and Contact: F. J. Moraga

Authors: D. A. Drew and R. T. Lahey, Jr.

Organization: Center for Multiphase Research, Rensselaer Polytechnic Institute, Troy, NY, 12180-3590

Resources: Linux Supercluster, *Huinalu*, at MHPCC

Sponsorship: Office of Naval Research (ONR)

Acknowledgement: We thank the Iowa Institute for Hydraulic Research for providing us with their code, CFDSHIP-Iowa, to calculate the liquid flow around the ship.

MatlabMPI Improves Matlab Performance By 300x

Jeremy Kepner

The true costs of high performance computing are currently dominated by software. Addressing these costs requires shifting to high productivity languages such as Matlab. MatlabMPI is a Matlab implementation of the Message Passing Interface (MPI) standard and allows any Matlab program to exploit multiple processors. The performance has been tested on both shared and distributed memory parallel computers (Sun, SGI, HP, IBM, and Linux). A test image filtering application using MatlabMPI achieved a speedup of ~300 using 304 CPUs and ~15% of the theoretical peak (450 Gigaflops) on an IBM SP at the Maui High Performance Computing Center. In addition, this entire parallel benchmark application was implemented in 70 software-lines-of-code (SLOC) yielding 0.85 Gigaflops/SLOC or 4.4 CPUs/SLOC. The MatlabMPI software will be available for downloading.

Research Objectives: Matlab¹ is the dominant programming language for implementing numerical computations and is widely used for algorithm development, simulation, data reduction, testing, and system evaluation. The popularity of Matlab is driven by the high productivity that is achieved by users because one line of Matlab code can typically replace ten lines of C or Fortran code. Many Matlab programs can benefit from faster execution on a parallel computer and there have been many previous attempts to provide an efficient mechanism for running Matlab programs on parallel computers (see Reference 4 for a complete list of these efforts).

The Message Passing Interface² is the de facto standard for implementing programs on multiple processors. MatlabMPI⁵ consists of a set of Matlab scripts that implements a subset of MPI and allows any Matlab program to be run on a parallel computer. The key innovation of MatlabMPI is that it implements the widely used MPI "look and feel" on top of standard Matlab file I/O, resulting in a "pure" Matlab implementation that is exceedingly small (~250 lines of code). Thus, MatlabMPI will run on any combination of computers that Matlab supports.

Results: MatlabMPI has been run on Sun, HP, IBM, SGI, and Linux platforms. These results indicate that for large messages (~1 MByte), MatlabMPI is able to match the performance of MPI⁵ written in C. In addition, MatlabMPI performance scales well to multiple processors (see Figure 1). To further test the scalability of MatlabMPI, a simple image filtering application was used based on the key computations used in many DoD sensor processing applications (e.g., wide area Synthetic Aperture Radar). The image processing application was implemented with a constant load per processor (1024 x 1024 image per processor) on a large shared/distributed memory system (the IBM SP at the Maui High Performance Computing Center). In this test, the application achieved a speedup of ~300 on 304 CPUs, as well as achieving ~15% of the theoretical peak (450 Gigaflops) of the system (see Figure 2).

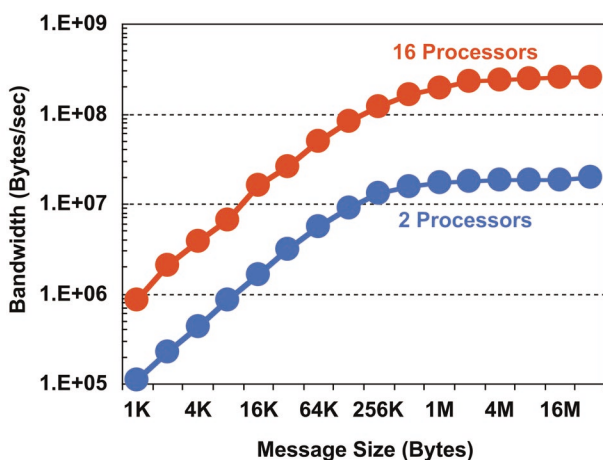


Figure 1. Bandwidth on a Linux Cluster. Send/receive benchmark run on an eight node (16 cpu) Linux cluster connected with Gigabit ethernet.

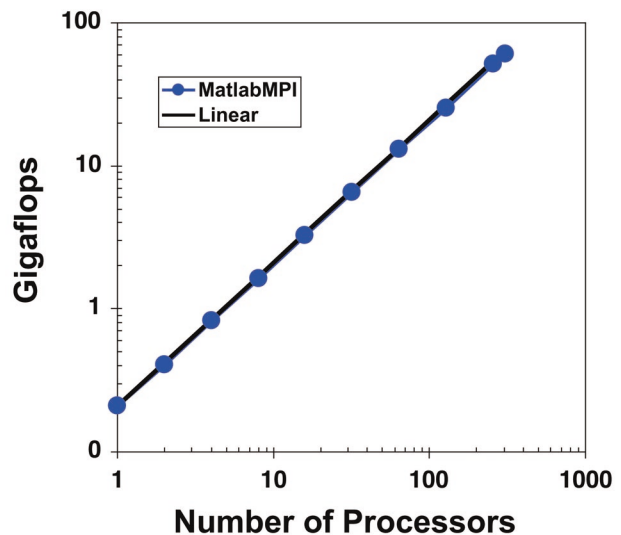


Figure 2. Shared/Distributed Parallel Speedup. Measured performance on the IBM SP of a parallel image filtering application.

Note: This work is sponsored by the High Performance Computing Modernization Office, under Air Force Contract F19628-00-C-0002. Opinions, interpretations, conclusions, and recommendations are those of the author and are not necessarily endorsed by the Department of Defense.

The ultimate goal of running Matlab on parallel computers is to increase programmer productivity and decrease the large software cost of using HPC systems. Figure 3 plots the software cost (measured in Software Lines of Code or SLOCs) as a function of the maximum achieved performance (measured in units of single processor peak) for the same image filtering application implemented using several different libraries and languages (VSIPL, MPI, OpenMP; using C++, C, and Matlab⁶). These data show that higher level languages require fewer lines to implement the same level of functionality. Obtaining increased peak performance (i.e., exploiting more parallelism) requires more lines of code. MatlabMPI is unique in that it achieves a high-peak performance using a small number of lines of code.

Two useful metrics we have developed for measuring software productivity on high performance parallel systems are Gigaflops/SLOC and CPUs/SLOC. The test application does extremely well in both of these measures, achieving 0.85 Gigaflops/SLOC and 4.4 CPUs/SLOC.

Conclusions: MatlabMPI provides the highest productivity parallel computing environment available. However, because it is a point-to-point messaging library, a significant amount of code must be added to any application in order to do basic parallel operations. In the test application presented here, the number of lines of Matlab code increased from 35 to 70. While a 70-line parallel program is extremely small, it represents a significant increase over the single processor case.

Future Work: Our future work will aim at creating higher-level objects (e.g., distributed matrices) that will eliminate this parallel coding overhead. The resulting "Parallel Matlab Toolbox" will be built on top of the MatlabMPI communication layer, and will allow a user to achieve good parallel performance without increasing the number of lines of code.

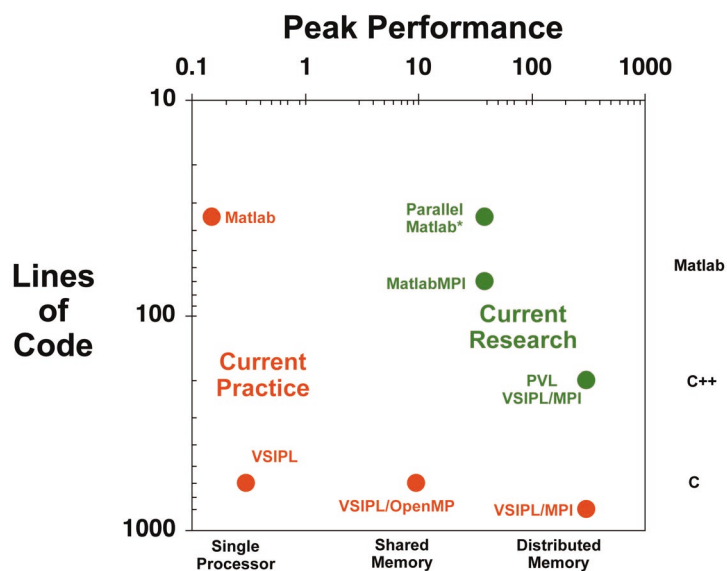


Figure 3. Productivity vs Performance. Lines of code as a function of maximum achieved performance (measured in units of single processor theoretical peak) for different implementations of the same image filtering application.

References:

- 1) Matlab, The MathWorks, Inc., <http://www.mathworks.com/products/matlab/>.
- 2) Message Passing Interface (MPI), <http://www.mpi-forum.org/>.
- 3) MATLAB*P, A. Edelman, MIT, <http://www-math.mit.edu/~edelman/>.
- 4) Parallel Matlab Survey, R. Choy, MIT, <http://supertech.lcs.mit.edu/~cly/survey.html>.
- 5) J. Kepner, Parallel Programming with MatlabMPI, 2002, High Performance Embedded Computing (HPEC) Workshop, MIT Lincoln Laboratory, Lexington, MA <http://arXiv.org/abs/astro-ph/0107406>.
- 6) J. Kepner, A Multi-Threaded Fast Convolver for Dynamically Parallel Image Filtering, 2002, accepted *Journal of Parallel and Distributed Computing*.

Author and Contact: Jeremy Kepner
 Organization: MIT Lincoln Laboratory, Lexington, MA, 02420
 Resources: IBM SP at MHPCC
 Sponsorship: DoD High Performance Computing Modernization Program (HPCMP)

A Study of Airfoil Spin Characteristics Using Computational Fluid Dynamics

Cadet First Class Jon Wentzel and Jim Forsythe

The United States Air Force Academy's (USAFA) Department of Aeronautics sponsored Cadet First Class Jon Wentzel's 2002 Summer research in the area of Computational Fluid Dynamics (CFD) at the Maui High Performance Computing Center (MHPCC). This research was in support of the DoD's High Performance Computing Modernization Program's (HPCMP) Challenge Project C-65, and it involved modeling of the flow around a spinning airfoil. The goal of the research was to validate Detached Eddy Simulation (DES) CFD codes with rotating grids. Once validated, these codes will be used to model flow over full aircraft in spin situations. The Gottingen 387FB airfoil was chosen to validate these codes due to the large amount of experimental data available. Cadet Wentzel will continue his research utilizing MHPCC resources remotely from the U.S. Air Force Academy.

Research Objectives: In order to validate new Computational Fluid Dynamics (CFD) methods, their results must be tested against experimental data. Detached-Eddy Simulation (DES), a new method of modeling turbulence designed by Dr. Philippe Spalart (Boeing Commercial Airplanes) and co-workers, has been subjected to a large number of validation cases over the last few years, as part of Challenge Project C-65. DES was designed for the simulation of massive separation on full aircraft, a flight regime that has been out of reach of current CFD methods. The Challenge project supports an Air Force Office of Scientific Research (AFOSR) grant to develop a method to predict spin of full aircraft. The current effort supports this project by predicting the autorotation characteristics of a rectangular wing using DES. This effort uses NACA Paper 273 to obtain data on the spin characteristics of the Gottingen 387FB airfoil. A parallel effort is being made using the same methods to predict the spin characteristics of the F-15E Strike Eagle.

Methodology: NACA Paper 273 uses the drag polar graph and strip theory to predict the spin characteristics of wings. Thus, if the codes can match the drag polar of the experiment, the CFD will also match the spin characteristics. Since the drag polar consists of the lift and drag coefficients at different angles of attack, simulations will be run for both the Reynolds-Averaged Navier Stokes methods (RANS) and the DES at angles of attack ranging from -3 to 45 degrees. The results will then be graphed next to the experimental data. Extensive flow visualization will augment the numerical results.

Results: Results were achieved for the full drag polar for the RANS method. DES results are ongoing, however a partial DES result at 45 degrees angle of attack is included in this report.

Figure 1 illustrates the power of DES to resolve the time dependent turbulent structures. A surface of constant vorticity shows the three-dimensional turbulence on the DES side and the somewhat two-dimensional RANS result. Illustrations such as this make it easily apparent that RANS are generally incapable of resolving unsteady turbulent flows. Also of important note is that the DES simulation was able to resolve the wingtip vortices, whereas the RANS model quickly damped the vortex.

Future Research: The next step in this project is to complete the DES simulations of the Gottingen Wing. With a full comparison of the separated flow on hand, the project can move away from static CFD. By prescribing rotational motion about the velocity vector, the resultant rolling and yawing moments will indicate the dynamic response of this airfoil when in a spin situation. With successful completion of the prescribed motion stage, 1 degree of freedom (DOF) will be allowed into the code such that the airfoil can rotate at will about the velocity vector. Once validation of the 1 DOF case is complete, DES will be ready to be trusted to produce simulations of full aircraft in spins.

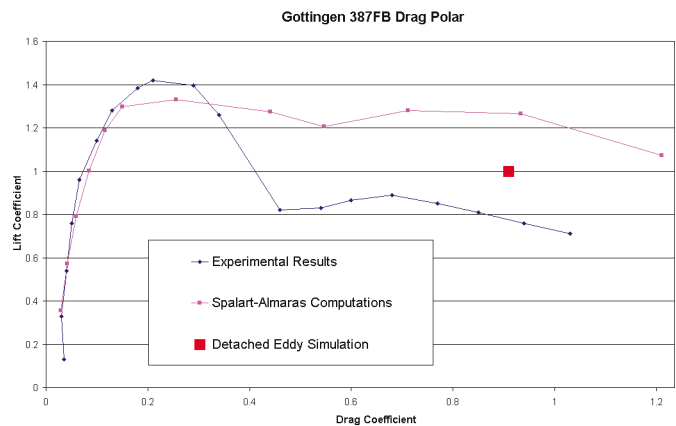


Figure 1. Graph illustrates the power of DES to resolve the time dependent turbulent structures.

Author and Contact: Cadet First Class Jon Wentzel

Author: Jim Forsythe

Organization: USAFA, Aeronautics Department, 2354 Fairchild Drive, Suite 6H27, USAF Academy, CO, 80840

Resources: IBM SP3 Tempest System and SGI Onyx3400 hardware at MHPCC. Cobalt, Gridgen, and Fieldview software at MHPCC.

Acknowledgement: Marie Greene (MHPCC) and Capt. Brian Beveridge (AFRL/DET 15) assisted with the research done by Cadet Wentzel.

Sponsorship: DoD High Performance Computing Modernization Program (HPCMP) Challenge Project

Ultra-High Bandwidth Control of Active Optics Using Chemo-Optical Computation

Joe Ritter

Proposed is the study of a bold new concept merging Ritter's optically addressable Active Optics (AO) with non-linear phase conjugation techniques in a closed loop in pursuit of an ultra-high bandwidth adaptive optic correction system controlled by a hybrid "chemo-optic" computer. This novel device will utilize nonlinear chemically generated conjugate laser beams for computation to control laser activated actuated optic deformable mirrors. Such a system would have capabilities far beyond the current state-of-the-art, yet would not require a digital computer for wavefront reconstructor determination and actuator control. The proposed effort has revolutionary implications for research in astronomy, for surveillance, and for high energy laser (HEL) beam propagation.

Research Objective: The objective is to develop a novel ultra-high bandwidth computation and control method for adaptive optical and other systems. The proposed technology is a light based physical computer closed loop correction of secondary optics which in turn control wavefront phasing, i.e., an optically addressed and controlled adaptive optics system with a physical as opposed to computer processor. This amazing possibility would have enormous bandwidth.

Methodology: The proposed hybrid computation control system would use light matter interaction of beams and molecules for computations and generation of conjugate laser beams used to control laser actuated optically addressable Adaptive Optic deformable mirrors. Wavefront

reconstructor determination and actuator control would all be performed by a nonlinear optical system. Such a system would eliminate digital computers in the control loop. This would eliminate the computational scaling problem associated with Large Apertures (e.g., proposed 30m telescopes) while simultaneously increasing correction bandwidth by at least an order of magnitude. This would enable systems far beyond current state-of-the-art. One benchmark for control authority is the amplitude of the wavefront phase changes. This is determined by the stroke of the actuators of the deformable mirror, and is usually a maximum of a few microns. A nonlinear phase conjugator would be preferable to conventional adaptive optics. Four-wave mixing (FWM) can produce an "effective stroke" on the order of millimeters. The temporal bandwidth of a phase conjugator is bottlenecked by the response of its slowest component. In conventional adaptive optics, travel of an actuator typically takes 1 millisecond (1000 Hz rep rate). The real bottleneck is usually in the reconstructor calculations.

FWM and other non-linear optical-phase-conjugation techniques (e.g., stimulated Brillouin scattering) are non-mechanical, light/matter-interaction-based systems with the demonstrated ability to correct for large jitter and figure errors which contribute to beam aberrations and affect propagation in laser systems. Because FWM relies on the motion of individual atoms or molecules, it has over 100 times the control authority of conventional adaptive optics systems.

A pumped FWM or similar system would be adapted to generate a conjugate laser beam which would then rapidly control deformation of a chromophore enhanced optic. In this way, reconstructor matrix calculations and complex calculations required for AO deformable mirror systems would be accomplished by a high speed hybrid chemical-optical computer, resulting in an ultra-high bandwidth closed loop adaptive optic system which does not require a digital computer

This would virtually eliminate the non-trivial computational complexity scaling issues associated with inversion of reconstructor/control matrices which proposed large aperture optics require. This would represent not only a great leap in adaptive optics performance, but also enable other areas such as optical computing, HEL beam propagation, ultra-high resolution surveillance, and the correction of ultra-large ultra-light deployable diffraction limited membrane space optics. A prototype photoactive mirror was developed by Joe Ritter in 2000.

Summary: The study will pave the way for a leap in novel lightweight active optics capabilities, revolutionizing wavefront control (increasing Strehl ratios in adaptive optics systems), enabling multiconjugate adaptive optics, enabling future optical computing techniques, and controlling enormous lightweight diffraction limited apertures for spacecraft.

References

- 1) J. Ritter, J. Newhouse, J. Brozik, D. Evans, Novel Ultra-Lightweight Space Telescopes Using Optically Active Polymer Membrane Mirror Shape Control, *MHPCC/AFRL Application Briefs 2001*.
- 2) J. Newhouse, D. Evans, J. Ritter, *Ab Initio* Calculations Characterizing an Effective Hamiltonian for Polymeric Photonic "Muscles", *MHPCC/AFRL Application Briefs 2001*.
- 3) Joe Ritter et al, NRA 00-055-06, Gossamer Spacecraft Exploratory Research and Technology Optically Active Polymer Membrane Mirror Shape Control Using Lasers, Dec. 2000.
- 4) Brozik, Evans, Hampton, Keller, Lopez, Nanoscale Photonic Muscles: Fundamentals and New Technologies, Proposal to (Department of Defense) Defense University Research Initiative on NanoTechnology (DURINT), FY2001.

Author and Contact: Joe Ritter

Organization: SAIC, Technology Research Group, 590 Lipoa Parkway, Building B, Kihei, HI, 96753

Resources: IBM SP3 and SGI dual R12000 at MHPCC

Acknowledgements: The author is grateful for the support from the Air Force Office of Scientific Research and the Air Force Directed Energy Detachment 15.

Non-Linear Imaging Algorithm Study

Kathy Schulze, Paul Billings, Chuck Matson, Bobby Hunt, Bob Dant

The primary mission of the Air Force Research Laboratory (AFRL) operating location on Maui, Hawaii is to conduct telescope operations at the Maui Space Surveillance Complex (MSSC) at the top of Haleakala. Images of earth-orbiting satellites acquired by ground-based telescopes are blurred by the earth's atmosphere, making the raw data generally unusable for intelligence gathering. A linear technique known as bispectrum has been in use for many years to mitigate the atmospheric turbulence in the raw data. Figure 1 shows a simulated raw data frame and a recovered image. The performance of the bispectrum technique is related to the careful collection of star calibration measurements that are not always available. Non-linear algorithms, such as blind deconvolution, do not require the additional star calibration measurements. We would like to know how these nonlinear algorithms function relative to the linear technique (bispectrum), in order to increase the resolution of the recovered imagery and decrease the noise without requiring the additional star calibration data. We further wish to develop an understanding of why non-linear algorithms sometime struggle to reconstruct fine details in images, change the overall morphology of the object, and produce correlated noise features that can appear to be object structure instead of noise. A supercomputer at the Maui High Performance Computing Center (MHPCC) is being used to perform the imaging algorithm research and data reduction.

Research Objectives: The objective of this research was to quantify the conditions where a linear technique, (bispectrum), and a non-linear technique, (blind deconvolution), would perform optimally. Also, we wanted to understand how to control noise artifacts and morphology changes introduced by the non-linear algorithm. Furthermore, we wanted to determine the best combination of both bispectrum and blind deconvolution techniques, with the goal of forming a more robust image recovery algorithm. This new combined algorithm would eliminate the need for additional star calibration data and would increase the resolution of the recovered imagery, while still controlling the noise artifacts and morphology changes.

Methodology: Raw data was simulated for a variety of seeing conditions and two

object sizes. Seeing conditions were selected based upon real MSSC conditions for data collection. 1600 frames of data were simulated for each scenario. This amount of raw data allowed reduction of the data using both 16 and 64 frames per recovery ensemble (group of data frames to form one image recovery), producing enough recoveries to allow meaningful statistics to be determined. The raw data was reduced using the bispectrum algorithm and the blind deconvolution algorithm.

Results: Figure 2 shows some results from our study. Since it is difficult to obtain meaningful metrics based upon the image domain (the satellite recovery) data, we focused on the Fourier domain information and initially only the phase. For each recovery in the set (e.g., 1600 raw frames/16 frames per recovery = 100 recoveries; or 1600 raw frames/64 frames per recovery = 25 recoveries), we calculate a phase-difference-squared metric. The phase-difference-squared metric is calculated by averaging the phase of each recovery in the set, minus the phase of the truth object quantity squared.

The areas of white in the phase metrics of Figure 2 show where the recovered phase and the truth phase are in good agreement over the ensemble of recoveries. We see in Figure 2 that both algorithms successfully reconstruct the low to mid-spatial frequencies. However, the blind deconvolution algorithm metric shows us that this algorithm was able to recover high spatial frequency information (i.e., the white strip going from the top right to the bottom left) that the bispectrum algorithm did not recover.

In Figure 3, we again we see good agreement in the phase metric at the low spatial frequencies. However, the black stripes in the blind-deconvolution results show us high frequency errors in the phase, which the bispectrum result does not contain.

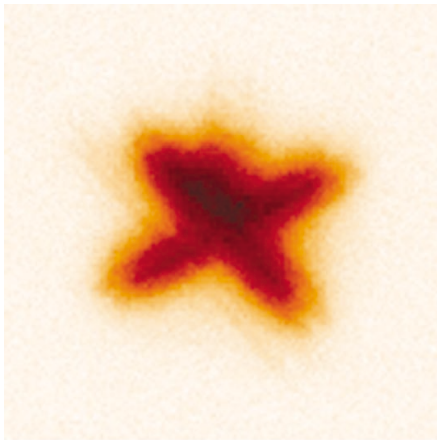


Figure 1. Raw data and recovered image.

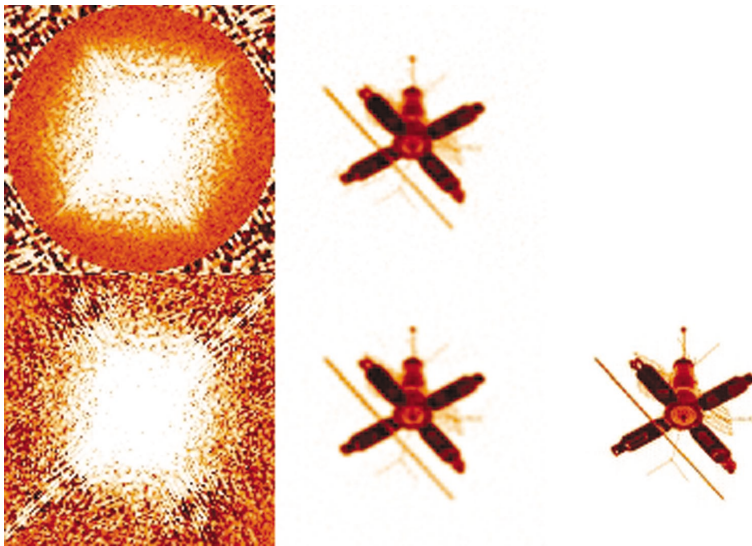


Figure 2. Raw Data Set - r0 8, bandwidth 200 visual magnitude 3 large object.
 Top Row -- bispectrum results, phase-difference-squared metric, 1st recovery in set.
 Bottom Row -- blind deconvolution results, phase-difference-squared metric, 1st recovery in set and truth object.

Significance: This study gives an initial indication of phase quality as it relates to a variety of seeing conditions and object sizes for both algorithms. In the area of low earth-orbit satellite imaging performed at MSSC, the turbulence is relatively benign and the target size is predominantly large. Our initial research shows that the bispectrum algorithm generally performs better than the blind deconvolution algorithm. However, when relatively few frames are used for the image reconstruction process, the blind deconvolution algorithm can perform comparably to the bispectrum algorithm. Removing the requirement for the additional star calibration measurements makes the blind deconvolution algorithm attractive for operational use. Our research further shows that the linear bispectrum algorithm typically performs better for smaller targets and substantially worse seeing conditions. We are now in the process of studying how best to merge these technologies to exploit their individual strengths. With the current space industry trend toward smaller and smaller satellites, this is one step down the road today to handle tomorrow's requirements.

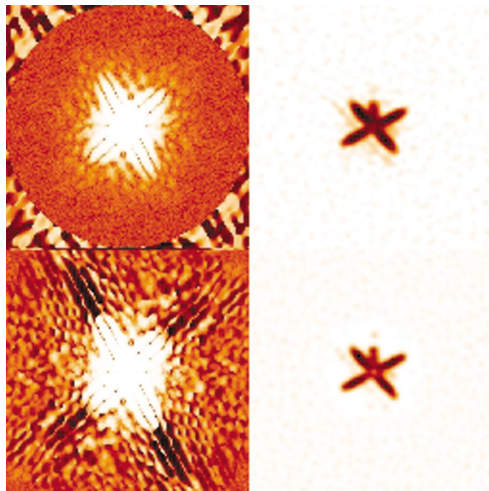


Figure 3. Raw Data Set - r0 8, bandwidth 200 visual magnitude 6 small object.
 Top Row -- bispectrum results, phase-difference-squared metric, 1st recovery in set.
 Bottom Row -- blind deconvolution results, phase-difference-squared metric, 1st recovery in set and truth object.

Author and Contact: Kathy J. Schulze
 Organization: KJS Consulting, PO Box 591, Georgetown, DE, 19947
 Author: Paul Billings
 Organization: Textron Systems, 535 Lipoa Parkway, Kihei, HI, 96753
 Author: Chuck Matson
 Organization: Air Force Research Laboratory, DEBI, 3550 Aberdeen Ave. SE, Kirtland Air Force Base, Albuquerque, NM, 87117
 Authors: Bob Dant and Bobby Hunt
 Organization: Maui High Performance Computing Center, 550 Lipoa Parkway, Kihei, HI, 96753
 Resources: IBM SP3, *Tempest*, at MHPCC
 Sponsorship: Air Force Research Laboratory

Novel Laser Actuated Optically Addressable Adaptive Optics

Joe Ritter, Jim Brozik, James Newhouse, David Keller

This novel effort is an investigation of the fundamental chemistry and physics of light-activated, polymeric photoisomer materials paving the way for a union of adaptive optics and nano-technology. In order to achieve a 100-fold improvement in spatial resolution, 10-fold improvement in bandwidth, and a factor of 10 reduction in production and deployment cost of adaptive optics, new directions for fundamental research in computation, nano-engineering, opto-mechatronic (OM) photochemistry, and nonlinear optics is being explored. This will entail the synthesis and incorporation of photoactive isomers into crystals and polyimides (as well as other matrices) to understand nanomachine "laser controlled molecular actuators." This will enable a new class of optical technologies, including a number of new devices such as inexpensive 10k-element ultra-high bandwidth adaptive optic correction systems. The proposed effort has revolutionary implications for research in astronomy, for surveillance, and for high-energy laser (HEL) beam propagation.

Research Objective: The goal is to synthesize and elucidate the fundamental physics of two types of molecular machine mechanisms; Cis-Trans photoisomer polyimide membranes, and Laminate structures (pi-pi and metal-metal stacking polymers), and to generate a picture of photoinduced molecular scale mechanical forces and geometric distortions. By combining this with macroscopic measurements, the team is gaining knowledge of these important yet poorly understood materials.

Photonic Muscles: It will soon be possible to build amazing molecular-scale machines and devices. This new technological thrust is partly inspired by biology and partly by the decreasing

dimensions of semiconductor devices, and will result in novel devices set apart from any others currently used and understood. Work on molecular machines today is as important and fundamental as work on semiconductors was 50 years ago.

Early work by Ritter investigated the use of Cis-Trans isomerization to effect figure change in membrane optics. When irradiated by the correct wavelength of light, some chromophores (e.g., azo derivatives) undergo a structure change (photoisomerization), which if placed in a matrix (polymer, crystal, or other) can cause movement of the matrix. This suggests the following uses: compensation for errors in membrane mirrors, inducing controlled deformations to correct wavefront aberrations induced by atmospheric propagation (AO systems), figure control of HEL mirrors, figure control of large space optics, and damping of oscillations caused by telescope repointing and environmental perturbations in a large deformable mirror allowing a robust response to pointing and slewing membrane space optics. Ritter's approach has numerous advantages over piezoelectric bimorphs, electrostatic actuation, electroactive, and ionic polymers.

Adaptive Optics (AO): Current AO correctors for 4 meter class telescopes are expensive, burn out when stressed, and limit the field of view that can be well corrected. Larger and multi-aperture telescopes require higher than currently available actuator density and number, and even larger deformable mirrors. Prototype correctors with a few thousand corrective elements have been produced at high cost, and they are far from the large aperture optically addressable mirrors proposed by Ritter.

This novel research effort is both a completely new production technique, along with a potentially vastly superior novel non-contact control technique. This technology opens up the possibility of a light-based, physical computer closed-loop correction of secondary optics, which in turn control wavefront phasing, i.e., an adaptive optics system with a physical (as opposed to computer) processor. This amazing possibility of having enormous bandwidth, also proposed by Ritter, is a likely spin-off of this effort.

Methodology: The primary goal is to synthesize and chemically alter photomechanical polymers to tune optical response, as well as to test existing samples. Several polymer backbones will be synthesized. Pendant groups will be attached to the backbone. Cross-linked materials will be synthesized. Cross-linkers will be incorporated into several polymeric materials. Additional studies will focus on the feasibility of incorporating chromophores into crystals, to make heat-resistant adaptive secondary mirrors. Such devices would be invaluable for defense missions, such as Space-Based Lasers, Airborne Lasers, etc.

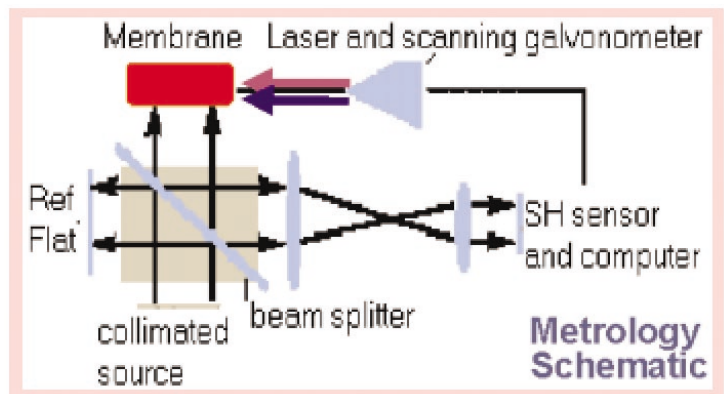


Figure 1. Schematic of novel control and metrology set up.

Spectroscopic studies will reveal the nature of the ground and lowest excited states, as well as the structural and dynamical nature of the excimer formation process and mechanisms involved in energy transfer in photo-mechanical devices. Energetics of excited states will be measured through steady-state emission. Exciton migration and trapping dynamics, and luminescence studies will be conducted. Transient luminescence spectroscopy will probe the behavior of exciton hopping and measure lifetimes of excimer states.

Metrology to test control authority of polymers and photocontractile organic lamellar optics will be accomplished on both a nano and macro scale. Scanning probe atomic force microscopy (AFM) will measure surface topography, time, and magnitude of response before, during and after photoexcitation. These data will be used to determine the basic physical model for force generation, and how this is related to structure and electronic properties. Thin membrane "mirrors" will be produced using novel materials. Incoherent monochromatic, as well as laser sources, will be used to effect shape control. Wavefront sensing techniques will be used to quantify the response of each sample. The beta version metrology and control setup is detailed in Figure 1.

The study will pave the way for a leap in novel lightweight active optics capabilities, revolutionizing wavefront control (increasing Strehl ratios in adaptive optics systems), enabling multiconjugate adaptive optics, fabricating enormous lightweight active diffraction-limited apertures for spacecraft, and laying the groundwork for future hybrid chemo-optic and bio-optic computers.

References:

- 1) J. Ritter, J. Newhouse, J. Brozik, D. Evans, Novel Ultra-Lightweight Space Telescopes Using Optically Active Polymer Membrane Mirror Shape Control, *MHPCC/AFRL Application Briefs 2001*.
- 2) J. Newhouse, D. Evans, J. Ritter, *Ab Initio* Calculations Characterizing an Effective Hamiltonian for Polymeric Photonic "Muscles", *MHPCC/AFRL Application Briefs 2001*.
- 3) Joe Ritter et al, NRA 00-055-06, Gossamer Spacecraft Exploratory Research and Technology Optically Active Polymer Membrane Mirror Shape Control Using Lasers, Dec. 2000.
- 4) Brozik, Evans, Hampton, Keller, Lopez, Nanoscale Photonic Muscles: Fundamentals and New Technologies, Proposal to (Department of Defense) Defense University Research Initiative on NanoTechnology (DURINT), FY2001.

Author and Contact: Joe Ritter

Organization: SAIC, Technology Research Group, 590 Lipoa Parkway, Building B, Kihei, HI, 96753

Author: James S. Newhouse

Organization: Maui High Performance Computing Center, 550 Lipoa Parkway, Kihei, Maui, HI, 96753

Authors: Jim Brozik and David Keller

Organization: University of New Mexico, Department of Chemistry, Albuquerque, NM, 87131

Resources: IBM SP3 and SGI Octane dual R12000 at MHPCC

Acknowledgements: The author is grateful for the support from the Air Force Office of Scientific Research and the Air Force Directed Energy Detachment 15.

The Impact of Initial Conditions on the Time-Space Distribution of Long-Term Atmospheric Predictability

Thomas Reichler and John Roads

The problem of forecasting the future state of the atmosphere depends on the range of lead and averaging time. Forecasts on the short to medium range (day 1-14) are dominated by initial conditions, and climate-range (3 months and longer) forecasts are completely determined by boundary conditions. Our research is focused on the long-range from 2 weeks to 2 months, where both initial and boundary conditions play a role. This range is the most difficult of all ranges, since the memory of the initial conditions is weak at these long-lead times, and the impact of boundary conditions is hard to detect because of the relative short averaging interval. The societal benefits of long-range forecasts, however, would be large because extreme atmospheric conditions could be anticipated many weeks ahead. This study is aimed at improving our ability to make long-range atmospheric predictions with Atmospheric General Circulation Models (AGCMs). AGCMs are complex 3-dimensional numerical models, which simulate as realistically as possible the complex physical and dynamical processes of the atmosphere.

Research Objectives: Atmospheric predictability is inherently limited by the chaotic nature of atmospheric flow. Predictability is increased by providing to the atmospheric model information about the real system in the form of (1) atmospheric initial conditions at the beginning of the forecast, and (2) lower boundary conditions during the forecast. Forecast errors that limit predictability are caused by uncertainties in the proper specification of initial and boundary conditions, and by errors in the model formulation. Here we conduct idealized AGCM experiments to find out how large predictability would be if the model had no errors, and if either initial or boundary conditions or both would be perfectly known. Our research is focused on the long-range of 2 weeks to 2 months, where both initial and boundary conditions are important. As Reichler and Roads (2002a) showed, boundary conditions are as important as the decaying influence of initial conditions after four weeks.

The purpose of this study is (1) to determine the 3-dimensional structure of monthly mean perfect model predictability as a function of lead time, and (2) to find out how important initial and boundary conditions are for regional patterns of predictability.

Methodology: The numerical model of this study was the seasonal forecasting model developed at the National Centers for Environmental Prediction. It simulates the global atmosphere with a horizontal resolution of approximately 300 km and 28 vertical layers. We performed three idealized experiments using different combinations of initial and boundary conditions. For experiment ICBC (Figure 1), proper boundary and initial conditions were used. Ocean boundary conditions were derived from the observed history of sea surface temperatures (SSTs) and sea ice, while land boundary conditions were produced internally by the land surface scheme of the model. The initial conditions were derived from a continuous 22 year-long integration with the same model that was forced with the same boundary conditions as ICBC. Experiment IC was started from identical initial conditions as ICBC, but was forced with the climatological mean seasonal cycle of sea surface temperatures, sea ice, soil moisture, and snow cover. For experiment BC, we used the same boundary conditions as for ICBC, but initialized the model from an atmospheric state, which was close to its climatological mean. Each experiment simulated the evolution of the Boreal wintertime atmosphere of 22 years (1979-2000). In each of the 22 years, the experiments were started on December 15th and run for 107 days through the end of March of the following year. Since the chaotic nature of the atmosphere requires a probabilistic approach, we repeated each run ten times by starting from slightly perturbed initial conditions but forcing with identical boundary conditions.

Results: Figure 1 shows the regional distribution of monthly mean predictability of the middle troposphere for different lead times and forcings. Predictability was measured at each grid point by the temporal anomaly correlation of monthly mean geopotential heights between experiment and reference run over the 22-year period. We applied the perfect model approach, where the ensemble mean of one forecast is verified against one member of a reference forecast with the same model. This way we eliminated errors concerning the model formulation and we focused better on the

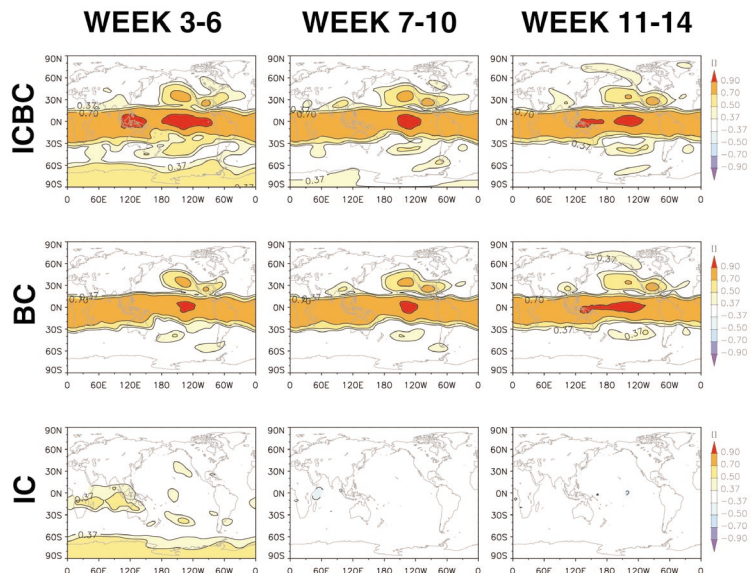


Figure 1. Regional distribution of monthly mean predictability of the middle troposphere for different lead times and forcings (ICBC, BC, IC). Predictability is being measured at each grid point by the temporal correlation (1979-2000) of the geopotential height of the 500 hPa surfaces between the experiment and the reference simulation ICBC. Shown are only statistically significant correlations given the 22 year-long time series ($r > 0.37$).

basic questions of this study. ICBC was used for all cases as a reference experiment, since it comes closest to the real atmosphere. The verification of ICBC against itself provides an upper predictability limit with this model, since both initial and boundary conditions are perfect for this experiment.

The perfect predictability experiment ICBC shows useful forecast skill (correlation > 0.5) at all lead times over the Tropics and over the Pacific-North American (PNA) region. For week 3-6, ICBC also shows high predictability over the Antarctic continent. This region of high predictability shrinks considerably during week 7-10, and disappears completely at maximum lead. This suggests that this region is related to the decaying influence of initial conditions. The skill of simulation IC, which comes from good initial conditions, and simulation BC, which comes from climatological initial conditions, confirm that the predictability over the Antarctic continent during week 3-6 is related to the long-term memory of the initial conditions. The tropical Indian Ocean is another region where the initial-condition influence seems to be important during week 3-6. This can be seen from experiment IC, and from the difference between BC and ICBC.

The height-latitude cross sections of zonal mean predictability (Figure 2) shows the vertical predictability structure of the atmosphere, and they demonstrate how signals from initial and boundary conditions propagate in space and time through the atmosphere. The effects of boundary forcing dominate the whole atmospheric column over the Tropics. To some extent, boundary forcing is also important for the well-known teleconnection regions in the extratropics and for the stratosphere. The effects of initial conditions are mostly limited to week 3-6, and to areas that are far from the tropical regions of strong boundary forcing, namely the Antarctic continent and the stratosphere. However, the comparison of experiment BC with ICBC also shows that for other areas and lead times, boundary conditions alone do not achieve the same forecast skill as initial and boundary conditions together.

Conclusions: We conducted three AGCM predictability experiments to determine the 3-dimensional structure of monthly mean predictability at different lead times, and to find out how important initial and boundary conditions are for this predictability. There is a surprisingly long-lasting effect of initial conditions for some areas. In particular, during week 3-6, the troposphere and stratosphere over the Antarctic continent is dominated by the effects of initial conditions. Initial conditions also seem to be important for the lower troposphere over the tropical Indian Ocean. The consequence for current long-range forecasts is that good atmospheric initial conditions are needed.

References:

- 1) Thomas J. Reichler, (2002): Seasonal Atmospheric Predictability, University of California San Diego, PhD thesis (in preparation).
- 2) Thomas J. Reichler and John O. Roads, (2002a): The Role of Boundary and Initial Conditions for Dynamical Seasonal Predictability, *Nonlinear Processes in Geophysics*, (in press).
- 3) Thomas J. Reichler and John O. Roads, (2002b): The Role of Atmospheric Initial Conditions for Long-Range Predictability, Workshop on Prospects for Improved Forecasts of Weather and Short-Term Climate Variability on Subseasonal (2 weeks to 2 months) Time Scales, Greenbelt, MD, April 2002.

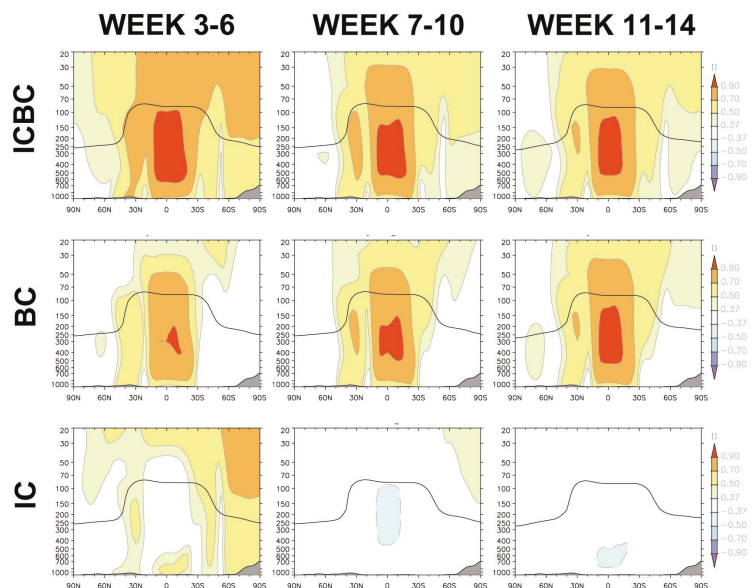


Figure 2. Height-latitude cross sections of monthly mean zonal mean predictability of geopotential height for different experiments and lead times. Predictability is measured at each grid point by the temporal correlation (1979-2000) of geopotential height at each pressure level between the experiment and the reference simulation ICBC. Shown are only statistically significant correlations given the 22 yearlong time series ($r > 0.37$). Black continuous lines indicate the location of the tropopause derived from the lapse rate criterion ($dT/dz > -2K/km$).

Author and Contact: Thomas Reichler
 Author: John Roads
 Organization: Scripps Institution of Oceanography, UCSD, 0224, La Jolla, CA, 92093
 URL: <http://ecpc.ucsd.edu>
 Resources: IBM SP at MHPCC and DEC Alphas at Scripps Institution of Oceanography
 Sponsorship: NOAA Office of Global Programs NA17RJ1231 grant to the Scripps ECPC

Experimental High-Resolution Forecasts/Analyses for the Hawaiian Islands

John Roads, Jongil Han, Francis Fujioka, Kevin Roe

One of the key aspects of disaster forecasting, response and mitigation planning is readily available, accurate, timely, local scale weather and climate information. In Hawaii, where weather and climate variations are affected by the steep island topography, there is a clear and acknowledged need for improved weather and climate forecasts at a variety of time and space scales. In that regard, nested mesoscale models could provide a valuable tool to resolve weather patterns and the Scripps Experimental Climate Prediction Center (ECPC), in collaboration with the Hawaiian Weather/Climate Modeling Ohana (HWCMO), has now implemented routine mesoscale weather forecasts. Near-real-time high-resolution weather forecasts are made available to the general public on our MHPCC Web site (<http://weather.mhpcc.edu/>), and we are also analyzing climatological characteristics of these forecasts. It should be noted that weather forecasts have not previously been systematically applied to the individual islands on scales less than ten kilometers, and MHPCC is the testing ground for future high-resolution operational forecasts.

Methodology: As described previously by Roads, et al. (2001); the HWCMO developed a dynamical/physical modeling capability to make short-term (out to 48 hours) weather predictions for the individual island counties of the state of Hawaii. We initially used a version of the Mesoscale Spectral Model (MSM), which was developed by the National Centers for Environmental Prediction (NCEP) from the Regional Spectral Model (RSM; Juang et al. 1997). The MSM is able to resolve weather parameters (such as temperature, humidity, winds, rainfall) on horizontal scales down to approximately two kilometers for Hawaii. Since the MSM is nested within the operational global model, the local forecast domain can be relocated anywhere in the world. These predictions can therefore provide local scale weather information (down to horizontal scales of at least two kilometers) for environmental disaster managers. Since March 1998, when we

ported and implemented the National Centers for Environmental Prediction (NCEP) Mesoscale Spectral Model on a single node of the MHPCC IBM SP2, we have made routine predictions (Roads et al. 1999, 2000). For example, we now routinely run the atmospheric model for individual counties with grid point resolutions of: 2 kms for Oahu and Kauai, 3 kms for Maui County, 4 kms for Hawaii County, and 10 kms for the entire Hawaiian Archipelago. Near-surface meteorological variables, including temperature, relative humidity, rainfall, and wind, as well as a derived Fire Weather Index and drought index (soil moisture) are computed by the model. We have also sponsored a number of international RSM workshops at MHPCC describing our experimental applications (Roads 2000).

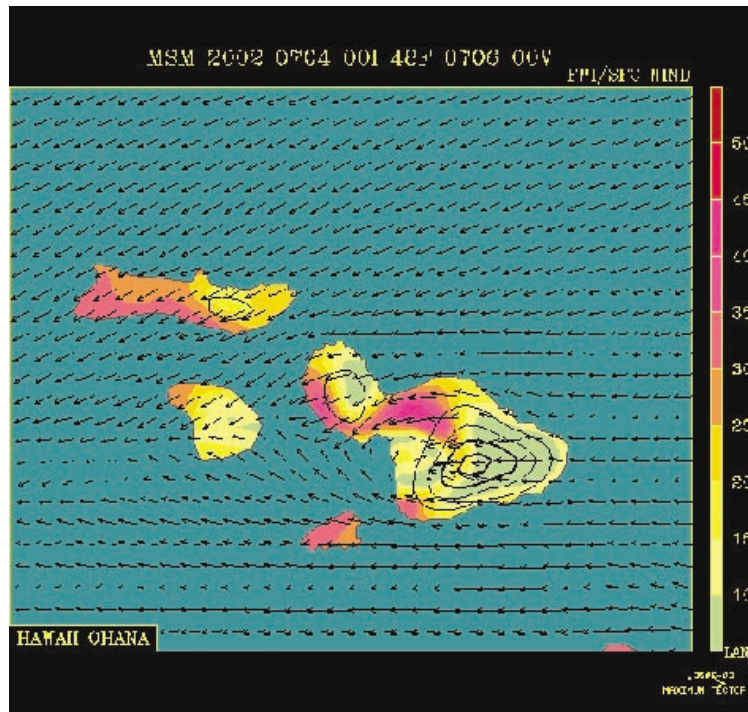


Figure 1. 48-hour Fire Weather Index (FWI) and surface wind forecast for Maui and surrounding islands at 3 km resolution. The forecast was initialized on July 4, 2002, at 00UTC and validated July 6, 2002 at 00UTC. This is a typical FWI forecast provided routinely on <http://www.mhpcc.edu/~swsx> for Maui and other Hawaiian islands. Red colors indicate regions of increased fire danger.

Results: We have made a number of significant improvements to the previous HWC MO forecasting system:

- (1) We switched the input NCEP files to come directly to NCEP, which significantly increased the forecast start time and increased the reliability of our quasi-operational system.
- (2) We increased the number of vertical levels to 42 to make the MSM more consistent with the operational global analysis and 3-day aviation forecast.
- (3) We adapted the MSM to the new open MP SP processors, which means that each county can use at least 4 processors for numerical computations and additional processors for graphics computations.
- (4) We experimented with making 72-hour forecasts but have since cut back to 48-hour forecasts to conserve resources while waiting for demand to build for these extended range forecasts.
- (5) We augmented current fire weather forecasts with fire danger and drought forecasts that are more compatible with standard USFS fire danger ratings.
- (6) As part of our work for the Pacific Disaster Center (PDC), we developed a user manual to describe our system and system output (this user manual has been posted on our Web site).
- (7) The entire MSM prediction system now runs on a single node, ensuring the timely completion each day of 48-hour forecasts for each island with minimal computing resources.

References:

- 1) H. Juang, S. Hong, M. Kanamitsu, 1997: The NMC Nested Regional Spectral Model, An update, *Bull. Amer. Meteor. Soc.*, 78, 2125-2143.
- 2) J. Roads, S. Chen, D. Stevens, C. McCord, H. Juang, F. Fujioka, 1999: Weather and Climate Analysis and Forecasts at MHPCC, Seventh International Conference on High Performance Computing and Networking, Amsterdam, The Netherlands, April 12-14, 1999.
- 3) J. Roads, S. Chen, F. Fujioka, Bob Burgan, D. Stevens, D. Funayama, B. Anderson, C. McCord, K. Roe, 2000: High-Resolution Forecasts/Analysis for the Pacific Disaster Center. Fire Conference 2000: The First National Congress on Fire Ecology, Prevention, and Management, San Diego, CA., Nov. 27-Dec. 1, 2000.
- 4) J. Roads, 2000: The Second International RSM Workshop: Meeting Summary, *Bull. Amer. Meteor. Soc.*, Vol. 81 (12), 2979-2980.
- 5) J. Roads, J. Han, D. Stevens, D. Funayama, C. McCord, K. Roe, F. Fujioka, 2001: Routine High-Resolution Forecasts/Analysis for the Pacific Disaster Center, *MHPCC 2001 Application Briefs*.

Author and Contact: John Roads

Organization: Scripps Institution of Oceanography, UCSD, 0224, La Jolla, CA, 92093-0224

Author: Jongil Han

Organization: World Weather Building, Room 806, 5200 Auth Road, Camp Springs, MD, 20746

Author: Francis Fujioka

Organization: Riverside Fire Laboratory, U.S. Forest Service, Riverside, CA

Author: Kevin Roe

Organization: Maui High Performance Computing Center, 550 Lipoa Parkway, Kihei, HI, 96753

URL: <http://www.mhpcc.edu/~ws wx>

Resources: IBM SP3 at MHPCC and DEC Alphas at Scripps Institution of Oceanography

Sponsorship: US Department of Agriculture, Forest Service; NOAA Office of Global Programs, NOAA CDEP Program

High-Resolution Weather Modeling for Improved Fire Management

Kevin Roe and Duane Stevens

Several weather variables, such as wind, temperature, humidity, and precipitation, make direct impacts on the practice of managing controlled burns and fighting wild fires. State-of-the-art Numerical Weather Prediction (NWP) enables the short-term forecasting of near-surface weather. This project integrates three complementary model types to aid federal agencies in real-time management of fire.¹ A highly complex, full-physics mesoscale weather prediction model, MM5, is applied in order to estimate the weather fields up to 72 hours in advance. A nested grid technique is used to incorporate terrain down to a one-kilometer grid scale.² A diagnostic fire behavior model, FARSITE, takes the near-surface weather fields and computes the expected expansion of wind, humidity, and fuel driven fire.³ A tracer, transport, and diffusion model is applied in order to provide estimates of smoke and haze.

Research Objectives: Fires are highly dependent on wind and terrain, which require the forecasts to be done at a high-resolution. Currently the National Weather Service produces forecasts on the order of 30-50 km resolution and has publicly stated that they do not intend to go below 10 km. Since fires can travel rapidly (especially uphill) and their spread rates are strongly dependent on winds, it is important to have wind forecasts and terrain information at a much finer resolution than 10 km. If the terrain data given to the NWP models is not at a fine level, they will miss details such as ridges and valleys, as well as make the model "think" the mountains

are smaller because it is only an average terrain height. An example of how this can be a problem is the Idaho/Montana fires of 2000 (Figure 1) where fire spread rapidly through mountainous regions. The fire fighters/incident managers were relying on coarse forecasts to predict how the weather would behave; this caused problems because the forecasts were generated using data that prevented the model from accurately seeing the terrain details. A resulting problem was higher wind speeds than what was predicted. Finer resolution (i.e., 1 km resolution) simulations may still not be completely accurate, as there may be deficiencies in the physics behind the model, unpredicted events, and sub-kilometer information that could be relevant for wind channel effects. Despite this, these simulations would be a significant improvement over what is currently available.

Methodology: The procedure for enabling incident managers to utilize fine resolution weather forecasts consists of many segments^{1,2} which occur as follows:

- (1) Prescribed burn or wildfire is identified.
- (2) Required resolution is requested (i.e., 3 km, 1 km, etc.).
- (3) Forecast length and interval output requirement is inputted into the model.
- (4) Nested domains are created to cover fire.
- (5) MM5³ collects global analysis data (and possibly observational data) and does pre-processing to put the data in a format usable by the model.
- (6) Simulation is run.
- (7) Data is converted to a format suitable for FARSITE⁴⁻⁷ and made ready for download.
- (8) Incident managers in the field download the data.
- (9) Incident managers do fire behavior simulations using this data.



Figure 1. The Pistol Creek fire swept down the canyon, crossed the middle fork, and blasted the hillside.

Results: Timing is crucial to make the above methodology work. In order for the incident managers to get the data they need when it is still a prediction, it is crucial to streamline the process. Below is an example of the time required given the current state of the project:

- (a) 2-3 hours to create domains that will accurately handle the required area to be covered.
- (b) MM5 collection of global analysis data from NCEP takes about fi hour to download. Observational data is harder to determine as it is dependent on the sources, but, since the data files are usually very small, it rarely takes more than a few minutes. Pre-processing usually takes about 5 minutes for a 24-hour forecast (10 minutes for a 48-hour forecast).
- (c) 3 hours for a 24-hour forecast. This is a rough number, as the required area coverage and resolution determine run size but 3 hours were required for a 1 km resolution, 24-hour MM5 simulation over the Little Pistol Creek fire of 2000 in Idaho. Run time would be linear if the forecast time is changed to a 48-hour forecast, under the same conditions, it would take approximately 6 hours.
- (d) Approximately fi to 1 hour to produce the required data for the fire behavior simulation (again depending on the length of the forecast).
- (e) Since the simulations that the incident managers do in the field (to determine the appropriate course of action) is beyond the scope of this paper, these simulations will not be included in the time estimation; although the simulations are generally done on laptops in a few minutes.

In short, an initial 24-hour forecast would require approximately 7 hours to complete (an initial 48-hour forecast would require 10 hours). Subsequent 24-hour forecasts in the same area would require 4 hours (7 hours for a 48-hour forecast).

Conclusions: We have created a methodology that will produce fine-resolution weather forecasts. These forecasts can provide useful information for the management of prescribed burns and wildfires. This methodology is focused on providing the required forecasts in a timely manner in order to be useful to the incident managers who will do simulations based on these forecasts and to more effectively manage their available resources.

Future work would entail increasing the resolution of the model (i.e., sub-kilometer resolution simulations), decreasing the response time of the entire operation, and expanding the coverage area. Other areas of potential work include: Improving the land-cover and vegetation data, working with other fire fighting organizations, and providing feedback to weather models from the actual fire's behavior (e.g., using a dispersion model).

References:

- 1) K. P. Roe, D. Stevens, C. McCord, "High Resolution Weather Modeling for Improved Fire Management", *Supercomputing 2001*, Denver, CO, 2001.
- 2) K. P. Roe, D. Stevens, C. McCord, "Real-time Fire Management Using Fine Scale Weather Modeling", *HPC Asia 2001*, Gold Coast, Australia, 2001.
- 3) J. Michalakes, The Same-Source Parallel MM5, *Journal of Scientific Programming*, 8 (2000), 5-12.
- 4) M. A. Finney, "FARSITE-A Fire Simulator for Managers", The Biswell Symposium: Fire Issues and Solutions in Urban Interface and Wildland Ecosystems, General Technical Report PSW-158, Berkeley, CA, USDA Forest Service, 1995.
- 5) M. A. Finney, "FARSITE: Fire Simulator-Model Development and Evaluation", USA Forest Service, Research Paper RMRS-RP-4, Rocky Mountain Research Station, Ft. Collins, CO, 1998.
- 6) M. A. Finney, D. B. Sapsis, B. Bahro, "Use of FARSITE for Simulating Fire Suppression and Analyzing Fuel Treatment Economics", *Fire in California Ecosystems: Integrating Ecology, Prevention and Management*, San Diego, CA, 1997.
- 7) P. L. Andrews and C. H. Chase, "BEHAVE: Fire Behavior Prediction and Fuel Modeling System-BURN Subsystem, Part 2", Gen. Tech. Rep., INT-260, Ogden, UT, U.S. Department of Agriculture, Forest Service, Inter-mountain Research Station, 1989.

Author and Contact: Kevin Roe

Organization: Maui High Performance Computing Center, 550 Lipoa Parkway, Kihei, Maui, HI, 96753

Authors: Duane Stevens

Organization: University of Hawaii at Manoa, Dept. of Meteorology, HIG 350, 2525 Correa Road, Honolulu, HI, 96734

URL: www.mhpcc.edu/projects/wswx/mm5

Resources: IBM SP3 at MHPCC

Sponsorship: USDA Forest Service

Ab Initio Calculations Characterizing an Effective Hamiltonian for Polymeric Photonic "Muscles"

James Newhouse, Debi Evans, Joe Ritter

Nanoscale "photonic muscles" are studied by a research group associated with Prof. Debi Evans at the University of New Mexico (UNM). The photonic molecular muscles act as nano-scale actuators to correct the less-than-ideal original figure of the space-based optics proposed by Dr. Joe Ritter. Dr. James Newhouse is using parallel machines at MHPCC to calculate parameters for the Effective Hamiltonian of the polymer/pyrene excimer/exciton system (one of several proposed) via *ab initio* calculations using Gaussian 98 A.11, and Q-Chem 2.0.1/1.2. The Effective Hamiltonian is used by Prof. Debi Evans in molecular dynamics simulations to simulate the force and throw of different variants of the molecular muscles, and the behavior of energy transport along the polymer/pyrene system to the site of excimer formation by means of Frenkel excitons. The Coulombic contribution to electronic coupling for energy transfer in these systems is obtained using the *ab initio* transition density cube method (Zindo CIS and CUBE keyword in Gaussian 98).

Research Objectives: This research group proposes to design, construct, and characterize a new class of molecular motors called polymeric muscles, which are polymer molecules that have the ability to contract and generate forces. Because they are the simplest to design and build, but still very versatile, they will focus on photon-powered polymeric muscles, or "photonic muscles". Structurally, photonic muscles are composed of two major parts: a parent polymer molecule (e.g., polystyrene) and a chromophore that forms tightly-bonded excimer pairs when excited by light (e.g., pyrene). The chromophores are attached to the parent polymer by linker arms at regularly spaced intervals, so when the photonic muscle is exposed to light, excimer pairs form and the polymer contracts.

Significance and Vision: The overall goal of the "photonic muscles" project is to develop a new kind of molecular machine, the polymeric muscle, and use it to build useful nano-devices. A polymeric muscle is a polymer molecule with the ability to contract and generate forces. The simplest photonic muscle is a polymer molecule with pendant groups spaced along its length (see Figure 1). The pendant groups form tightly bonded excimer pairs when excited by a photon, so the polymer molecule contracts when exposed to light and thus converts radiant energy into mechanical work. A simple example of such a photonic polymer has been synthesized, and the first experiments (which demonstrate its ability to contract when illuminated) have been carried out. The photonic muscle should be both strong (piconewtons at the single molecule level) and fast (tens of microseconds).

Methodology: The exciton model requires calculation of the adiabatic surfaces and the coupling between them. Given that an *ab initio* electronic structure calculation for the entire polymer is not feasible, a small fragment of the polymer (most likely a chromophore dimer) will be used to generate this data on the assumption that these dimer units are essentially uncoupled. As a starting assumption, distortion of only one mode will be considered. If more than one mode is strongly coupled to the dynamics, subsequent wavepacket propagation will be done using the time-dependent Hartree approximation, which scales favorably with the nuclear degrees of freedom.

Exciton properties, in the absence of coupling to the polymer backbone, will be accessed from electronic structure calculations. For localized excitations, the Frenkel-exciton model is directly applicable, and can be used to generate the necessary Hamiltonian for the dynamical processes. The Frenkel model describes a general aggregate made out of L interacting two-level chromophores. To describe its electronic states, we introduce the exciton creation (annihilation) operators (B_n^\dagger / B_n) which add (eliminate) an excitation on the nth chromophore that satisfy the fermion commutation relations. Using these operators, the Frenkel Hamiltonian reads:

$$\hat{H} = \sum_{kn} A_{kn} B_k^\dagger B_n + \sum_j H_{osc}(x_j) + \sum_{j,n} x_j \Delta_j^n B_j^\dagger B_n$$

The first term represents the purely excitonic system:

$$A_{kn} = \omega_k \delta_{kn} + J_{kn}$$

where ω_k are the on-site exciton energies, and J_{kn} are the site-to-site exciton transfer matrix elements. Diagonalization of A_{kn} would give the one-exciton eigenstates and energies of the system in the absence of coupling to the polymer vibrational modes. *Ab initio* simulations of chromophore dimers and trimers will be used to obtain the above matrix elements for the exciton states in the absence of nuclear interactions.

The polymer vibrational modes are taken to be harmonic [the second term in the Hamiltonian], and the coupling to the exciton motion is taken to be a bi-linear coupling [the third term in the Hamiltonian]. The dissipative effects of the polymer distortion are more difficult to obtain.

Ab initio calculations by Dr. James Newhouse have focused on the excited states of pyrene and characterization of the pyrene dimer by means of the CIS method in Gaussian. The *ab initio* transition density cube method (ZINDO CIS and CUBE keyword in Gaussian 98) was used for calculating the Coulombic contribution to electronic coupling for energy transfer.

Significance: Fundamental understanding of the behavior of exciton-energy transfer in the polymer/pyrene excimer/exciton system, the nature of the forces generated, and the distance over which the photonic muscles would act (throw) will result. The effective design of such nanoscale systems will be learned, making them useful in many different applications. Application to correcting space-based optics is a challenging example.

References:

- 1) Brozik, Evans, Hampton, Keller, and Lopez, "Nanoscale Photonic Muscles: Fundamentals and New Technologies", Proposal to (Department of Defense) Defense University Research Initiative on NanoTechnology (DURINT), FY2001.
- 2) Brent P. Krueger, Gregory D. Scholes, Graham R. Fleming, "Calculation of Couplings and Energy-Transfer Pathways between the Pigments of LH2 by the *Ab Initio* Transition Density Cube Method", *Journal of Physical Chemistry B*, Vol. 102, p. 5378, 1998.
- 3) Ritter et al 2001, Gossamer Spacecraft Exploratory Research and Technology Proposal: "Optically Active Polymer Membrane Mirror Shape Control Using Lasers".

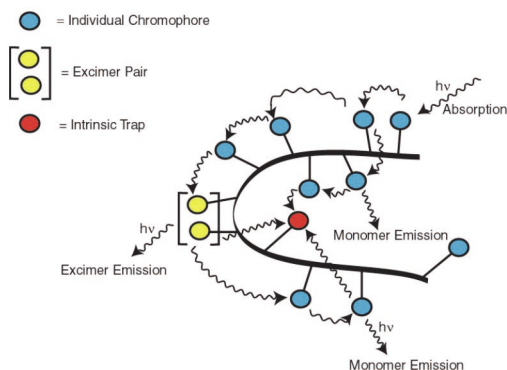


Figure 1. Paths of energy migration and deactivation from the "Nanoscale Photonic Muscles: Fundamentals and New Techniques" by Brozik, Evans, Hampton, Keller, and Lopez (University of New Mexico).

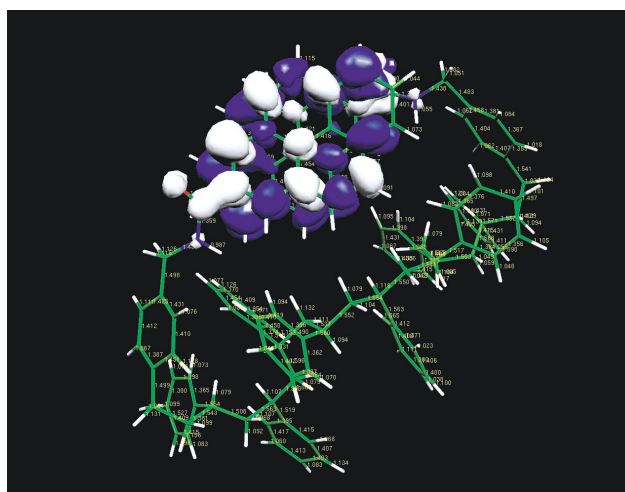


Figure 2. Ten polystyrene repeating units with attached pyrenes in approximate excimer orientation, which occurred after ~100 nanoseconds of molecular dynamics (mm+ force field). Electronic density difference plot: Blue-e-destination White-e-source

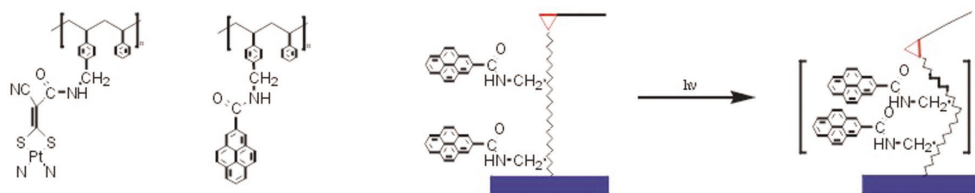


Figure 3. Conceptual model of "photomuscles". Average conformation will be greatly contracted in the excited state because excimer will hold the contracted geometry longer than a single randomly occurring fluctuation. From the "Nanoscale Photonic Muscles: Fundamentals and New Techniques" by Brozik, Evans, Hampton, Keller, and Lopez (University of New Mexico).

Author and Contact: James S. Newhouse
 Organization: Maui High Performance Computing Center, 550 Lipoa Parkway, Kihei, Maui, HI, 96753
 Author: Debi Evans
 Organization: University of New Mexico, Department of Chemistry, Albuquerque, NM, 87131
 Author: Joe Ritter
 Organization: SAIC, Technology Research Group, 590 Lipoa Parkway, Building B, Kihei, HI, 96753
 Resources: IBM SP3 and SGI Octane dual R12000 at MHPCC
 Sponsorship: Defense University Research Initiatives on NanoTechnology

Investigation of Small Boron Nitride Clusters

Sigrid Greene and Pui Lam

Solids can crystallize in different structures. Carbon, for example, can crystallize as graphite or diamond, with graphite being more stable at room temperature and pressure. Only at high temperature and pressure does diamond become the more stable structure. Therefore, in experiments one only produces diamond, if the temperature and pressure are sufficiently high. We are investigating the reasons behind the unconventional crystallizations of Boron Nitride (BN). It can crystallize in two different structures, hBN and cBN, of which cBN is more stable at room temperature and pressure. Nonetheless, experiments at ambient conditions produce the less stable hBN. This leads us to believe that, at the beginning of the crystal growth, the cBN structure is actually less stable than hBN, and that kinetics prevent it from switching between structures, once the crystal becomes larger. We are testing this hypothesis by performing *ab initio* quantum theory calculations to determine the stabilities of small clusters and then slowly combining them into bigger crystals.

Research Objectives: The stability of different crystal structures can be compared by calculating their respective binding energies. More strongly bound crystals are statistically more likely to be grown. When people started to produce Boron Nitride (BN),¹ they expected that it might have similar characteristics to carbon, as boron and nitrogen are the neighboring elements in the periodic table. When the early BN crystals showed graphite-like structure (hBN), the next step was to try and create diamond-like BN (cBN) under high temperature and pressure.² When theorists years later calculated the binding energies of the different crystal structures, they were surprised to learn that cBN seemed to be the more stable structure.³

Possibilities that the theoretical models were not accurate enough were tested, but then careful experimental measurements of the P-T diagrams confirmed that earlier measurements had not treated the dynamics involved in shock compressions accurately, and that cBN really is the more stable structure.⁴ While this solves one problem, it asks a new question: Why is it so difficult to produce the crystal structure that is energetically favored? In our research project we seek to answer this question by looking at the growth of the crystal. Even if cBN is the more stable structure for the bulk crystal, small clusters of atoms might prefer the hBN structure, and once the crystal has reached a critical size only then does the cBN structure become favored.⁵ At that stage of the growth, the energy barrier between the two structures might already be too big, so the crystal cannot change from hBN into cBN at ambient conditions. To test this hypothesis we calculate the binding energies of small clusters of Boron and Nitrogen atoms, and then start stacking them in two and three dimensions to simulate growth in the two different crystal structures.

Methodology: For our quantum theory calculations of the binding energies of Boron-Nitrogen clusters, we use the FHI98MD program.⁶ This program is based on the density functional theory⁷ and employs periodic boundary conditions with a plane wave basis set. This enables us to go from individual clusters to infinite crystals within the framework of the same program. As the supercell, in which the calculations are being carried out, is periodically repeated, we have to make sure to include enough vacuum around the clusters to prevent interactions from one cell into the neighboring cells. As an easy visual test, we check that the electron density does not form bonds through the cell boundaries and has decreased to less than 0.02% of its maximum value at the edges of the cell. The cut-off energy for our plane wave expansion is 60 Ry. The number of k-points is $2 \times 2 \times 2$ for most clusters, but we changed that for some of the very unstable geometries to see if we could improve convergence. For semi-periodic structures (infinite layers, infinite stacks) and bulk crystals, the number of k-points is obviously increased. To test which geometric arrangement gives the strongest binding energy, we do runs with changing starting configurations: linear, 2-dimensional, and 3-dimensional. The cluster structure is being relaxed according to the forces on the ions in a steepest descent, so we will get the geometries and energies of metastable structures. All starting geometries are slightly distorted, so the relaxation is not impeded by initial symmetries.

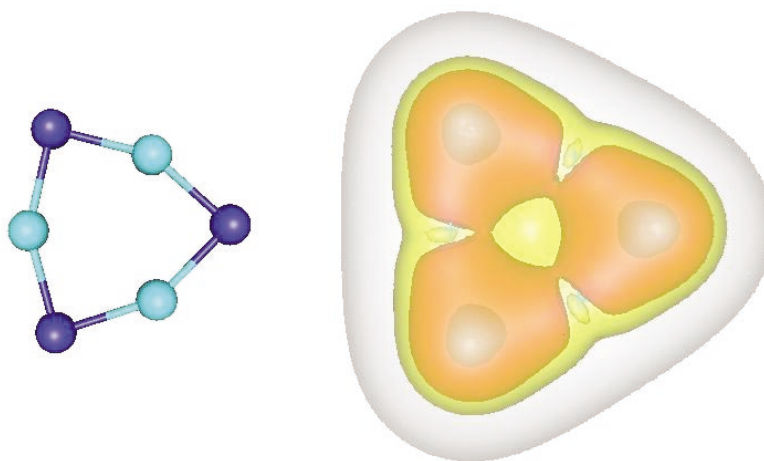


Figure 1. Geometry (left) and Electron Density (right) of the Hexagonal Boron Nitride Ring.

Results: We did calculations for clusters with 2, 3, 4, and 6 atoms. We found that once the strong Nitrogen-Nitrogen molecular bond is broken, the atoms seek Boron-Nitrogen bonds. By the time we reach a 6 atom cluster of three Boron and three Nitrogen atoms, this cluster is more strongly bound per atom than the Nitrogen molecule, and is stable against dissociation. The energetically most favored geometry for this cluster is a distorted hexagonal ring with angles of 153° (N-B-N) and 87° (B-N-B) (Figure 1). This ring can easily be combined into a 2-dimensional graphite-like net that produces the hBN crystal, with rather weak bonds from one crystal layer to the next. In order to grow cBN, these hexagonal rings have to create 3-dimensional bonds, and the rings themselves need to buckle. Preliminary calculations indicate that buckling only becomes advantageous when one has multiple (3 or more) layers *and* no room for the rings to spread out. So, one already needs a rather large number of atoms involved before the cBN structure becomes energetically favored, and this reduces the probability of this rearrangement being possible, as one has to overcome the energy barrier between the two structures.

Conclusion: We were able to find a stable building block for a Boron-Nitride crystal, and could confirm that Boron and Nitrogen like to mix in equal stoichiometry and will not segregate. Our preliminary results indicate that no matter if the growth occurs in layers or stacks, the hexagonal rings will not buckle until you have enough material in all three dimensions. Therefore, the growth always starts in an hBN-like crystal structure and can easily be trapped in this structure, which explains the unexpected metastable bulk crystals.

References:

- 1) R. S. Pease, "An X-ray Study of Boron Nitride", *Acta Crystallographica*, 5 (1952), 356.
- 2) R. H. Wentorf Jr., "Cubic Form of Boron Nitride", *Journal of Chemical Physics*, 26 (1957), 956.
- 3) P. K. Lam, R. M. Wentzcovitch, M. L. Cohen, "High Density Phases of BN", *Material Science Forum* 54/55 (1990) 165.
- 4) V. L. Solozhenko, "Thermodynamics of Dense Boron Nitride Modifications and a New Phase P, T Diagram for BN", *Thermochimica Acta*, 218 (1993), 221.
- 5) P. K. Lam, "Phase Diagram, Cluster Stability, and Growth Mechanism of Boron Nitride", *Proceedings of AIRAPT-17*, Vol. 2 (1999), 935.
- 6) M. Bockstedte, A. Kley, J. Neugebauer, M. Scheffler, "Density-Functional Theory Calculations for Poly-atomic Systems: Electronic Structure, Static and Elastic Properties, and *Ab Initio* Molecular Dynamics", *Computer Physics Communications*, 107 (1997), 187.
- 7) P. Hohenberg, W. Kohn, "Inhomogenous Electron Gas", *Phys. Rev.*, 136B (1964), 864.

Author and Contact: Sigrid Greene

Author: Pui Lam

Organization: Dept. of Physics and Astronomy, University of Hawaii at Manoa, 2505 Correa Rd, Honolulu, HI, 96822

Resources: : IBM SP3 at MHPCC and Pentium PC running Linux at the University of Hawaii

Sponsorship: NSF Grant and the Hawaii Institute of Geophysics and Planetology

Measuring the Carrier-Envelope Phase of Few-Cycle Laser Pulses Using Attosecond Cross Correlation Technique in Atoms and Molecules

André D. Bandrauk, Szczepan Chelkowski, Nguyen Hong Shon

The directional asymmetry of photoionization in an H atom and a H₂⁺ molecular ion under the action of combined infrared (IR) femtosecond (fs) and ultraviolet (UV) attosecond (asec) laser pulses are numerically investigated. It is shown that the ionization signal in the combined field is much higher (by several orders) as compared to the signal produced by a single fs or asec pulses alone. As a function of the time delay between two pulses, the *difference* of ionization signals in two opposite directions (along the polarization vector of laser pulses) is modulated at the period of the IR laser pulse and reproduces well the profile of the electric field in the IR pulse. This phenomena can be used for directly measuring the absolute phase of few-cycle laser pulses with an error ~1%. Simultaneously this technique can also be used to evaluate the duration of UV asec pulses.

Research Objectives: In the interaction of intense ultrashort laser pulse with atoms and molecules, most effects depend on the evolution of the laser field within an optical cycle. This evolution is affected by the relative phase of the carrier wave with respect to the pulse envelope (the so-called carrier-envelope or absolute phase φ). In a pulse containing less than three oscillations, the effects of this phase can be significant. For measuring and stabilizing the absolute phase in a few-cycle laser pulse, different schemes have been proposed (e.g., recent references. 1-6). In particular, the possibility of measuring the absolute phase of circularly polarized laser pulses, based on asymmetric angular distributions of photoelectrons, was theoretically investigated in reference 6 and experimentally demonstrated in reference 3. The main idea of this technique is the following: when atoms are ionized by a short laser pulse, and the photoelectrons are recorded with two opposing

detectors in a plane perpendicular to the laser beam, the anticorrelation in the electron yield serves as a measure for determination of the absolute phase. In this paper⁷ we have proposed and investigated a technique for measuring the absolute phase of linearly polarized few-cycle laser pulse by measuring the *ratio* between ionization signals in opposite directions along the polarization vector of the laser pulse.

Methodology: In this paper we propose a new technique for measuring the absolute phase of linearly polarized light pulses. The idea of this technique is also based on the symmetric spatial distribution of photoionization, but we introduce two important modifications. First, we use additional UV asec pulse to enhance the ionization signals. The UV photon energy is chosen to induce resonant transition (*1s-2p* in H atom, LUMO-HOMO in molecules). It will be shown that under the action of combined IR fs and UV asec pulses, the ionization signal increases by several orders as compared to single fs or asec pulse. Second, instead of the *ratio* we measure the *difference* of ionization signals in the two opposite directions along the polarization vector of laser fields. This automatically eliminates a background in the photoelectron yield produced by the above-threshold ionization (ATI) primarily along the polarization vector of the pulses. For the asec-pulse duration shorter than T/4 (T is the optical period) this *difference* is modulated at the period of the IR laser field, and reproduces very well the profile of the electric field inside the laser pulse.

Results: Our investigation is based on the numerical solution of the 3D (for an H atom⁷) or 1D non-Born-Oppenheimer (for H₂⁺ ion⁸) Schrödinger equation in the field of linearly polarized laser pulses. The electric fields are given by:

$$E(t) = E_I(t) + E_{as}(t), \text{ where } E_j(t) = -(1/c)(\partial A_j / \partial t),$$

$$A_j(t) = -\frac{c I_j^{1/2}}{\omega_j} f_j(t - t_j) \sin[\omega_j(t - t_j) + \varphi_j] \quad j = I, as.$$

where ω_j , φ_j and I_j are frequencies, carrier-envelope phases and intensities, and $f_j(t)$ and t_j are field-envelopes and the peak-positions of pulses, respectively. The method of solution, of the Schrödinger equation, is described in details in references 7 and 8.

As an example, we show in Figure.1(b) the results of calculations for an H atom, which is in the initial stationary *1s* state. We use two laser pulses, both have the *sin-square* pulse-envelopes. The 800-nm, 5-fs driver pulse has the peak intensity $I_I = 4 \times 10^{13}$ W/cm². The 115-nm 0.6-fs pulse has the peak intensity $I_{as} = 1 \times 10^{13}$ W/cm². It is clear that the ionization signal (blue dots) reproduces well the profile of IR fs pulse (red dashed line). By simply fitting obtained data with free parameters, I_I and φ_{as} , we can determine the absolute phase with an error ~1%. Our technique also suggests a potential way for measuring the duration of UR asec pulse. For this, one may proceed as indicated in reference 9, i.e., to simulate the cross-correlation data with a single fit parameter t_{as} . The best fit can provide the UV pulse duration with an error of a few tenths of a percent.

References:

- 1) M. Hentschel et al., *Nature*, 414, 509 (2001).
- 2) M. Drescher et al., *Science*, 291, 1923 (2001).
- 3) G. G. Paulus et al., *Nature*, 414, 182 (2001).
- 4) A. Baltuska, T. Fuji, T. Kobayashi, *Phys. Rev. Lett.* 88, 133901 (2002).
- 5) T. Brabec and F. Krausz, *Rev. Mod. Phys.*, 72, 545 (2000).
- 6) P. Dietrich, F. Krausz, P. B. Corkum, *Opt. Lett.*, 25, 16 (2000).
- 7) S. Chelkowski and A. D. Bandrauk, *Phys. Rev.*, A 65, 061802 (2002).
- 8) S. Chelkowski, C. Foisy, A. D. Bandrauk, *Phys. Rev.*, A 57, 1176 (1998).
- 9) A. Scrinzi et al., *Phys. Rev. Lett.* 86, 412 (2001).

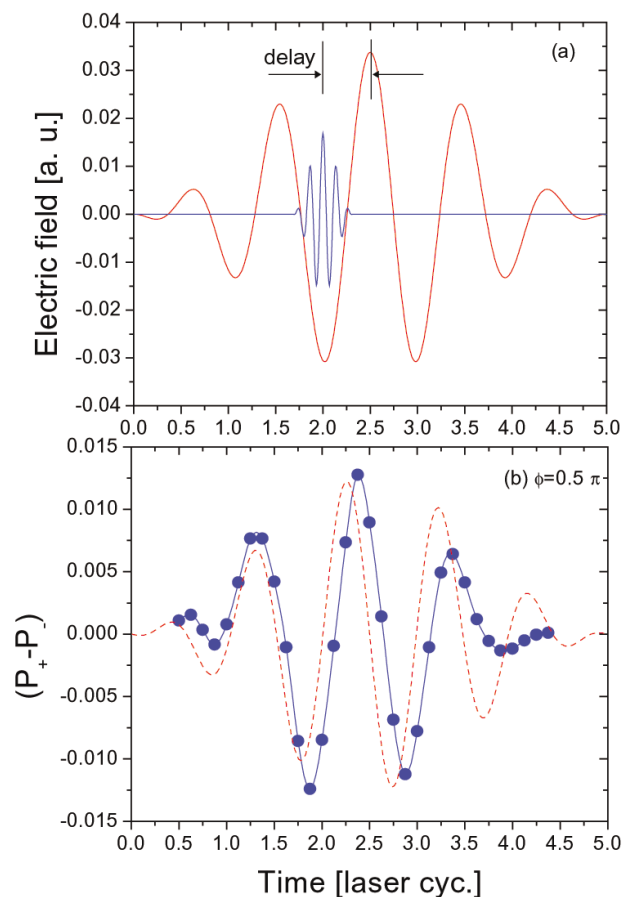


Figure 1. (a) Electric Field of 800-nm, 5-fs laser pulse (red-line) and of 115-nm, 0.6 fs laser pulse. (b) Difference of photoelectron yield in forward and backward directions (blue dots-line). For comparison, the normalized electric field of UV-pulse (red dashed-line) is shown.

Author and Contact: André D. Bandrauk

Authors: Szczepan Chelkowski and Nguyen Hong Shon

Organization: Laboratoire de Chimie Théorique, Université de Sherbrooke, Sherbrooke, Québec, Canada, J1K 2R1

URL: www.cacpus.usherb.ca

Resources: IBM SP at MHPCC

Acknowledgements: Natural Sciences and Engineering Research Council of Canada and Canadian Institute for Photonics Innovations

3D Visualization Concept for Complex Battlefield Simulations

Marie Greene, Mark Elies, Jonathan Baliqat, Peter Lentz, Ted Meyer,
Michael Shrive, Brent Swartz, J. D. Vargas-Garcia, Betsy Ward

The University of Hawaii Maui Community College (MCC) students attending the spring session of MCC's Advanced Animation Course developed a mockup animation of a 3D complex battlefield situation. This movie demonstrates new ways to view urban battlefield complexity and can aid in the decision of the next-generation Playback Tool for the Marine Corps Combat Development Command's (MCCDC) Project Albert Program.

Research Objectives: In support of MCCDC's Project Albert, the Maui High Performance Computing Center (MHPCC) has developed visualization tools that allow MCCDC's analysts to explore the outcome of combat simulations. One of these tools is known as the Playback Tool, and it depicts combatants in a 2D landscape with simple terrain. However, MCCDC has a need to explore more complex battlefield situations, such as combat in an urban environment. To achieve this goal, a next-generation 3D Playback Tool will be developed by MHPCC, which can depict more complex environments, including an urban landscape.

In order to assess what features this tool should incorporate, Maui Community College agreed to collaborate with MHPCC to produce a 3D mockup movie. Students from the Advanced Animation Course were tasked with creating the movie as a class project. This movie depicts agents in an urban environment, exploring different display concepts. Upon viewing this movie, analysts can further decide how the next-generation Playback Tool could best display agents and terrain (including buildings) in three dimensions.

Results: This 3D movie represents friendly (blue), enemy (red), and non-combatant (green) agents moving in an urban environment containing multiple multi-story buildings. An agent can represent a soldier, a squad, a tank, a non-combatant person, etc. The next-generation 3D Playback Tool may incorporate these features to allow analysts to explore the results of Project Albert computer simulation runs. Three different renditions of the urban environment are shown.

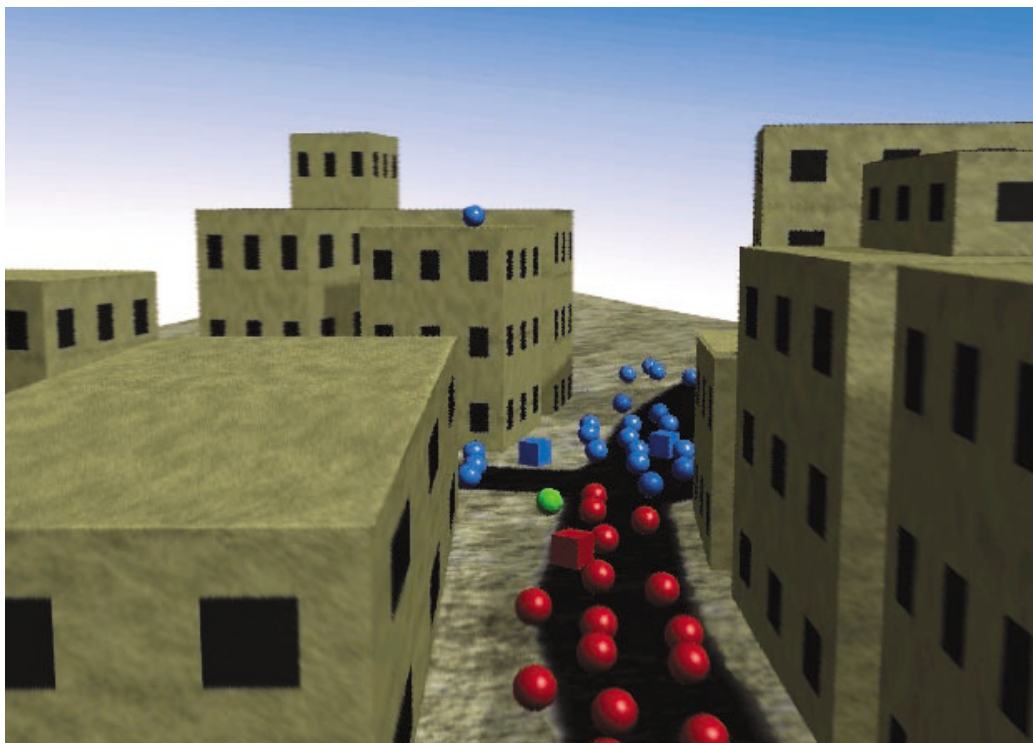


Figure 1. *The opaque rendition shows what the urban landscape would look like to the naked eye.*

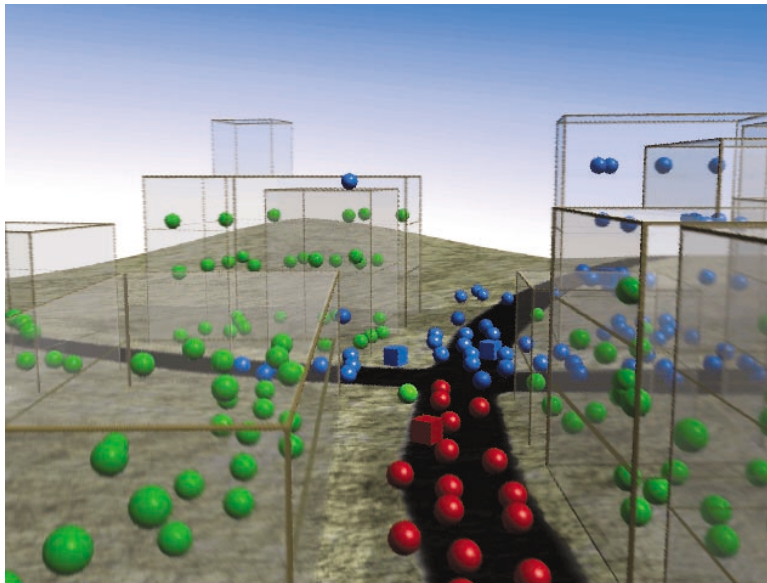


Figure 2. *The transparent rendition shows all agents in the urban scene, as if the viewer possessed "X-ray vision", allowing the viewer to see "ground truth" or reality.*

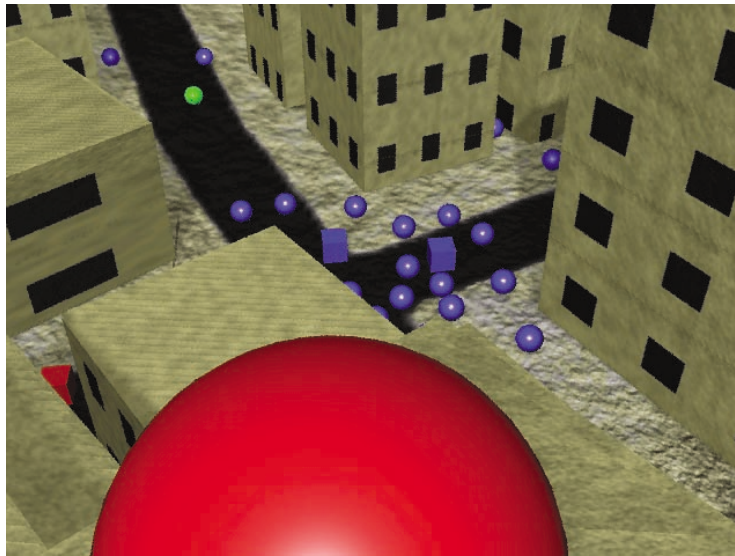


Figure 3. *Also shown is the view of the battlefield from the perspective of a single agent, including what that agent perceives is happening (as opposed to what reality may be).*

Author and Contact: Marie Greene

Author: Brent Swartz

Organization: Maui High Performance Computing Center, 550 Lipoa Parkway, Kihei, HI, 96753

Authors: Jonathan Baliquat, Mark Elies, Peter Lentz, Michael Shrive, J. D. Vargas-Garcia, Betsy Ward

Organization: University of Hawaii, Maui Community College, 310 Ka'ahumanu Ave, Kahului, HI, 96732

Author: Ted Meyer

Organization: MITRE Corporation, Quantico Site, 2750 Killarney Dr., Woodbridge, VA, 22192

Resources: SGI Onyx3400 and the Visualization Facility at MHPCC and Alias/Wavefront Maya 4 on PCs and workstations running MS2000 at MCC

Acknowledgement: MHPCC and MCC would especially like to thank the project author, Mark Elies.

Minima of Kr_n-H for $n = 1$ to 13

Emanuele Curotto and Jonathan H. Skone

We have constructed a simple model for the potential energy surface of clusters consisting of n krypton atoms and one hydrogen. We have used the model to obtain structural and energetic information about the system by employing minimization techniques. Of particular importance to us are the cohesive energies of hydrogen. The data we generate is essential for further experimental and theoretical studies. The hydrogen atom is weakly bound to the Kr framework. However, the systems should be long lived at achievable temperatures in jet expansions to allow for empirical studies.

Research Objectives: The present work is part of a larger project where a hierarchy of quantum - stochastic approaches are developed and applied to obtain spectroscopic properties of LJ_n-H and LJ_n-H_2 clusters at ultra-cold temperatures. The methods we are developing are based on linear scaling, large scale repeated diagonalization techniques which have been recently tested with relatively low dimensional parametric Hamiltonians in the discrete variable representation (DVR).¹ In the present brief, we report the results of a systematic characterization of the potential energy surface of Kr_n-H in the $n=1$ to 13 range. We use a dual numerical strategy to carry out the characterization. A Metropolis² walk at 40 K is used to generate candidate structures. Every 1400 moves, a configuration is

compared structurally with a database of minima already at hand. Structural comparisons are carried out using an algorithm we developed recently.³ If the configuration is sufficiently different structurally from the minima in the database, it is quenched using a dissipative Newtonian algorithm.

Results: Homogeneous Lennard-Jones clusters have very different structures compared to the bulk solid matter. With the exception of few large sizes,⁴ clusters global minima have icosahedral geometry. The icosahedral structure is the result of the large surface tension generated by their nanoscale size. The completion of icosahedral layers explains the occurrence of magic numbers in the cohesive energy per atom (i.e., the "unusual" stability of special sizes, $n = 13, 19, 55, 147, \dots$) in LJ_n . In the $n = 1$ to 13 range the icosahedral growth pattern of LJ_n is evident for $n > 6$ where the global minimum has a characteristic pentagonal symmetry systematically capped as atoms are added. Most global minima of Kr_n-H have a krypton framework identical to the homogeneous Lennard-Jones cluster in the range studied. The hydrogen coordinates 3 surface krypton atoms (for $n > 2$). The cohesive energy of H for most clusters with $n > 2$ is about 160 cm^{-1} . We do find one exception with the $Kr_{10}-H$ cluster, however. The $Kr_{10}-H$ global minimum is a square anti-prism framework of Kr atoms completely caging the hydrogen atom (see Figure 1). For $Kr_{10}-H$ the hydrogen cohesive energy is approximately two and a half times larger than the typical tri-coordinated surface hydrogen.

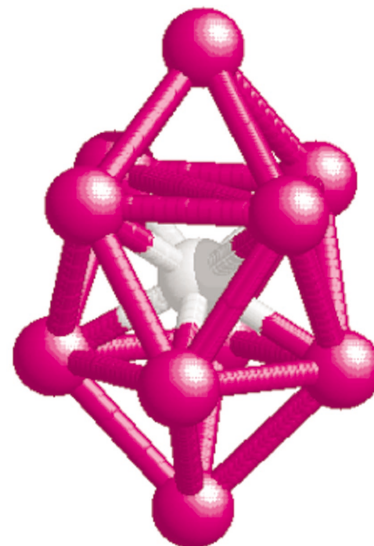


Figure 1. The structure of $Kr_{10}-H$. The global minimum is a square anti-prism with the hydrogen atom in the center. The minimum with icosahedral - like geometry and the H atom on the surface is 24 cm^{-1} higher in energy.

References:

- 1) J. H. Skone and E. Curotto, *J Chem. Phys.*, 116 , 3210 (2002).
- 2) N. Metropolis, A. Rosenbluth, N. M. Rosenbluth, A. Teller, E. Teller, *J. Chem. Phys.*, 21, 1087 (1953).
- 3) E. Curotto, Alex Matro, David L. Freeman, J. D. Doll, *J. Chem. Phys.*, 108, 729 (1998).
- 4) D. J. Wales and Jonathan P. K. Doye, *J. Phys. Chem.*, 101, 5111 (1997).

Author and Contact: Emanuele Curotto

Organization: Department of Chemistry & Physics, Arcadia University, 450 South Easton Road, Glenside, PA, 19038-3295

Author: Jonathan H. Skone

Organization: Department of Chemistry, Pennsylvania State University, 152 Davey Laboratory, University Park, PA, 16802-6300

URL: <http://gargoyle.arcadia.edu/Faculty/Curottom>

Resources: IBM SP at MHPCC and Silicon Graphics 02 and Linux workstation at Arcadia University

Acknowledgements: The Stacy Ann Vitetta '82 Professorship Fund and the Ellington Beavers Fund for Intellectual Inquiry is gratefully acknowledged. This research has also been supported in part by the Phillips Laboratory, Air Force Material Command, USAF, through the use of the MHPCC. The views and conclusions contained in this document are those of the author and should not be interpreted as necessarily representing the official policies or endorsements, either expressed or implied, of the Phillips Laboratory or the U.S. Government.

2D MHD Simulations Using Lattice Boltzman Methods

Linda Vahala, George Vahala, Angus Macnab, Min Soe

The Lattice Boltzmann method utilizes two distribution functions on an octagonal velocity lattice, a scalar distribution function for the velocity field, and a vector distribution for the magnetic field. The Lattice Boltzmann code is ideally parallelized, and with runs on *Tempest* at the Maui High Performance Computing Center (MHPCC), we have examined the evolution of plasma sheets in 2D flows.

Research Objectives: Our primary interest is to develop quantum lattice codes for MHD. However, as a preliminary to developing 2D codes, we are first considering the Lattice Boltzmann approach. The lattice Boltzmann method utilizes two distribution functions on an octagonal velocity lattice, a scalar distribution function for the velocity field, and a vector distribution for the magnetic field.

Methodology: A coupled set of Lattice Boltzmann BGK kinetic equations are solved in 2D such that under Chapman-Enskog expansions one recovers the dissipative MHD equations:

$$\begin{aligned} \partial_t \rho + \nabla \cdot (\rho \mathbf{v}) &= 0 \\ \rho [\partial_t \mathbf{v} + \mathbf{v} \cdot \nabla \mathbf{v}] &= -\nabla \left[P + \frac{B^2}{2} \right] + \mathbf{B} \cdot \nabla \mathbf{B} + \nu \nabla^2 (\rho \mathbf{v}) \\ \partial_t \mathbf{B} + \mathbf{B} \cdot \nabla \mathbf{v} &= \mathbf{v} \cdot \nabla \mathbf{B} + \mu \nabla^2 \mathbf{B} \end{aligned}$$

with the viscosity $\nu = \frac{1}{4} \left(\tau_v - \frac{1}{2} \right)$ and the resistivity $\mu = \frac{\alpha}{2} \left(\tau_\mu - \frac{1}{2} \right)$ for arbitrary α . The τ s are the relaxation rates in the BGK equations.

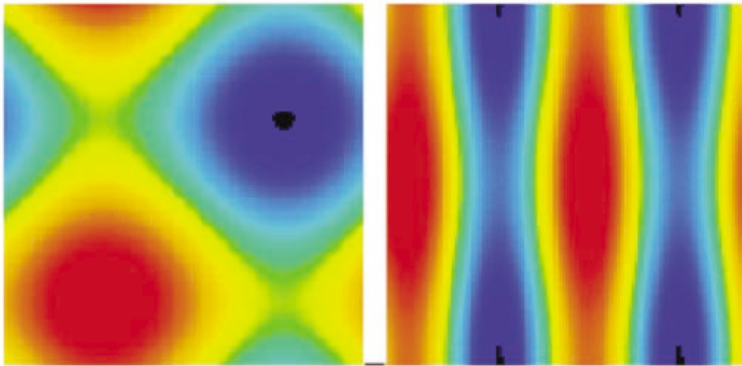


Figure 1a. Initial vorticity.

Figure 1b. Initial current density.

Results: The Lattice Boltzmann code is ideally parallelized, and with runs on *Tempest* (MHPCC), we have examined the evolution of plasma sheets in 2D flows. In Figure 1 we see the initial vorticity (a) and current sheets (b).

After about 1,000 iterations, the large structures give way to localized vortex and current sheets (Figures 2a and 2b).

We are planning on developing a quantum algorithm to solve these MHD equations and test the results of such simulations against the Lattice Boltzmann results.

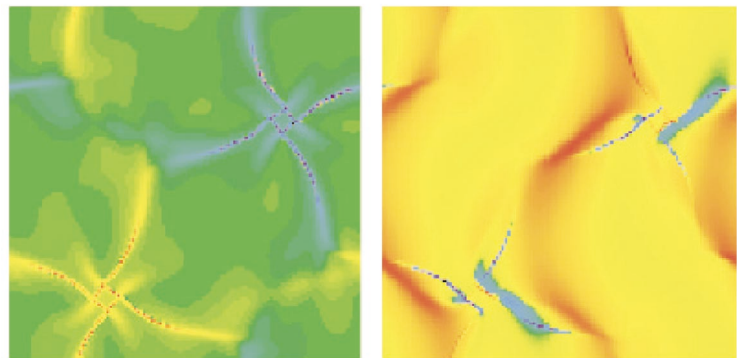


Figure 2a. Vorticity after 1K iterations.

Figure 2b. Current density after 1K iterations.

Author and Contact: Linda Vahala

Authors: George Vahala and Angus Macnab

Organization: Old Dominion University, Norfolk, VA, 23529

Author: Min Soe

Organization: Rogers State University, 1701 W. Will Rogers Blvd., Claremore, OK, 74017

Resources: IBM SP3 *Tempest* at MHPCC

First-Principle Methodologies for Ferroelectromagnetic Materials

Alessio Filippetti and Nicola A. Hill

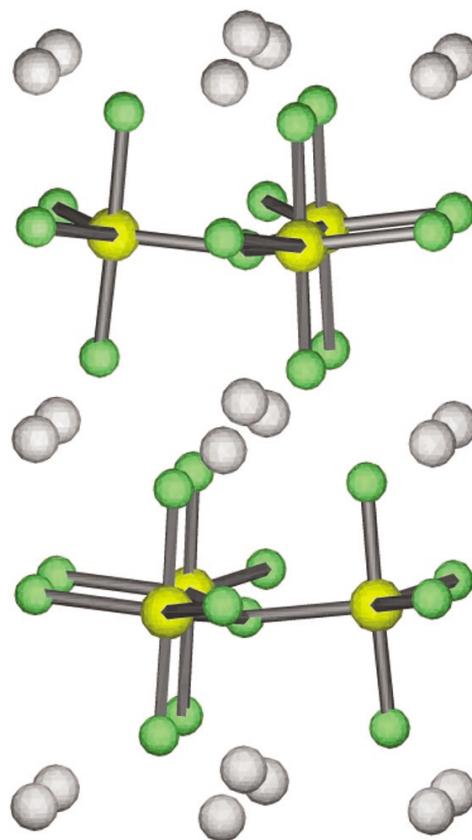
First-principles condensed matter theories are aimed at calculating the fundamental properties of materials within a purely theoretical, quantum-mechanical approach, i.e., without the aid of models or input parameters derived from experimental sources. Within the context of Density Functional Theory (DFT) formulated in 1965, the basic properties which identify the equilibrium ground state (e.g., structural, electronic, magnetic, piezoelectric), as well as the dynamical and optical properties of a vast range of compounds are now accessible.^{1,2,3} With this goal, the increasing power of modern computers represents the necessary complement of the theory itself, and the very efficient *Tempest* IBM SP3 parallel computer of the Maui High Performance Computing Center (MHPCC) is an ideal instrument for solving the demanding numerical equations which stand at the basis of our approach. Our project carried out with the MHPCC resources follows two main paths. On one hand, we work on methodological developments aimed at improving the accuracy of DFT for those materials whose description is difficult using the conventional formalism (magnetic and strongly-correlated materials). On the other hand, we apply the DFT to the study of specific problems within solid state physics. In particular, we are interested in ferroelectromagnetic materials; i.e., materials which are both magnetic and ferroelectric within the same bulk phase (e.g., hexagonal YMnO_3). These might be potentially interesting as building blocks in the so-called spintronic technology, which aims to take advantage of the electronic, as well as the magnetic state of matter, to design new and more powerful devices.⁴

Technicalities: Our initial theoretical framework was based on the DFT within the Local Spin Density Approximation (LSDA) for the exchange-correlation energy, and employs plane wave basis functions and ultrasoft pseudopotentials. A ferroelectric material must be an insulator, otherwise it cannot sustain a spontaneous electric polarization, but the LSDA describes this system as a metal.⁷ This is a typical error due to the presence in the LSDA energy of the spurious self-interaction of the strongly localized 3d and 2p states. To overcome this shortcoming we developed a self-interaction corrected pseudopotential scheme (pseudo-SIC),⁹ which promises to be able to correct to a large extent the LSDA faults occurring in the description of magnetic and strongly-correlated compounds with a minor increase of computing cost. The application to YMnO_3 is an example of the capability of our methodology.

Figure 1. Structure of the hexagonal ferroelectric YMnO_3 . Mn atoms (yellow) are placed within bi-pyramidal cages of five oxygens (green), whose triangular basis is tilted with respect to the hexagonal planes. Y atoms (gray) are seven-fold coordinated with oxygens. The electric polarization is orthogonal to the hexagonal (001) plane.

Introduction: Multiferroic, or ferroelectromagnetic materials, possess both magnetic and ferroelectric ordering; thus they retain all the potential applications of their parent ferroelectric and ferromagnetic compounds, and in addition, can be used for a whole range of new applications that exploit the coupling of these two orders.^{4,5} For example, multiple state elements, where data are stored both in the electric and the magnetic state of polarization, or novel memory media which might allow writing of a ferroelectric data bit and reading of the magnetic field generated by association. Example of such compounds are YMnO_3 ^{6,7} and BiMnO_3 .⁸

Structure and Main Features: In Figure 1 we report the structure of ferroelectric hexagonal YMnO_3 . The Mn ions, sited on close-packed hexagonal positions, are surrounded by corner sharing bi-pyramidal cages of five oxygens which are seven-fold coordinated with Y (in total there are 8 layers and 30 atoms per cell). The structure is ferroelectric for temperatures below $T_c=900$ K and antiferromagnetic below $T_N=80$ K. The spontaneous electric polarization, P , is directed along the c axis, and the magnetic ordering is A-type antiferromagnetic (each Mn layer is individually ferromagnetic, with an alternating spin direction along [001]).



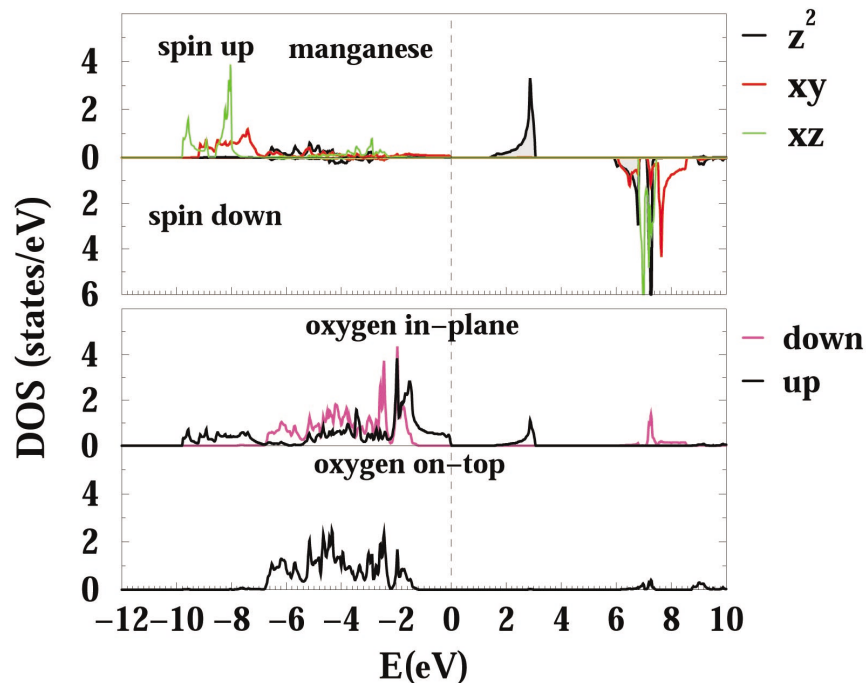


Figure 2. Orbital-resolved density of states of individual Mn and O atoms calculated within pseudo-SIC. For the on-top oxygen, up and down spin densities are equal by symmetry.

Results: In Figure 2 we report the orbital-resolved Density of States (DOS) of individual spin-polarized Mn and O atoms calculated within pseudo-SIC. The antiferromagnetic symmetry enforces the DOS of the up-spin and down-spin Mn atoms to be equal under exchange of up and down components. In the hexagonal crystal field, the local orbitals with d-like angular character are split into two doublets (d_{xz} , d_{yz}) and (d_{xy} , $d_{x^2-y^2}$) and one singlet d_{z^2} . The two doublets are fully spin-polarized, thus they furnish a magnetic moment close to $4 \mu_B$, whereas the singlet lies higher in energy and is separated from the valence band top by an energy gap of 1.5 eV, i.e., the system is properly described as an insulator.

Through the application of the pseudo-SIC method, we have been able to calculate structural and electronic properties of YMnO_3 ,^{6,7} to rationalize the microscopic mechanisms leading to ferroelectric distortions and, in turn, to understand the principles which permit the coexistence of ferroelectric and magnetic ordering.^{5,6,7}

References:

- 1) R. O. Jones and O. Gunnarson, *Rev. Mod. Phys.*, Vol.61, 689 (1989).
- 2) W. E. Pickett, *Rev. Mod. Phys.*, Vol.61, 433 (1989).
- 3) R. Resta, *Rev. Mod. Phys.*, Vol.66, 899 (1994).
- 4) D. D. Awschalom, M. E. Flatté, N. Samarth, *Scientific American*, June 2002.
- 5) N. A. Hill, *J. Phys. Chem.*, B, Vol.104, 6694 (2000).
- 6) A. Filippetti and N. A. Hill, *Journal of Magnetism and Magn. Mat.*, Vol.236, 176 (2001).
- 7) A. Filippetti and N. A. Hill, *Phys. Rev.*, B Vol.65, 195120 (2002).
- 8) N. A. Hill and K. M. Rabe, *Phys. Rev.*, B Vol.59, 8759 (1999).
- 9) A. Filippetti and N. A. Hill, to be published.

Author and Contact: Alessio Filippetti

Author: Nicola A. Hill

Organization: Materials Research Laboratory, University of California, Santa Barbara, CA, 93106

Resources: IBM SP3 at MHPCC

Sponsorship: NSF, MRL Central Facilities

Cluster Computing: Communication Performance and Scalability

Daniele Tessler

Cluster computing has emerged as a viable alternative to massively parallel supercomputers to cope with the computing demands of scientists and HPC application developers. Cluster machines, built on top of Commodity Off The Shelf components and based on open source software are becoming very popular. This project is aimed at evaluating the performance that these machines actually deliver to scientific and industrial applications. For such a purpose, we have analyzed the performance achieved by a large IBM NetFinity when processing a few numerical algorithms. Statistical techniques, such as clustering and fitting, have been used to characterize the actual performance of the machine. Performance models have been derived for investigating the scalability of analyzed numerical algorithms.

Research Objective: In the High Performance Computing (HPC) scenario, the idea of exploiting the aggregated computational power of inexpensive personal computers and workstations has long been pursued. Started as a pile-of-pcs, today's cluster might be composed of hundreds of commodity processors connected via specialized, high performance, interconnection networks. Indeed, several of these superclusters are ranked in the top 500 most powerful computers.

Methodology: It is then important to investigate the performance that these machines actually deliver to scientific and industrial HPC applications. For such a purpose, we have analyzed the performance of one of the largest Linux clusters, which is the IBM NetFinity at the Maui High Performance Computing Center. A bottom-up methodology has been adopted to characterize the performance. Basic machine performance has been analyzed by means of low level kernels from the ParkBench suite.

Results: Analytical models for the severity of the communication versus computation performance have been derived. We have then investigated the behavior of a few kernels from the NAS Parallel Benchmarks suite. These kernels resemble the computational cores of many scientific and industrial applications. Matrix LU factorization, multigrid V cycle, linear equation systems solver, Fast Fourier Transform, and Montecarlo simulations are examples of considered algorithms.

The aim of this analysis is to characterize the kernels' performance when executed over either Myrinet and Ethernet networks. Figure 1 shows the time spent in computation activities, on a per kernel basis, varying the number of allocated processors. Note that logarithmic scales have been used on both axes. As can be seen from the figure, the time spent on computational activities scales proportionally to the number of allocated processors.

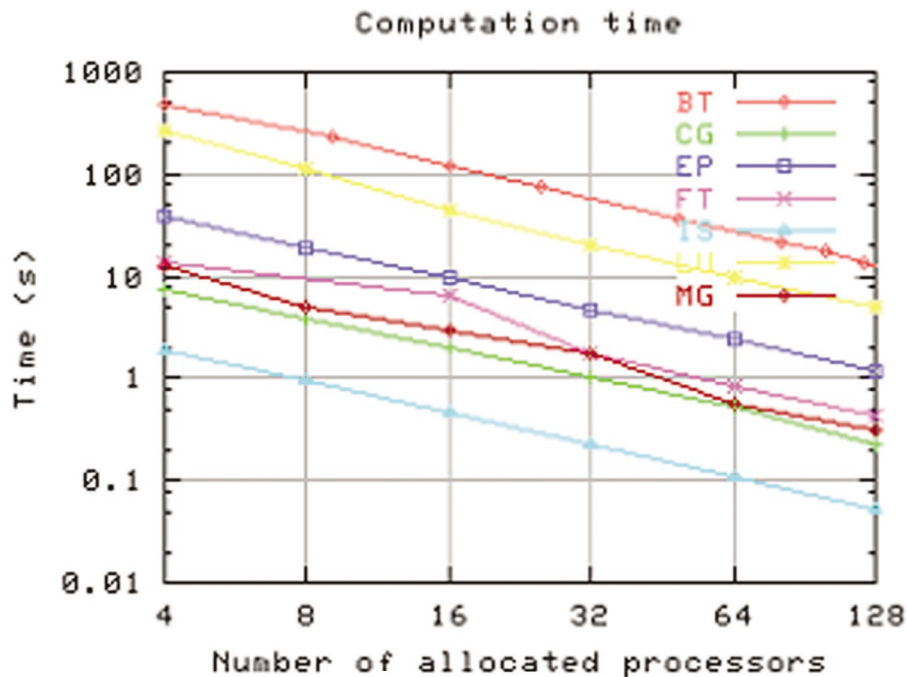


Figure 1. Computational time, on a per kernel basis, as a function of the number of allocated processors.

Figure 2 plots the time spent by each kernel in communications activities, as a function of the number of allocated processors, over both Myrinet and Ethernet interconnection networks. Executions over Myrinet, even when a large number of processors is allocated, do not experience significant increases of the communication time. As can be seen from the figure, Ethernet limits the scalability of the considered kernels. An in-depth analysis of the communication times, on a per protocol basis, has outlined that the best performance over Ethernet is achieved by blocking protocols (e.g., MPI_Send and MPI_Recv). On the other hand, Myrinet performance benefits from using blocking sends and non blocking receives (e.g., MPI_Send, MPI_Irecv).

Significance: Future works will be aimed at identifying workload models for classes of numerical algorithms, as well as investigating the impact of the processor allocation policies on the performance.

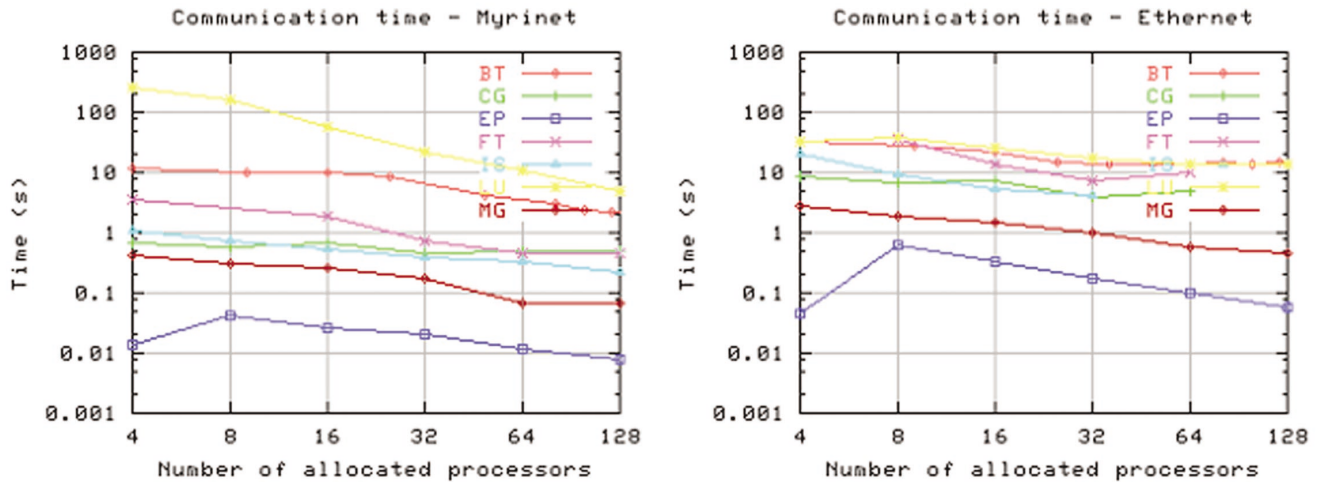


Figure 2. Communication time for each kernel executed over both Myrinet and Ethernet, as a function of the number of allocated processors.

Author and Contact: Daniele Tessera

Organization: Department of Computer Science, University of Pavia, Via Ferrata, 1 I-27100 Pavia, Italy

URL: <http://mafalda.unipv.it>

Resources: IBM NetFinity Supercluster, *Huinalu*, at MHPCC

Sponsorship: This work has been partially funded by the Italian Research Council under the grant CNRG0032FB "Agenzia 2000" and in part, by the Air Force Research Laboratory, Air Force Materiel Command, USAF, under cooperative agreement number UNIVY-0282-U00.

Electron-Impact Ionization of Hydrogen

Igor Bray

One of the last frontiers of atomic collision theory has been the problem of electron-impact ionization of atomic hydrogen. Recently, Rescigno et al (1999) solved this problem using a technique specifically designed for this problem. Here we show that a much more generally applicable and widely used method is also able to solve this problem.

Research Objectives: Electron-impact ionization of atomic hydrogen is a prototype Coulomb three-body problem. Its solution has recently been claimed by Rescigno et al. (1999). They developed an Exterior Complex Scaling (ECS) method to solve the problem and yielded generally excellent agreement with their experiment.

Methodology: Our own convergent close-coupling (CCC) method is based on ideas developed in the early 1930s, and refined continuously since that time. The close-coupling based theories are the most successful and applicable to a wide range of electron-atom collisions. They were not designed with ionization in mind, but we have shown how they may be simply adapted to treat ionizing collisions (Bray and Fursa 1996).

Results: The CCC method utilizes discrete square-integrable states to treat the target continuum, while using plane waves for the projectile continuum. Thus, the most difficult ionization kinematical regime is when the two outgoing electrons have the same energy. This makes them experimentally indistinguishable, unlike the CCC theory. However, in Figure 1 we show that agreement between the absolute (+/-40%) experiment, ECS and CCC theories is excellent.

References:

- 1) I. Bray and D. V. Fursa, *Physical Review, A* 54, 2991 (1996).
- 2) T. N. Rescigno, M. Baertschy, W. A. Isaacs, C. W. McCurdy, *Science*, 286, 2474 (1999).

MURDOCH
UNIVERSITY
PERTH, WESTERN AUSTRALIA

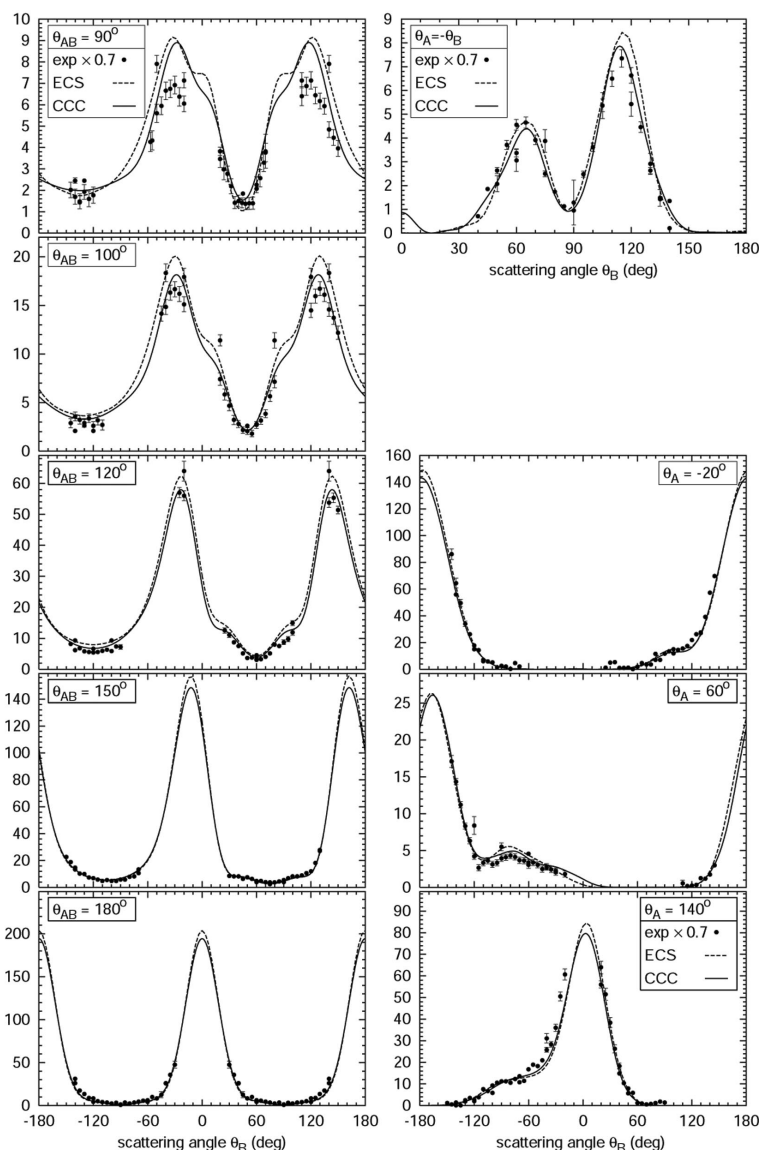


Figure 1. 17.6 eV e-H ionization fully differential cross section for 2 eV outgoing electrons.

Author and Contact: Igor Bray

Organization: Professorial Fellow, Physics & Energy Studies, Murdoch University, GPO Box S1400, Perth, Western Australia, 6849

URL: <http://atom.murdoch.edu.au>

Resources: IBM SP at MHPCC and SUN E450 at the Murdoch University of Western Australia

Sponsorship: Australian Research Council

INDEX OF AUTHORS

B

David Bacon 14
Jonathan Baliquat 40
Andre Bandrauk 38
Paul Billings 6, 24
Alfred Brandstein 12, 16
Igor Bray 48
Bob Brem 6
Jim Brozik 26

C

Emily Carter 4
Szczepan Chelkowski 38
Margaret Chen 2
Flo Cid 6
Emanuele Curotto 42

D

Bob Dant 24
Chip DeMeo 6
D. A. Drew 19
Bruce Duncan 6, 8, 12, 16
Thomas Dunn 14

E

Mark Elies 40
Debi Evans 34

F

D. J. Fabozzi 12, 16
Alessio Filippetti 44
James Forsythe 10, 22
Francis Fujioka 30

G

Dean George 8
Steve Gima 6, 8
Marie Greene 40
Sigrid Greene 36

H

Mary Hall 14
Jongil Han 30
Nicola Hill 44
Gary Horne 12, 16
Bobby Hunt 24

J

Emily Jarvis 4
Joel Johnson 1

K

David Keller 26
Jeremy Kepner 20
John Kresho 12, 16

L

R. T. Lahey, Jr. 19
Pui Lam 36
Pius Lee 14
Peter Lentz 40

M

Agnes Macnab 43
Chuck Matson 24
Mary McDonald 12, 16
Ted Meyer 12, 16, 40
F. J. Moraga 19
Scott Morton 10
Maria Murphy 12, 16

N

Chelsea Nesbitt 8
James Newhouse 26, 34

P

Frank Price 18

R

Mark Radleigh 8
Thomas Reichler 28
Nathan Reish 8
Joe Ritter 23, 26, 34
John Roads 28, 30
Kevin Roe 30, 32

S

A. Sarma 14
Kathy Schulze 6, 24
Nguyen Hong Shon 38
Michael Shrive 40
Jonathan Skone 42
Min Soe 43
Phillipe Spalart 10
Kyle Squires 10
Duane Stevens 32
William Strang 10
Bob Swanson 12, 16
Brent Swartz 12, 16, 40
Eric Szarmes 18

T

Daniele Tessera 46
Joshua Testerman 8
Robert Tomaro 10

U

Steve Upton 12, 16

V

George Vahala 43
Linda Vahala 43
J. D. Vargas-Garcia 40
Shirley Verbisk 8
Ron Viloria 12, 16

W

Jason Wachi 8
Betsy Ward 40
Jon Wentzel 22
Kenneth Wurtzler 10

INDEX OF ORGANIZATIONS

A

Aerospace Corporation 2
Air Force Research Laboratory 22, 24
Akimeka 8
Arcadia University 42
Arizona State University 10

B

Boeing Commercial Airlines 10
Boeing LTS 6

C

Cobalt Solution, LLC 10

K

KJS Consulting 6, 24

M

Marine Corps Combat Development Command . . . 12, 16
Maui High Performance Computing Center
..... 6, 8, 12, 16, 24, 26, 30, 32, 34, 40
MIT Lincoln Laboratory 20
MITRE Corporation 12, 16, 40
Murdoch University 48

N

NOAA Office of Global Programs 28

O

Ohio State University 1
Old Dominion University 43

P

Pacific Northwest National Laboratory 10
PEC Solutions 8
Pennsylvania State University 42

R

Rensselaer Polytechnic Institute 19
Riverside Fire Laboratory 30
Rogers State University 43

S

Science Applications International Corporation (SAIC)
..... 12, 14, 16, 23, 26, 34
Scripps Institution of Oceanography 28, 30

T

Textron Systems 6, 24

U

Unites States Air Force Academy 10, 22
U.S. Department of Agriculture 30
U.S. Forest Service 30
Université de Sherbrooke 38
University of
California at
Los Angeles 4
Santa Barbara 44
Hawaii at
Manoa 18, 32, 36
Maui Community College 40
New Mexico 26, 34
Pavia 46

V

Veridian-MRJ 8

W

World Weather Building 30